SET-THEORETIC CONTROL OF A PRESSURIZED WATER NUCLEAR POWER PLANT

by

ABDELHAMID CHENINI

B.S., Alexandria University (Egypt)
(1970)
D.E.A., University of Algiers (Algeria)
(1974)
M.S., Rensselaer Polytechnique Institut, (N.Y., USA)
(1978)

SUBMITTED IN PARTIAL FULFILLMENT
OF THE REQUIREMENTS FOR THE
DEGREES OF

NUCLEAR ENGINEER
AND
MASTER OF SCIENCE IN NUCLEAR ENGINEERING

at the

MASSACHUSETTS INSTITUTE OF TECHNOLOGY

September 1980

Signature of Author ______________________________
Department of Nuclear Engineering
August 25, 1980

Certified by ______________________________
Leonard A. Gould
Thesis Supervisor

Accepted by ______________________________
Allan F. Henry
Chairman, Department Committee

SET-THEORETIC CONTROL OF A PRESSURIZED WATER NUCLEAR POWER PLANT

by

ABDELHAMID CHENINI

Submitted to the Department of Nuclear Engineering on August 25, 1980 in partial fulfillment of the requirements for the Degrees of Nuclear Engineer and Master of Science in Nuclear Engineering

ABSTRACT

A Set-Theoretic approach for solving practical full-state feedback control problems when some or all of the states are not accessible and for which the available controls are limited and it is desired to keep the system states or outputs within prescribed bounds in the presence of input disturbances is developed.

The input disturbance is represented by an unknown-but-bounded process, a reduced-order observer is employed to reconstruct the inaccessible states, and the control and state constraints are treated directly. By treating the constraints directly, this technique ensures that all the constraints will be satisfied and a once-through design results.

The control problem associated with the operation of a pressurized water nuclear power plant is investigated and the Set-Theoretic Control technique is applied to demonstrate its applicability to practical control problems.

Thesis Supervisor: Leonard A. Gould

Title: Professor of Electrical Engineering and Computer Science

ACKNOWLEDGEMENT

To Professor Leonard A. Goud I express my greatest respect. Since his warm reception for the first time when he suggested the thesis topic, I found with him comprehension and understanding.

I am particularly indebted to Professor G. Verghese for his valuable suggestions and guidance, and to Dr. P.B. Usoro for his direct involvement in this research.

I would like to express my appreciation to Professors E.P. Gyftopoulos, F.C. Schweppe, J.E. Meyer, M.S. Kazimi and D.D. Lanning for their comments and advice.

I am very grateful to Professor T.W. Kerlin of the Department of Nuclear Engineering at the University of Tennessee for his explanatory letter. His advice and the material that he provided to me were of great help in the development of this research.

I am particularly indebted to my friend Kamal Youcef Toumi. His direct involvement in this work and his encouragements at times of hardship contributed to the success of this work.

I also wish to thank my colleagues, Mssrs. Shahriar Negahdaripour and Ryan Kim for their suggestions and interesting discussions.

I would like to thank Mr. M.P. LeFrancois of Maine Yankee for providing information about the tolerances in a

PWR power plant.

I would like to thank the University of Algiers for sponsoring my studies at the USA.

I give a very special word of thanks to Miss Cathy Lydon for her cooperation, patience and efficiency in typing this thesis. Miss Jennice Phillips was also of great help.

I would like to take advantage of this opportunity to remember my parents and all members of my family, especially my wife, Soheir, to whom I owe my success. Also I would like to remember, of course, my dearest children: Abir (chou-chou de papa) and Mohamed-Tarek (my Ibni). Finally, I remember my two intimate friends, A. Gharmoul and M. Abdellatif for their continued moral support.

TABLE OF CONTENTS

Table of Contents (cont'd)

Table of Contents (cont'd)

LIST OF TABLES

LIST OF FIGURES

List of Figures (cont'd)

NOMENCLATURE

For the sake of continuity and for a minimum of confusion, all symbols used in the main text and the appendices are defined immediately. However, the following symbols are redefined in order to eliminate any confusion:

β^*	fraction of delayed neutron
β	a free parameter that enters in the construction of the ellipsoid
ρ, ρ_{ext}	nuclear reactor reactivities
$\rho_{subscripts}$	are densities
S_i^*	are numbers $i=1,2,2,\ldots$
S, S_1 and S_2	are matrices
T_j^*	are numbers $j=1,2,3,\ldots$
T	is a transformation matrix
L_T	turbine power output
L	a matrix
η_i	numbers $i=1,2,3,\ldots$
$\underline{\eta}$	vector
'	on a matrix, it means its transpose
'	on a variable, it means a prime
"	on a variable, it means double prime
ε	if used as an operational symbol it means element of
ε	if used as a variable, it means main steam valve coefficient.

Abbreviations

PWR	Pressurized water reactor
LTI	Linear time-invariant
STC	Set-Theoretic Control
HP	High pressure
LP	Low pressure
UTSG	U-tube steam generator

Chapter 1

INTRODUCTION

1.1 Background

By far, the largest fraction of electrical supply in most parts of the world today is produced in central power stations which employ steam-driven turbines to drive the electric generators. Most such plants have in common what is termed in the industry as a "Steam Supply System." The name implies producing high pressure steam from water. In pressurized water nuclear power plants, which share this feature, the energy needed to produce the steam is provided by nuclear fission of uranium, which takes place in the core of a nuclear reactor. In any power plant and consequently in a PWR (pressurized water reactor) power plant, the one basic operating objective is to produce electrical energy as required by the load demand for that power plant. In order to meet the load demand, the power produced in the reactor core, its transfer through the various power conversion systems, and the power delivered by the turbine must be controlled. Such a control system must provide a simultaneous coordinated control for both the reactor and the turbine. A close coordination of the reactor and turbine controls will prevent large deviations in plant variables. Keeping the plant variables within prespecified bounds at all times is a vital requirement since violation of limiting constraints can result in poor performance, and could subject the power plant to extensive damage.

In summary, the problem considered is to develop a control for load changes in a PWR power plant which can maintain plant variables within prescribed bounds at all times.

In this study, this class of problems is addressed by using "Set-Theoretic Control (STC)", synthesis technique (1). In this design approach, satisfaction of system state or outputs and control constraints requires that the variables and controls lie within bounded sets. The bounded sets are approximated by bounding ellipsoids for the ease of calculations. In the development of this design approach, the control system that yields the maximum tolerable amplitude of the input disturbance that the system can tolerate without violation of the state and control constraints is determined.

1.2 Review of Literature in Set-Theoretic Control

The foundation of the "Set-Theoretic Control" concept is based on the "unknown-but-bounded" representation of uncertainties (2,3). This representation assumes no statistics for the uncertainty and the only information that is known about its identity is that it belongs to a bounded set. With this formalism, the idea of "using only available amount of control effort is re-stated as "using control from a bounded set of controls" and the idea of "keeping the system states within prescribed bounds at all times" is re-stated as "keeping the system states within a prespecified sequence of bounded sets," where the prespecified sequence of bounded sets defines what is termed a "Target Tube." Hence, the control objective is to keep the system state in a Target Tube, using control from a bounded control set, in the presence of unknown-but-bounded input disturbances.

Earlier work (2,4,5,6,7,8) in Set-Theoretic Control was done in the field of prediction and estimation. Further work (9,10,11,12,13) on Target Tube reachability problems provided more insight into the applicability of the Set-Theoretic concept to control system design. Glover and Schweppe (12) used the Target Reachability results to describe the control problem as a Dynamic Programming Problem. They showed that a solution of this problem, if it exists, would prescribe a sequence of admissible control sets that would meet the control objective but where a solution does exist, no specific control is defined at any particular instant of time. Sira-Ramirez(13) extended the Target Reachability Concept to the coordinated control of large scale systems and as in (11,12), the control solution was defined in terms of a sequence of sets which may or may not exist and no procedure was defined for determining a specific control to use at any given time. Usoro (1) proceeded a step further by defining a specific class of control systems (hypothesizing a full state feedback control structure) and then selecting the best control in this class which yields non-violation of state and control constraints in the presence of the input disturbance. In his development, he reformulated the Set-Theoretic Control problem as "attempting to maximize the amplitude of the unknown-but-bounded input disburbance instead of defining a prespecified bound on it."

Moore (14) applied set-theoretic concept, to a limited extent, to the control of nuclear power plant load changes by considering a state constraint set which is reduced by the effect of stochastic observation noise.

1.3 Research Objectives

The main objectives of this study are:

(1) To extend the Set-Theoretic Control synthesis technique as reformulated in (1) to include more practical situations. Note that the hypothesized structure for the control used in (1) is a full-state-feedback which assumes knowledge of the entire state variables. Unfortunately, in most

practical systems, the complete state is not always available for measurement and so there is a need to reconstruct the state via a device called "Observer." This subject is addressed in this study.

(2) To apply Set-Theoretic control to the PWR power plant as an example of a solution to a practical control problem.

1.4 Modern Versus Classical Control Techniques in Nuclear Power Plants

In the U.S. the design of control systems for nuclear power plants is mostly based on conventional frequency domain analysis methods and process computers have not been used extensively. However, the use of computers for data acquisition, logging, plant performance monitoring, etc., and the tendency toward adopting advanced control techniques are growing at a rapid rate (15). In Norway, an extensive program has been underway at the OECD Halden Reactor Project using "Linear Quadratic Gaussian". technique (16, 17). Frogner (18, 19) has applied this technique to the control of a boiling water nuclear power plant.

The lack of acceptance of modern control methods is due to two main shortcomings (15).

(1) Although the theoretical background is very well developed, the practical design methods have not been yet established.

(2) Most of the modern control methods result in systems which are best implemented by computers thus resulting in additional issues related to the licensing of the plant.

However, we hope that in spite of these shortcomings, the special advantages of Set-Theoretic Control will lend it attractive to implementation.

It is worthwhile to note that in nuclear power plants the control system is separated from the protection system. U.S. Regulations require that credit cannot be taken for the control system performance in the plant safety analysis (15). Although the control system may guide the plant in a safe direction during an emergency condition, this contribution is not to be incorporated in the safety analysis. Regulations (20) require an RPS (Reactor Protection System) which is a special quadruply redundant dedicated control sytem whose function is to trip the reactor if any one of several potentially unsafe conditions appear to exist.

1.5 Organization of Thesis

This thesis is organized in seven chapters. The second chapter describes a typical pressurized water nuclear power plant with its steady state control program. Some of the control systems are reviewed and a mathematical model of the plant is presented. Chapter 3 treats the reconstruction of state by using observers. Chapter 4 underlines the formulation of the Set-Theoretic Control synthesis technique and the observation/control problem is stated. In Chapter 5, the solution procedure is discussed and the relevant parts of the algorithm, used in the solution of the problem are presented. Applications are presented in Chapter 6. Explanatory examples are solved first and the procedure is applied to the PWR power plant. The effectiveness of the technique is evaluated through simulations of the time responses of the system. Conclusions and recommendations are given in the last chapter.

Chapter 2

PRESSURIZED WATER NUCLEAR POWER PLANT

2.1 Introduction

The basic objective of a power plant is to produce electrical energy as required by the load demand for that power plant. The load demand from the power distribution system is directly applied to the turbine-generator of the plant. In a nuclear power plant, several energy conversions take place, from nuclear energy to electrical energy. In order to meet the load demand, the different power conversion systems must respond with the correct flow of preconditioned steam to the turbine. Therefore in satisfying the basic objective, the energy release and energy transfers through the plant must be controlled. Hence the first specific control requirement is to coordinate the reactor control rods and the turbine throttle valves so as to avoid large deviations in plant variables.

In recent years, the problem of maintaining plant variables within prescribed bounds at all times during perturbations has become more demanding (21) because plants are larger, power levels are higher, and margins imposed by regulatory agencies are tighter. The effectiveness of any control system is in fact evaluated in terms of its ability to maintain the plant state variables within prescribed bounds, using only available control effort, in the presence of input disturbances.

In this study, the PWR power plant is described by a mathematical model derived from physical laws. The emphasis is placed on modeling for analyzing normal operational transients and for designing control systems. The model is linearized and assumed time-invariant. Thus, it is represented by a set of equations of the form:

$$\dot{\underline{n}} = A\underline{x} + B\underline{u} + \underline{G}w \qquad (2.1.1)$$

$$\underline{z} = M\underline{x} \qquad (2.1.2)$$

$$\underline{y} = H\underline{x} \qquad (2.1.3)$$

where,

$\underline{x}$ is an nxl state vector

$\underline{u}$ is an rxl input control vector

w is a scalar input disturbance

$\underline{z}$ is an mxl measurement input vector

$\underline{y}$ is a pxl system output vector

A,B,H and M are matrices and $\underline{G}$ is a vector with appropriate dimensions.

A full-state feedback control law is designed by using the Set-Theoretic Control synthesis technique (1) as we shall see in Chapter 4. This law requires knowledge of the entire state vector $\underline{x}$. However, not all components of this vector can be detected. For this reason, the unavailable state variables are first reconstructed via an observer as we shall see in Chapter 3.

A typical PWR power plant is discussed in this chapter. Control strategies for this type of power plant are reviewed in section 2.2 with a general description. Some control systems of the power plant are discussed in section 2.3 and a mathematical model of the plant is presented in section 2.4.

2.2 Control Strategies for a PWR Power Plant

Let us begin this section with a brief description of a pressurized water nuclear power plant in order to follow the control strategies applied.

2.2.1 General Description

All PWR power plants (22,23) employ a dual system for transferring energy from the reactor fuel to the turbine as shown schematically in Fig. 2.2.1. The major subsystems are reactor core, primary water loop, pressurizer, steam generator, secondary water loop, throttle valves, turbine, by-pass valve, condenser and feedwater system.

Heat is produced in the reactor core by nuclear fission. Primary water flows downward around the core and then upward through the fuel elements. It is maintained at high pressure (about 2250 psi) and is heated to about 600°F without boiling. Primary water carries energy from the reactor to the steam generators through a pipe called the hot leg. PWR systems usually have two, three, or four reactor coolant

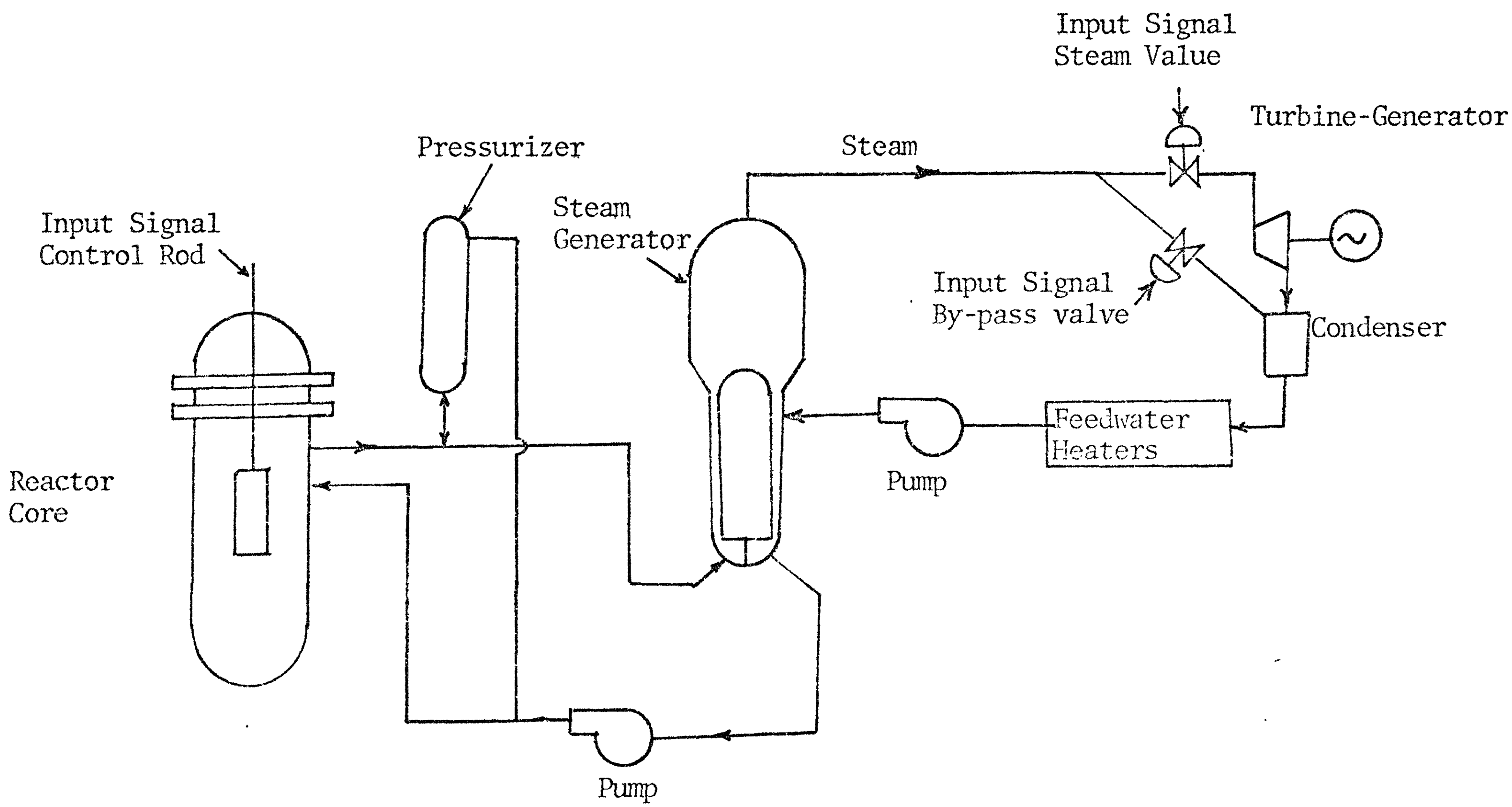

Fig. 2.2.1 Schematic Diagram of a PWR Power Plant.

loops (depending on the plant rating) with each loop having one steam generator. Reactor coolant loops and steam generators are, thus, operating in parallel. In each steam generator, the high-pressure primary water circulates through tubes whose outer surfaces are in contact with a stream of secondary water returning from the turbine condenser (this is called the feedwater). The feedwater is at considerably lower pressure and temperature than the primary coolant water and heat transferred from the hot primary water inside the tubes causes the feedwater to boil and produce steam. The steam generator tubes thus separate the reactor coolant from the secondary-side water. Reactor coolant is pumped within its closed loop from steam generator to reactor vessel via a pipe called the cold leg. Steam produced in the top of the steam generators passes through steam separators. The throttle valves admit steam to the turbine. The turbine produces shaft power from the expansion of the steam. From the turbine, the steam is admitted in the condenser and then to the condensate system and through the feedwater system to repeat the cycle. Alternatively, by-pass valves admit steam from the steam generator directly to the condenser by by-passing the turbine.

2.2.2 Steady State Control Programs

It has been mentioned in section 2.1 that the first specific control requirement is to coordinate the reactor control rods and the turbine throttle valves so as to avoid large deviations in plant variables In PWR power plants, this coordination is accomplished according to a well determined program (21,24). This program favors the tendency that primary loop variables must be kept within acceptable limits and favors the tendency that steam must be delivered to the turbine at acceptable pressures.

Why should primary loop variables be kept within acceptable limits and why should steam be delivered at acceptable pressures?

Let us first see the aspects of keeping primary loop variables within acceptable limits. This means

(1) to maintain the state variables of the nuclear reactor within limits by keeping the reactivity equal to zero at all times; and

(2) to maintain the volume changes in the pressurizer within limits.

For the control problems of interest here, the time constants are of the order of seconds. It follows that reactivity is affected only by the following three mechanisms.

(1) control rods;

(2) moderator temperature changes; note that the moderator is also the reactor coolant;

(3) fuel temperature changes; this is also known as Doppler effect.

Suppose that the average temperature of the reactor coolant changed. Then the reactivity in the core will vary due to both moderator and/or fuel temperature variations, and the control rods must be moved in order to keep a zero reactivity. In addition, the pressurizer must accomodate the volume changes of the reactor coolant. In this case, the control rods and the pressurizer increase the capital cost of the plant. Of course if the average temperature of the coolant were not changing, then this incremental capital investment would not have been required.

Now let us understand the other aspect of the problem which is to deliver steam at acceptable pressures.

Steam must be delivered to the turbine at a sufficiently high pressure to maintain turbine plant efficiency (25). Fig. 2.2.2 shows the variation of steam pressure as a function of steam temperature in the case of the saturated steam which is produced in steam generators of PWR power plants. It is clear from this figure that a change in steam temperature results in a sizable change in the steam pressure. Acceptable pressures are meant to hold steam temperature constant in order to avoid a large difference between the no-load steam pressure and the full-load steam pressure. In this way an optimum turbine performance is achieved in case of a constant steam temperature and pressure.

Therefore in combining the two aspects, the primary

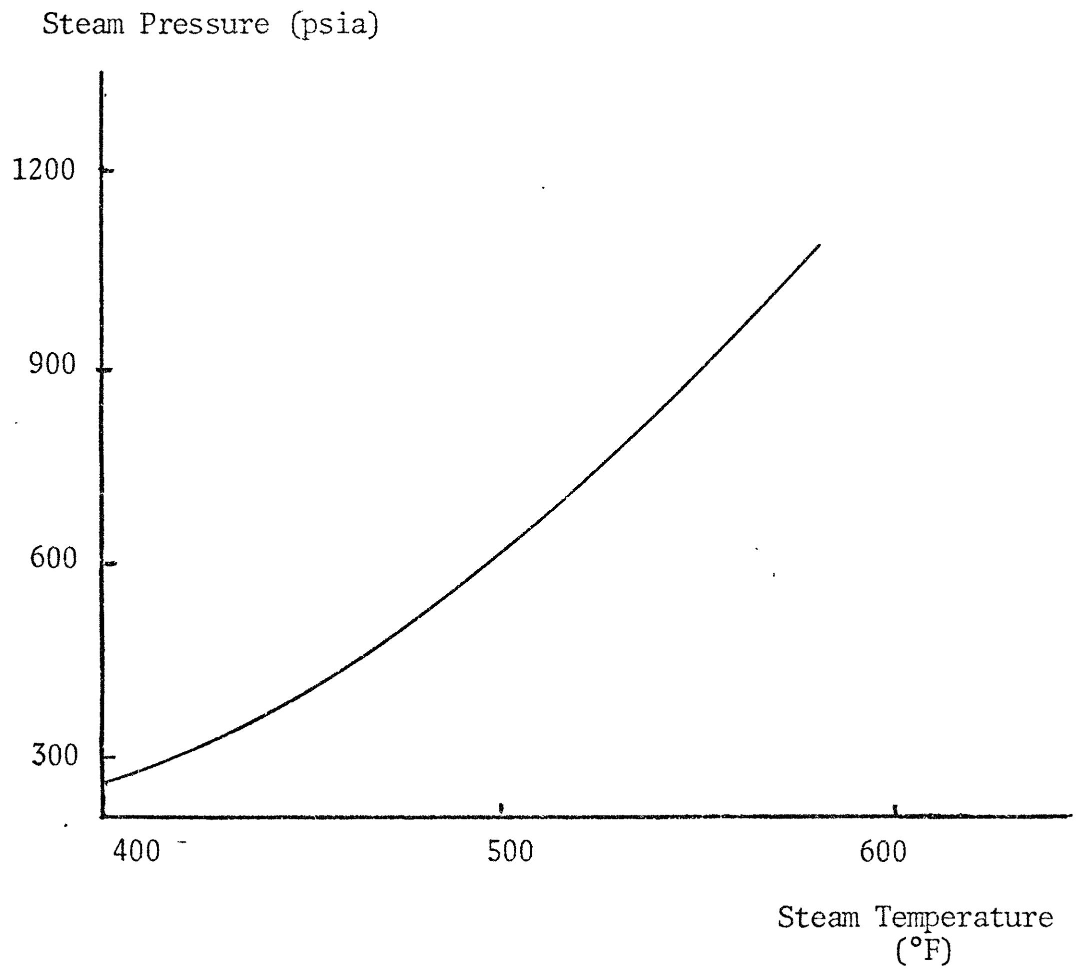

Fig. 2.2.2 Steam Pressure as a Function of Steam Temperature.

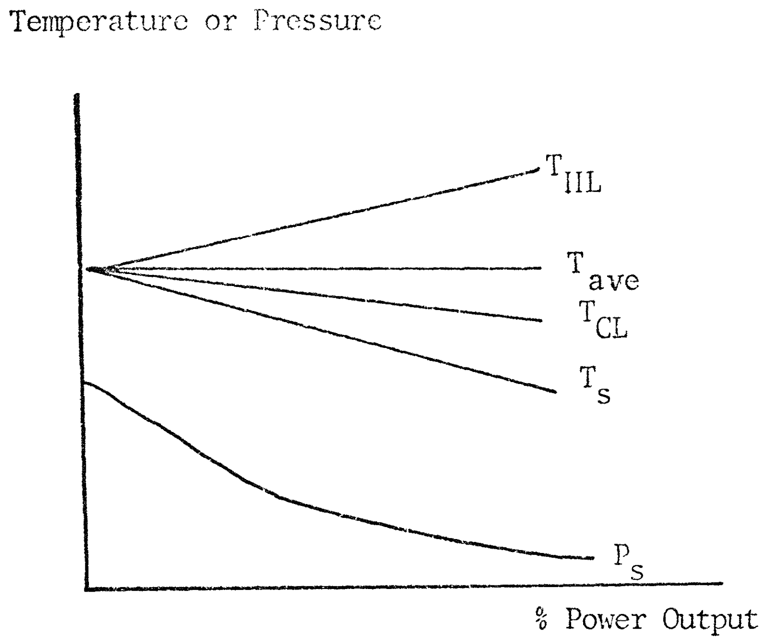

Fig. 2.2.3 Constant-Average Temperature Program.

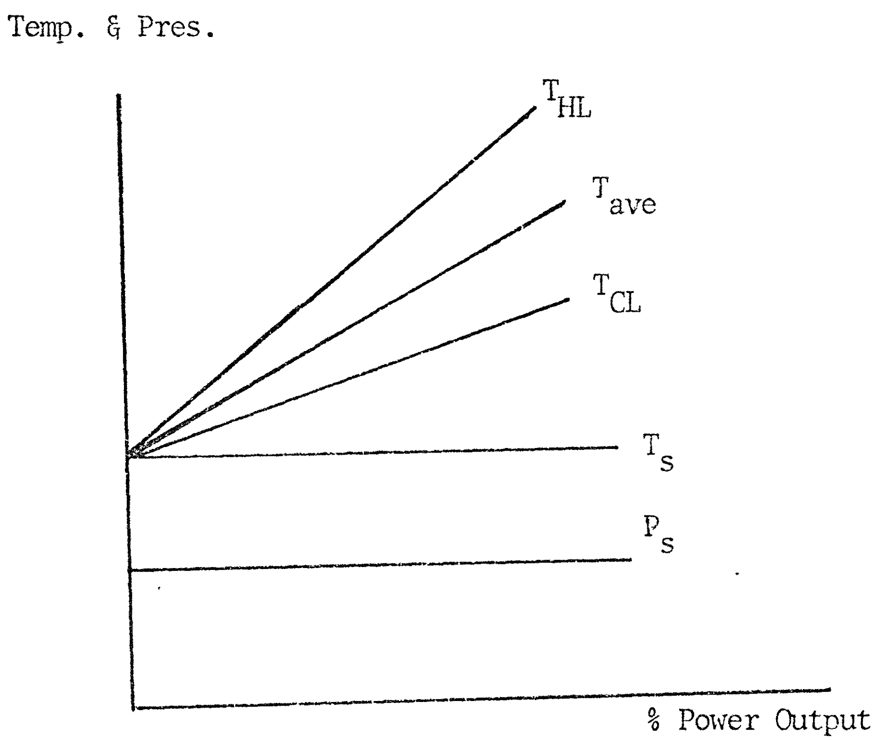

Fig. 2.2.4 Constant-Pressure Program.

loop prefers a constant coolant average temperature T_{ave} as shown in Fig. 2.2.3 and the secondary loop prefers a constant steam temperature as shown in Fig. 2.2.4. This is readily seen by writing the energy balance between the primary loop and the secondary loop (21).

$$P_{SG} = (h_{eff}A)_{SG} \, (T_{ave} - T_s) \qquad (2.2.1)$$

Where

P_{SG} = power delivered to the secondary fluid

h_{eff} = average effective primary-to-secondary heat transfer coefficient for the whole steam generator

A = heat transfer area in steam generator

T_{ave} = coolant average temperature

= $1/2\,(T_{HL}+T_{CL})$, where T_{HL} is hot leg temperature and T_{CL} is cold leg temperature

T_s = average steam temperature.

Eqn. (2.2.1) shows that the right-hand side must increase with increasing power demand. This indicates that T_{ave} and T_s cannot both remain constant with increasing load demand unless $(h_{eff}A)_{SG}$ increases.

In PWR power plants, there are two types of steam generators. The U-tube recirculation type steam generators used by Westinghouse (24) and the once-through steam generators used by Babcock & Wilcox (20). The former generate saturated steam and have a substantial energy storage; the latter generate superheated steam and have a higher thermodynamic efficiency but also a smaller energy reservoir (26). In this study a U-tube recirculation-type is considered and it is abbreviated as (UTSG).

For a UTSG, the term $(h_{eff}A)_{SG}$ does not change appreciably with load (21). Therefore the difference $(T_{ave}-T_S)$ must change with load. It is quite obvious that it is not possible to have a constant T_{ave} in the primary loop and a constant T_s in the secondary loop at all power levels.

A control strategy adopted in current PWR power plant practice (with UTSG) is a compromise with T_{ave} and T_s (and consequently P_s) used as set points both varying with load as shown in Fig. 2.2.5 . The relation between T_{ave} and P_s set points as functions of power levels is called a steady state program.

According to this program, when load increases, T_{ave} increases and because more energy is added to the reactor coolant, the control rods move out in order to offset the negative reactivity feedback due to the moderator and Doppler effects.

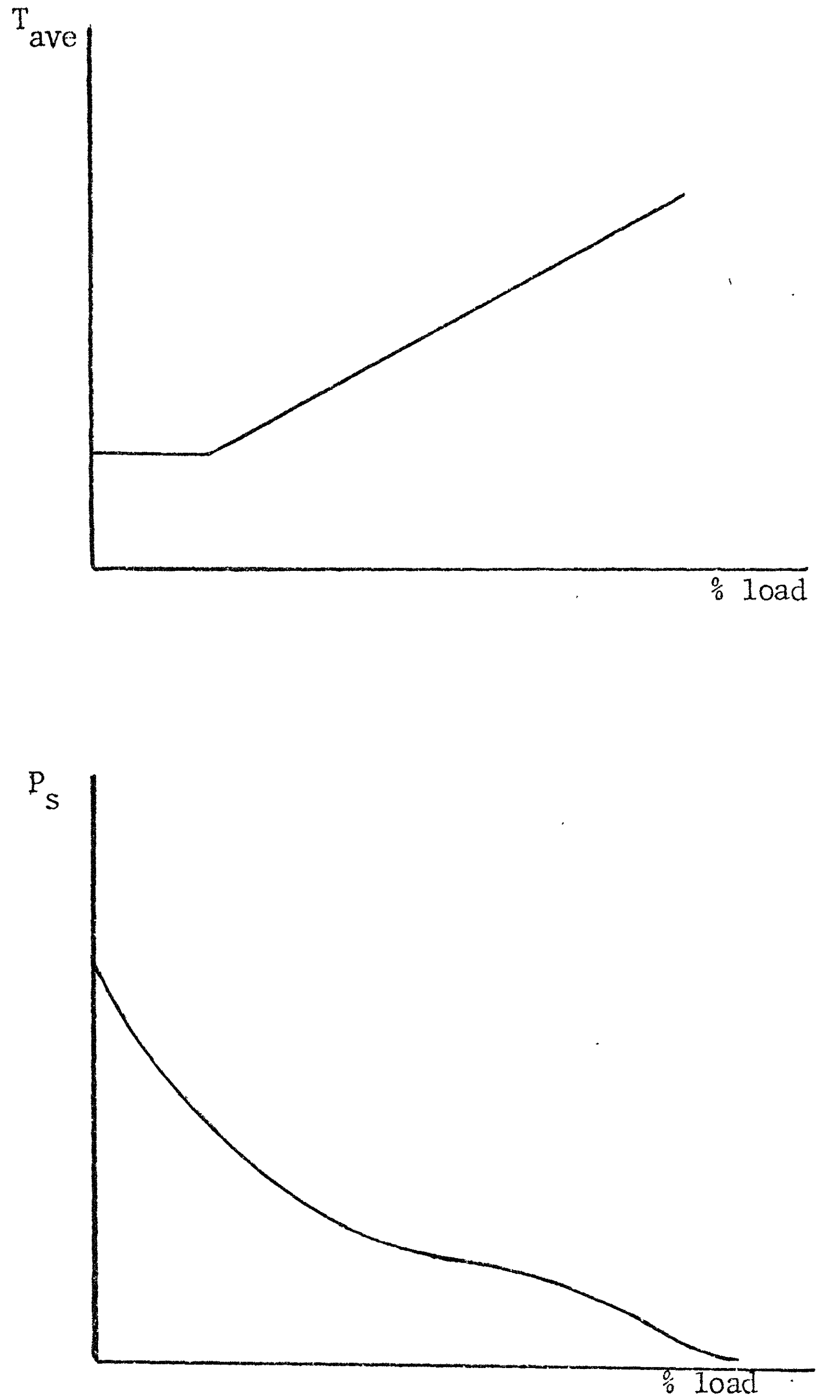

Fig. 2.2.5 Average-Temperature Program

2.3 PWR Power Plant Control Systems

In today's PWR power plants with a power exceeding 1200 MWe there is a multitude of variables to be observed. Present control methods applied conventionally assign single loop controllers to single variables and the coupling phenomena between them is handled individually. Kerlin (21) mentioned 10 measurable system variables of potential value as control signals and 7 potential system inputs for control actions. This makes 70 possible control loops. In current practice, the interaction between different control loops is supervised by a main control loop which can represent a specific control system in the power plant. For load changes control, we are mainly concerned with the following control systems:

(1) reactor control system

(2) steam by-pass control system

(3) steam generator control system

(4) pressurizer pressure and level control systems.

In this study, the feedwater flow to the steam generator is assumed to be controlled perfectly. This means that the steam flow rate is equal to the feedwater flow rate at all times. For this reason, the steam generator control system is not considered. Concerning the pressurizer, pressure changes have a feedback on the rest of the plant system through the pressure coefficient of reactivity, α_p.

This coefficient is very small and can be neglected. The water level in the pressurizer has no feedback on the rest of the plant system. Therefore the pressurizer and level control systems are both neglected.

The remaining control systems are seen as playing an important role if coordinated by avoiding large deviations in plant variables when the case is to meet large and fast load changes. The reactor control system and the steam bypass control system are described separately in the next two sections.

2.3.1 Reactor Control System

The main purpose of the reactor control system is to force the average reactor coolant temperature, T_{ave}, to follow as closely as possible the average temperature set point, $T_{ave\ set}$, determined by the steady state control program shown in Fig. 2.2.5. T_{ave} is measured by measuring hot leg T_{HL} and cold leg T_{CL} temperatures since $T_{ave} = 1/2 (T_{HL}+T_{CL})$. Temperatures are measured by using platinum resistance thermometer detectors (RTD) (24).

There are three inputs to the reactor control system as shown in Fig. 2.3.1:

(1) signal of the average temperature set point, $T_{ave\ set}$;

(2) signal of the average coolant temperature T_{ave} as measured via T_{HL} and T_{CL}; and,

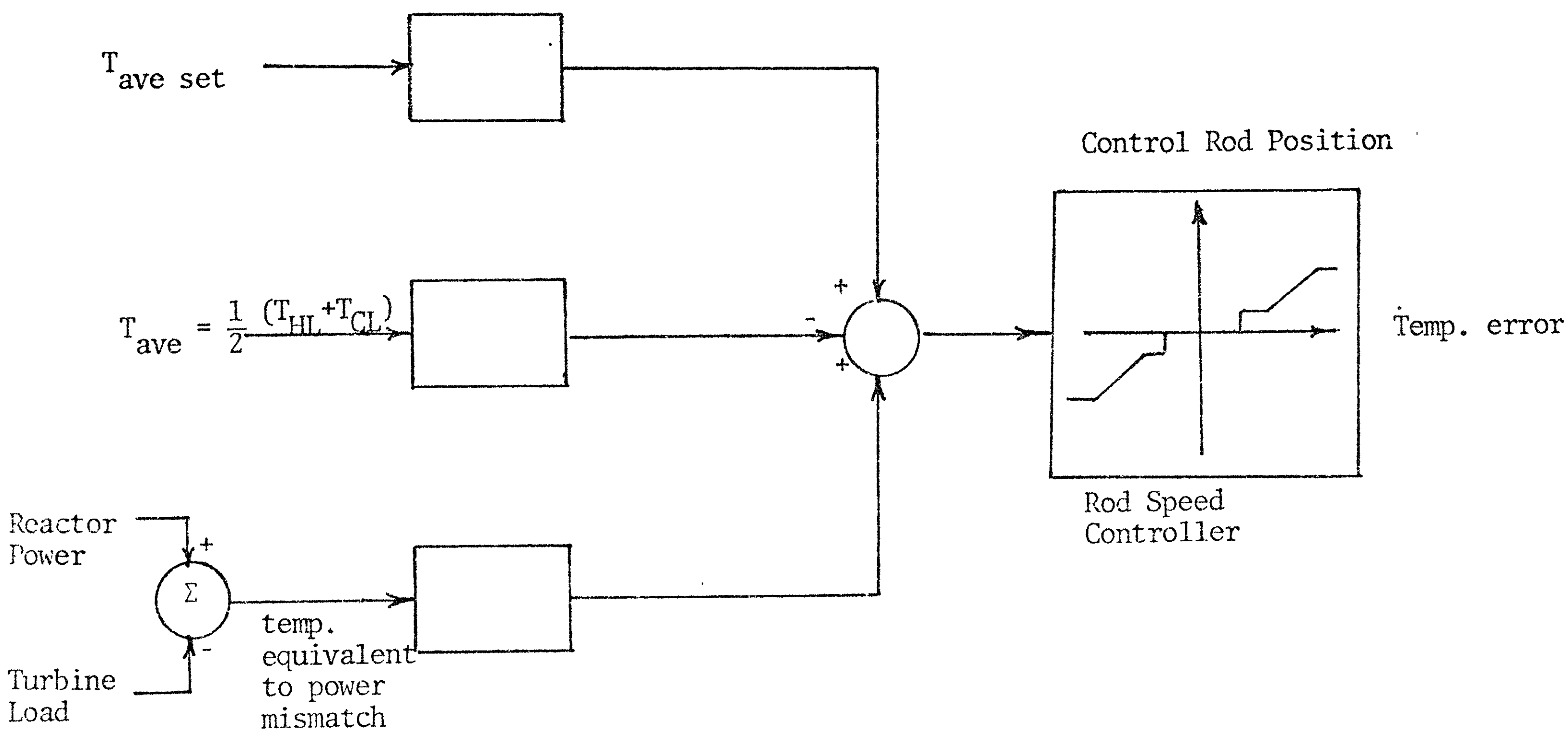

Fig. 2.3.1 Reactor Coolant Temperature Controller

(3) signal of a temperature equivalent of a power mismatch

A power mismatch occurs when reactor power is different than turbine load. When turbine load changes stepwise, the reactor power cannot change in a step manner to the new steady state power level but rather it is delayed due to the fact that control rods must be withdrawn to offset the Doppler and moderator reactivity effects for a period of time. But later in the transient the reactor power must exceed the turbine load in order to make up for the energy removed from the reactor coolant. The result is that there is an overshoot in the reactor power following a step increase in the turbine load as shown in Fig. 2.3.2 (25). The overshoot must be kept below a certain level in order to avoid a reactor trip according to design criteria. This is usually accomplished by moving the control rods at maximum speed at the beginning of the transient, thus reducing the overshoot. A signal of a power mismatch represented by a temperature is sent to the summation point of the rod speed controller via the third channel.

Note that in Fig. 2.3.1 signals of the power mismatch and $T_{ave\ set}$ are added positively while the signal of the measured T_{ave} is added negatively in order to make a temperature error signal. This error signal is sent to the rod speed controller. For positive error signal, the reactivity

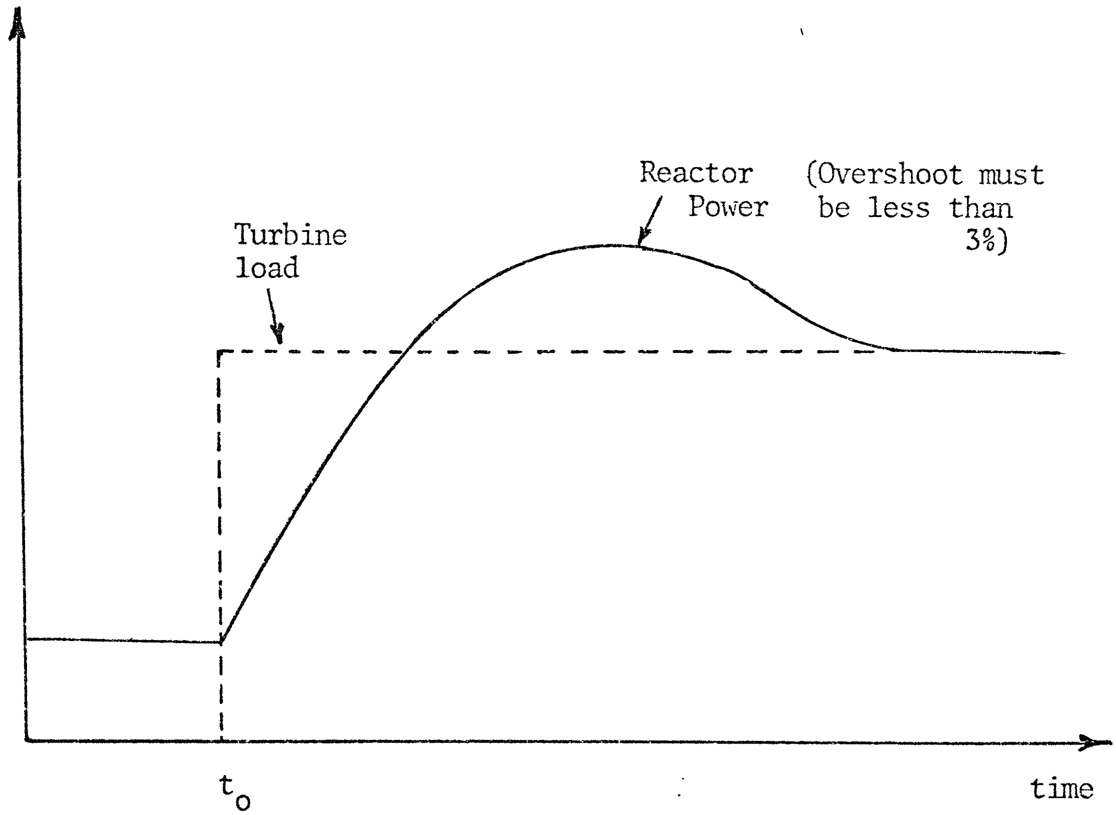

Fig. 2.3.2 Reactor Response Following a Stepwise Load Increase.

induced is positive and for negative error signal, the reactivity induced is negative which is consistent with the steady state program. The automatic rod control system is designed to maintain a programmed average temperature in the reactor coolant by varying reactivity within the core. This system is capable of restoring T_{ave} to within $\pm$ 3.5°F of $T_{ave\ set}$ including a + 2°F instrument error and a $\pm$ 1.5°F deadband following load changes (25).

2.3.2 Steam By-Pass Control System

The main purpose of the steam by-pass control system is to limit high reactor coolant average temperature excursions on turbine load reduction.

A typical steam by-pass valve system associated with steam dump system as shown in Fig. 2.3.3(a) would allow a 95% step load reduction (50% on some plants) without a reactor trip (25). This system is not actuated for load losses less than 15%. For a plant designed to take a 95% load rejection without a reactor trip, the total capacity of the steam dump system is 85%. Thus a 95% load reduction followed by steam dump appears to the steam generators, Reactor Coolant System (RCS), and nuclear reactor as a step decrease in load of approximately 10%. In addition a steam dump (25)

(1) permits to remove stored energy and residual heat following a reactor trip without actuation of the

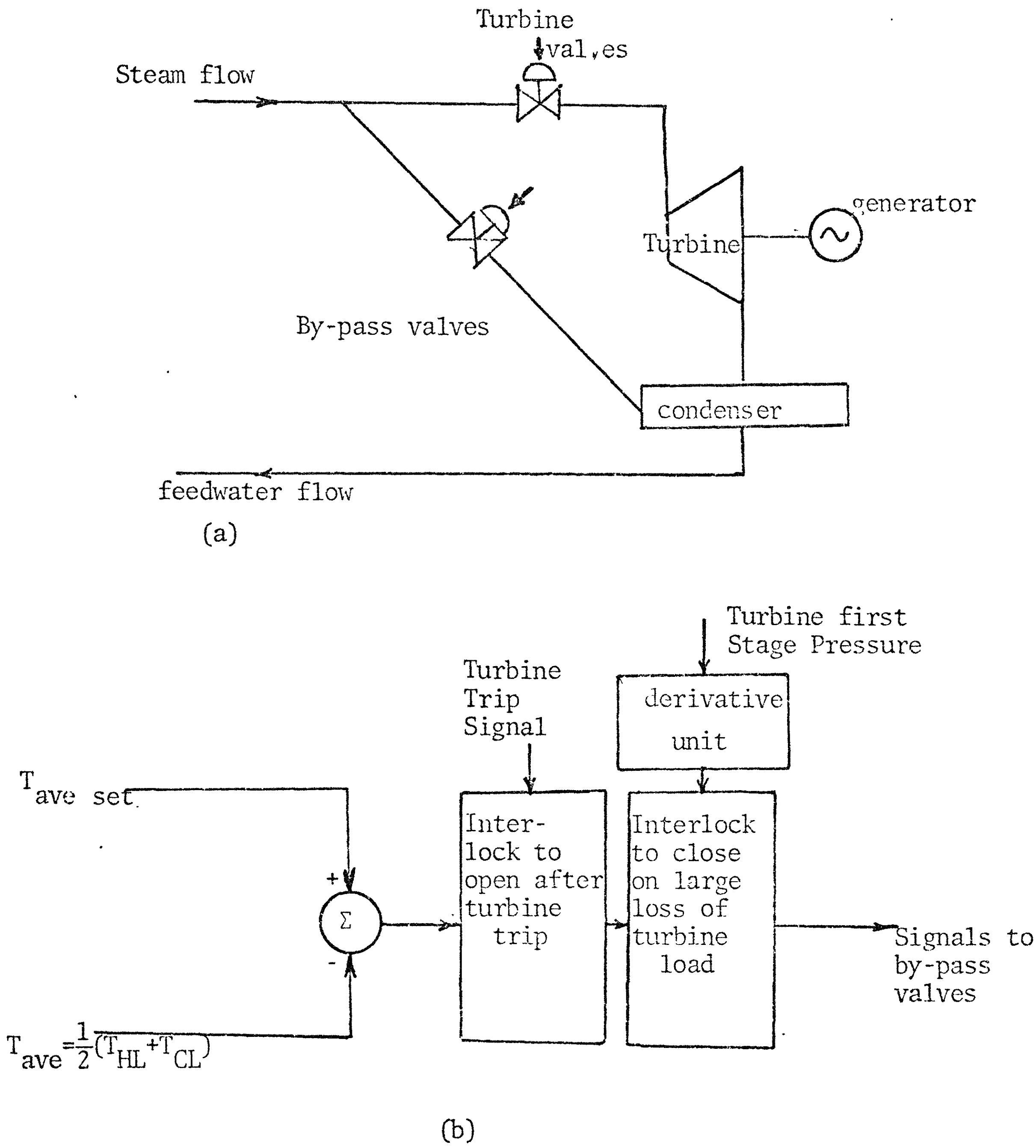

Fig. 2.3.3 (a) By-pass Valves System; (b) Functional Block-Diagram of Steam By-Pass Control System.

steam generator safety valves

(2) permits control of the steam generator pressure at no-load conditions and permits a manually controlled cooldown of the plant.

Similarly to the reactor control system, the steam dump control system is actuated through the reactor coolant average temperature control signals. Following a load reduction, both of the two control systems become operative upon coincidence of an abnormal increase in T_{ave} error signal and the signal derived from a large reduction in turbine load (function of turbine first stage pressure) as shown in Fig. 2.3.2(b). The by-pass valves open to the condenser and the rod control system is actuated to reduce reactor coolant average temperature to its new programmed set point.

2.4 System Model

A typical PWR power plant is represented by a mathematical model in order to:

(1) establish the control law for a full-state feedback;

(2) Predict maximum input disturbance which the system can tolerate without violating the state and control constraints; and

(3) Predict dynamic responses of potential system states and controls.

A mathematical model of a pressurized water nuclear power plant is presented in Appendix A. For the primary side this modeling follows the procedure presented in (21) and applied in (27,28,29) and, for the secondary side the modeling procedure adopted in (29,30). Other modeling procedures are found in (31,32,33).

The model presented in the appendix is linearized about operating values. It is of high order (a set of 31 linearized first order differential equations). In general, if the system model were of order n with r controls and m measurements (Eqns (2.1.1), (2.1.2) and (2.1.3)), the number of independent variables that we have to search over for the solution of the problem in this study will be equal to (1+nxr+(n-m)xm). A high order model will increase the computational time significantly; hence a low order system model is desirable but it must be accurate enough to predict the actual measurements fairly well.

Several methods of model reduction have been reported in the literature. Davison (43) described a computational approach of linear model reduction that eliminates the fast modes of the model. Another approach using an canomical form is described in (44). In (29), the authors investigated two methods of model reduction: the physical method and the pole-zero deletion method. The first method was applied to a 57th order PWR system model and resulted in a 25th order model. The low order model predicted the turbine mechanical shaft power equally as well as the high order model. But if other output variables of the system are of interest, some small differences exist between the two models. This is primarily due to the nonlinear reactor control system of the high order model. The second method was applied to a 23rd order model and resulted in a 9th order approximation. It was found that as more pole-zero pairs were deleted a point was reached where the reduced response no longer resembled the full order response.

Though the 31st order model presented in Appendix A is a reduced version of the 57th order PWR model given in (29), it is still of too high an order. For the purpose of this study, it is desirable to reduce the model to a lower order without losing its validity. In this section, the system model presented in Appendix A is reduced to a model of ten state variables. The response characteristics of the 10th order model will be investigated by simulation studies of their transient responses to the input disturbance in Chapter 6. The maximum amplitude of the input disturbance is determined by using the Set-Theoretic Control synthesis technique presented in Chapter 4 following the solution procedure presented in Chapter 5.

2.4.1 Reactor Core Model

The reactor core design used in this study is typical of of PWR's manufactured today. The essential design parameters are given in Table 2.4.1. The numerical values of the parameters listed in this table are taken from (29) and are typical of a Westinghouse PWR plant.

The theoretical model representing the reactor core is a linear time-invariant state-variable model that includes the neutron kinetics, the core heat transfer and the transport of the coolant in the piping connecting the core to the steam generators.

(1) Neutron Kinetics:

The major justification for using point kinetics in Appendix A is that the observer/controller does not need information about spatial flux transients to coordinate between the reactor control rods and the turbine valve when the objective is to meet the load demand. There are seven linearized point kinetic equations (Eqns. (A.3) and (A.4)},one for power and six for delayed neutron precursors.

Onega and Karcher (33) studied the sensitivity of the results to the number of delayed neutron precursors. For a step input reactivity of 30 cents, they compared the results of one precursor model to those of a six precursor model (27). They found that the final equilibrium power, average fuel temperature, and bulk coolant temperature were 2378.36 MWth, 1679.87 °F and 574.56 °F respectively,

Table 2.4.1

Essential Design Parameters

For the Reactor Core Model

* Kinetic Characteristics

Fuel Temperature Coefficient α_F (1/°F)	-1.1×10^{-5}
Moderator Temperature Coefficient α_c (1/°F)	-2.0×10^{-4}
Moderator Pressure Coefficient α_p (1/psi)	-1.0×10^{-6}
Neutron Generation Time Λ (sec)	17.9×10^{-6}
Total Delayed Neutron Group Fraction β^*	6.898×10^{-3}
Averaged Delayed Neutron Decay Constant λ(sec^{-1})	0.082246

Delayed Neutron Constants:

Group	Decay Constant (λ_i sec^{-1})	Fraction β_i^*
1st	0.0125	0.000209
2nd	0.0308	0.001414
3rd	0.1140	0.001309
4th	0.3070	0.002727
5th	1.1900	0.00925
6th	3.1900	0.000314

Table 2.4.1 (continued)

*<u>Core Thermal and Hydraulic Characteristics</u>	
Initial Power Level P_o (MWth)	3436.0
Mass of Fuel M_f (lbm)	222739.0
Specific Heat of the Fuel C_{Pf} (Btu/lbmF)	0.059
Total Heat Transfer Area A (ft^2)	59900.0
Fraction of the Total Produced in the Fuel f	0.974
Average Fuel Temperature (°F)	1600.0*
Overall Heat Transfer Coefficient from	
Fuel to Coolant, h_{eff} (Btu/hr ft^2F)	200.0
Volume of Coolant in Upper Plenum V_{UP} (ft^3)	1376.0
Volume of Coolant in Lower Plenum V_{LP} (ft^3)	1791.0
Volume of Coolant in Hot Leg Piping V_{HL} (ft^3)	250.0
Volume of Coolant in Cold Leg Piping V_{CL} (ft^3)	500.0
Total Volume of Coolant in Core V (ft^3)	540.0
Total Mass flow rate in core in (lbm/hr)	1.5×10^8
Hot Leg Temperature at 100 % Power T_{HL} (°F)	592.5
Cold Leg Temperature at 100 % Power T_{CL} (°F)	542.5
Nominal Reactor Coolant System Pressure P_{po} (psia)	2250.0
Coolant Density at System Pressure and	
Average Temperature ρ_c (lbm/ft^3)	45.71
Coolant Specific Heat at System Pressure	
and Average Temperature C_{PC} (Btu/lbm °F)	1.390

* This value has been calculated.

for the six precursor model, and 2379.14 MWth, 1683.4 °F, and 574.57 °F, respectively, for the one precursor model. These results indicate that one averaged precursor is adequate. The one precursor constants are given by:

$$\overset{*}{\beta} = \overset{*}{\beta} \text{ and } \lambda = \beta^{*} / \sum_{i=1}^{6} \overset{*}{\beta i}/\lambda i \qquad (2.4.1)$$

Thus the neutron kinetics model is reduced to two equations. One more equation can be eliminated by adopting the prompt jump approximation (35). Then Eqn. (A.3) becomes:

$$\frac{\delta P}{P_o} = \frac{\Lambda\lambda}{\beta^*} \delta C + \delta\rho \qquad (2.4.2)$$

and the neutron kinetics are governed by

$$\frac{d}{dt} \delta C = \frac{\beta^*}{\Lambda} \delta\rho \qquad (2.4.3)$$

As it can be seen from Eqn. (A.5) the reactivity $\delta\rho$ contains the different feedbacks.

(2) Core heat transfer model

This model involves the heat conduction in the fuel and the heat transfer in the coolant. The fuel temperature is introduced in the overall system model to account for the Doppler feedback. The coolant temperature is introduced in the overall system model to account for the moderator temperature feedback.

In PWR's, fuel rods are cylindrical. Generally, radial conduction dominates over axial or azimuthal conduction (21). In this context, it is common to divide the fuel into nodes as shown in Fig. 2.4.1. A heat balance, as given by Eqn. (A.7) may be performed for each node. The average time it takes the heat to be transferred from the fuel to the coolant includes the gas gap and the cladding. By defining the average fuel temperature as given by Eqn. (A.8) one can use the nodal approach to select one single node representing the average condition in the fuel, gap, clad assembly.

The heat transfer in the coolant is an axial convection which takes place in a channel when the coolant moves upward. Models for time domain analysis are usually based on a nodal approximation. Kerlin et al (27) formulated two core heat transfer models: a detailed one with 45 nodes (15 for fuel and 30 for coolant), and a simplified one with 3 nodes (1 for fuel and 2 for coolant). For a step insertion of 7.1¢ reactivity the results of the two models are in good agreement. Because of these results, the low order model shown schematically in Fig. 2.4.2 is used. Kerlin et al (27) state that this modeling approach (of two coolant nodes for each fuel node) provides better representation than the well-mixed or arithmetic average

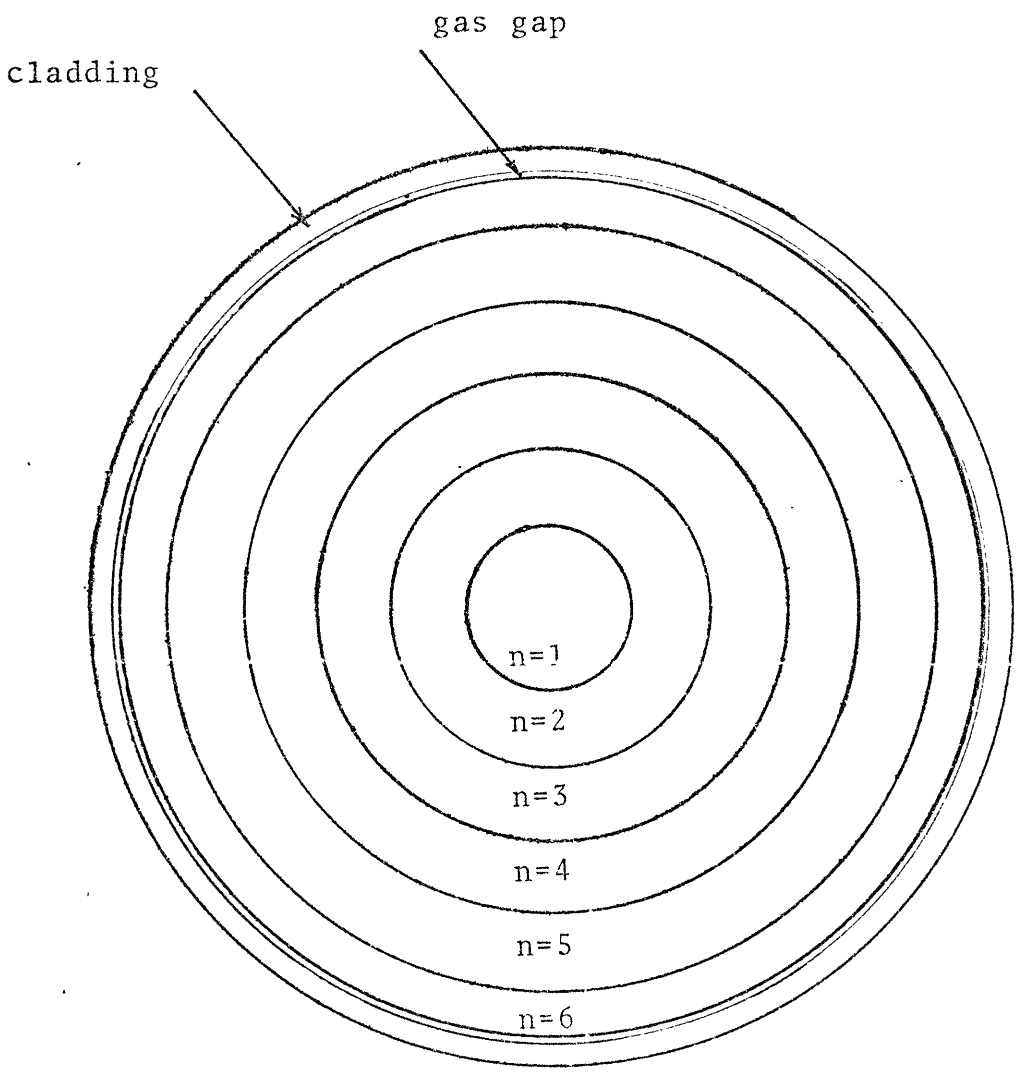

Fig. (2.4.1) A Nodal Model for Fuel Heat Transfer.

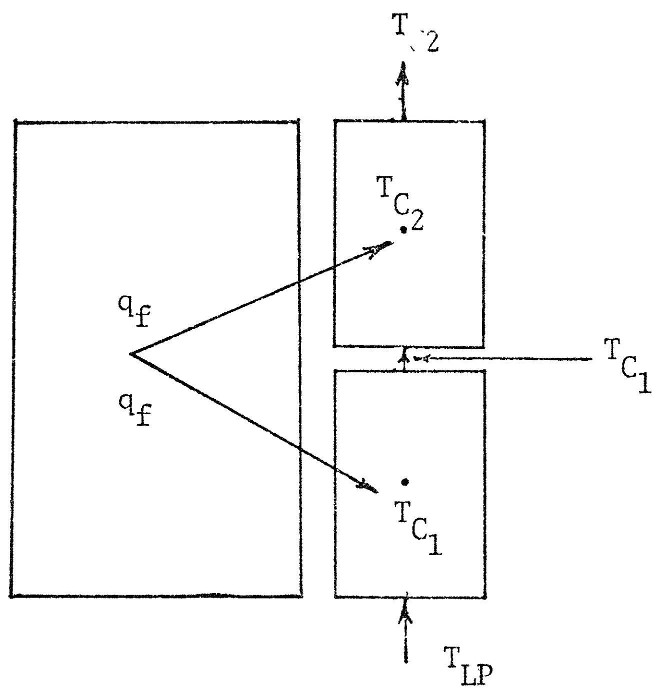

Fig. 2.4.2. Schematic of the Fuel-Coolant Heat Transfer Model.

average approximation (31). It gives a good approximation to the average coolant temperature T_{c1}. This temperature is taken as the temperature to determine the heat transfer rate. The outlet temperature is taken as the average of the second node, T_{c2}. Half of the heat rate is transferred to each fluid section. The governing equations of T_{c1} and T_{c2} are given by Eqns. (A.11) and (A.12).

The lumped parameter model of the core heat transfer is represented in this study by the three linearized equation (A.13), (A.14), and (A.15).

$$\frac{d}{dt}\,\delta T_f = \frac{fPo}{(mc_p)_f}\,\frac{\delta P}{Po} - \frac{A_f h_{eff}}{(mc_p)_f}\,[\delta T_f - \delta T_{c1}] \tag{2.4.4}$$

$$\frac{d}{dt}\,\delta T_{c1} = \frac{(1-f)Po}{(mc_p)_{c1}}\,\frac{\delta P}{Po} + \frac{A_f h_{eff}}{2(mc_p)_{c1}}\,[\delta T_f - \delta T_{c1}] - \left(\frac{\dot{m}}{m_{c1}}\right)[\delta T_{c1} - \delta T_{LP}] \tag{2.4.5}$$

$$\frac{d}{dt}\,\delta T_{c2} = \frac{(1-f)Po}{(mc_p)_{c2}}\,\frac{\delta P}{Po} + \frac{A_f h_{eff}}{2(mc_p)_{c2}}\,[\delta T_f - \delta T_{c1}] - \left(\frac{\dot{m}}{m_{c2}}\right)[\delta T_{c2} - \delta T_{c1}] \tag{2.4.6}$$

where $\frac{\delta P}{Po}$ is substituted by its equivalent given by Eqn. (2.4.2), and all terms are defined in Appendix A.

(3) Reactivity Feedback

The inherent feedbacks to the reactor used in this study are the Doppler feedback and the moderator temperature feedback. The primary pressure P_p of the reactor coolant system has some feedback on the rest of the system but the pressure coefficient of reactivity, α_p is small and so this feedback is neglected. The core reactivity $\delta\rho$ as given by Eqn. (A.5) is the sum of an externally inserted reactivity $\delta\rho_{ext}$, such as from control rod motion and the feedbacks.

$$\delta\rho = \delta\rho_{ext} + \frac{1}{\beta^*}[\alpha_f \ \delta T_f + \frac{1}{2}\ \alpha_c \ \delta T_{c1} + \frac{1}{2}\ \alpha_c \ \delta T_{c2}] \quad (2.4.7)$$

(the second term in the right hand side is divided by β^* because $\delta\rho_{f.b.}$ is expressed in units of β^*).

where,

α_f = fuel coefficient of reactivity (1/°F)

α_c = coolant coefficient of reactivity (1/°F)

Equation (2.4.7) is substituted into Eqns. (2.4.2) and (2.4.3). The governing equation of the precursor concentration is

$$\frac{d}{dt}\ \delta C = \frac{\alpha_f}{\Lambda}\ \delta T_f + \frac{1}{2}\ \frac{\alpha_c}{\Lambda}\ \delta T_{c1} + \frac{1}{2}\ \frac{\alpha_c}{\Lambda}\ \delta T_{c2} + \frac{\beta^*}{\Lambda}\ \delta\rho_{ext} \quad (2.4.3)$$

The fractional change in nuclear power, Eqn. (2.4.2) becomes

$$\frac{\delta P}{P_o} = \frac{\Lambda\lambda}{\beta^*}\,\delta C + \frac{\alpha_f}{\beta^*}\,\delta T_f + \frac{1}{2}\,\frac{\alpha_c}{\beta^*}\,\delta T_{C1} + \frac{1}{2}\,\frac{\alpha_c}{\beta^*}\,\delta T_{C2} + \delta\rho_{ext} \tag{2.4.2}$$

2.4.2 <u>Piping and Plenum Model</u>

Overall system model must include representations of the fluid transport in piping and plenums to account for the time lag which takes place. There is some heat transfer to the metal walls but it is usually ommitted (21). The flow in pipes results in axial mixing of the fluid. It is modeled somewhere between two extremes. One extreme, the slug flow model for temperature is given by $T_{out}(t) = T_{in}(t-\tau)$ where τ is the residence time. The other extreme is the well-mixed model which is given by:

$$\frac{d}{dt} T_{out} = \frac{1}{\tau}(T_{in}-T_{out})$$

The second model is convenient for time domain analysis using state variable models. The hot leg and cold leg pipes as well as the reactor and steam generator plenums are represented by Eqns. (A.16) to (A.21). Four equations out of six can be eliminated by combining the reactor upper plenum, hot leg, and steam generator inlet plenum volumes, V_{UP}, V_{HL}, V_{IP} respectively into one volume.

By this way the hot leg temperature is represented by a single time constant

$$\tau_{HL} = \frac{\rho_{ave}}{\dot{m}} \left[\frac{V_{UP}}{NUTSG} + V_{HL} + V_{IP}\right] \qquad (2.4.8)$$

where

ρ_{ave} = average coolant density

$\dot{m}$ = coolant flow rate

NUTSG = number of steam generators

The same assumption can be made on the steam generator outlet plenum V_{OP}, cold leg V_{CL}, and reactor lower plenum V_{LP}. The cold leg time constant is

$$\tau_{CL} = \frac{\rho_{ave}}{\dot{m}} \left[V_{OP} + V_{CL} + \frac{V_{LP}}{NUTSG}\right] \qquad (2.4.9)$$

The governing equations of T_{HL} and T_{CL} become

$$\frac{d}{dt}\,\delta T_{HL} = \frac{1}{\tau_{HL}}(\delta T_{c2} - \delta T_{HL}) \qquad (2.4.10)$$

$$\frac{d}{dt}\,\delta T_{CL} = \frac{1}{\tau_{CL}}(\delta T_{p} - \delta T_{CL}) \qquad (2.4.11)$$

2.4.3 Pressurizer Model

The reactor coolant is connected to the pressurizer by a surge line from the hot leg piping to the bottom of the pressurizer tank, as shown in Fig. (2.4.3). The change in reactor coolant average temperature with load

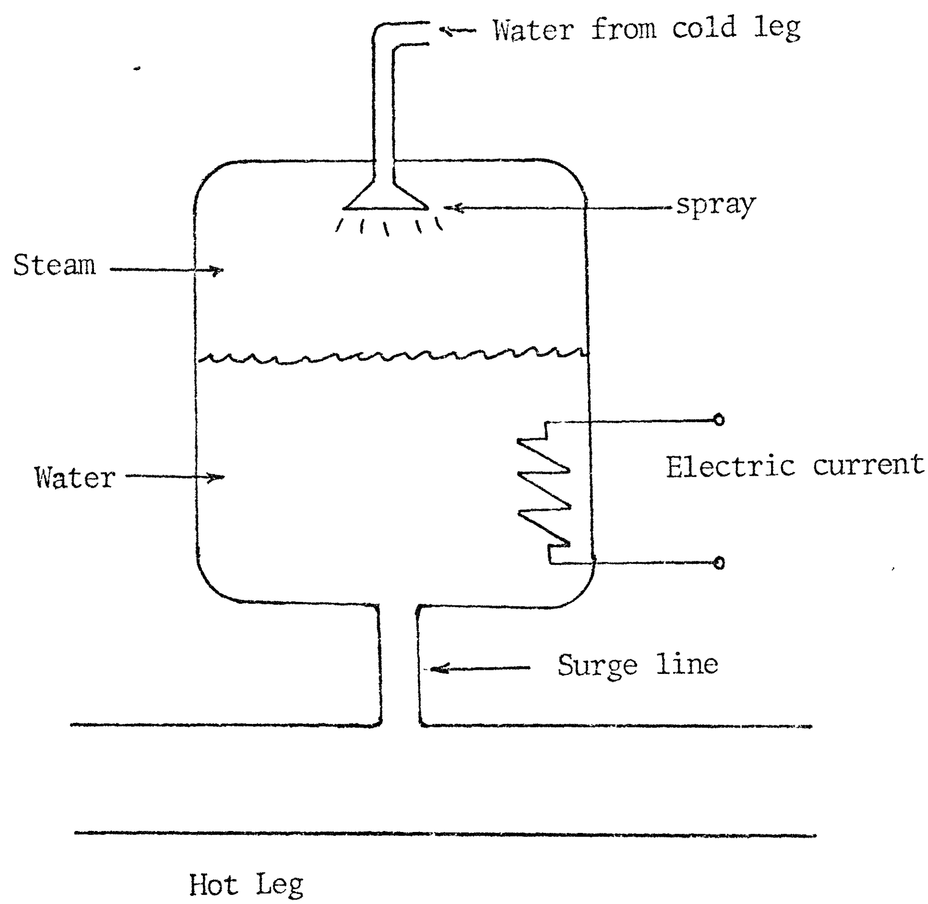

Fig. (2.4.3) Pressurizer Model Schematic Diagram.

results in a change in reactor coolant density with load. Density changes will cause a change in the pressurizer water level. The main function of the pressurizer is to provide a surge chamber and a water reserve to accomodate changes in the reactor coolant density and consequently volume. This is accomplished by maintaining water and steam in the pressurizer at the saturation temperature corresponding to the system pressure. As the pressure decreases below the desired value of 2250 psia the heaters are energized. This heats the water in the pressurizer and boils water to return the pressure to the nominal value. When the pressure increases above 2250 psia spray is used to condense steam and return the pressure to 2250 psia. Details about the function of the pressurizer are found in (21,25,29,38,39,40). The governing equation of the pressurizer pressure is given by Eqn. (A.22).

The only feedback this model has on the rest of the system is through the pressure coefficient of reactivity α_ρ. Because this coefficient is so small (on the order of 10^{-6}/psia) this model can be eliminated by assuming that α_ρ is equal to zero. Eqn. (A.22) will not be included in the system model.

2.4.4 The Steam Generator Model

The steam generator considered in this study is a vertical, U-Tube recirculation type steam generator (UTSG).

Fig. 2.4.4 shows a steam generator schematic diagram. The steam generator is essentially a boiler where the energy transferred from the reactor coolant flowing on the primary side (with the UTSG) boils water on the secondary side to generate the steam to drive the turbine. The steam passes through moisture separators and dryers before leaving the UTSG with a quality of approximately 99.75%. The essential data for generating a typical UTSG model are given in Table 2.4.2 (29).

The lumped parameter model of the UTSG consists of a primary coolant lump, a heat conducting metal lump, and a secondary coolant lump. The governing equations in linearized form are (A.23), (A.24) and (A.25). This model does not describe the downcomer water level. For applications where the primary concern of the overall system model is to deal with load demand, the downcomer level will not need to be described (29). The model as described by Appendix A with the three linearized equations is retained without reduction. These equations are:

$$\frac{d}{dt}\,\delta T_p = \left(\frac{\dot{m}}{m}\right)_p (\delta T_{IP} - \delta T_p) - \frac{(h_{eff}A)_{pm}}{(mc_p)_p} (\delta T_p - \delta T_m) \tag{2.4.12}$$

$$\frac{d}{dt}\,\delta T_m = \frac{(h_{eff}A)_{pm}}{(mc_p)_m} (\delta T_p - \delta T_m) - \frac{(h_{eff}A)_{ms}}{(mc_p)_m} \left(\delta T_m - \frac{\partial T_{sat}}{\delta P_s} \delta P_s\right) \tag{2.4.13}$$

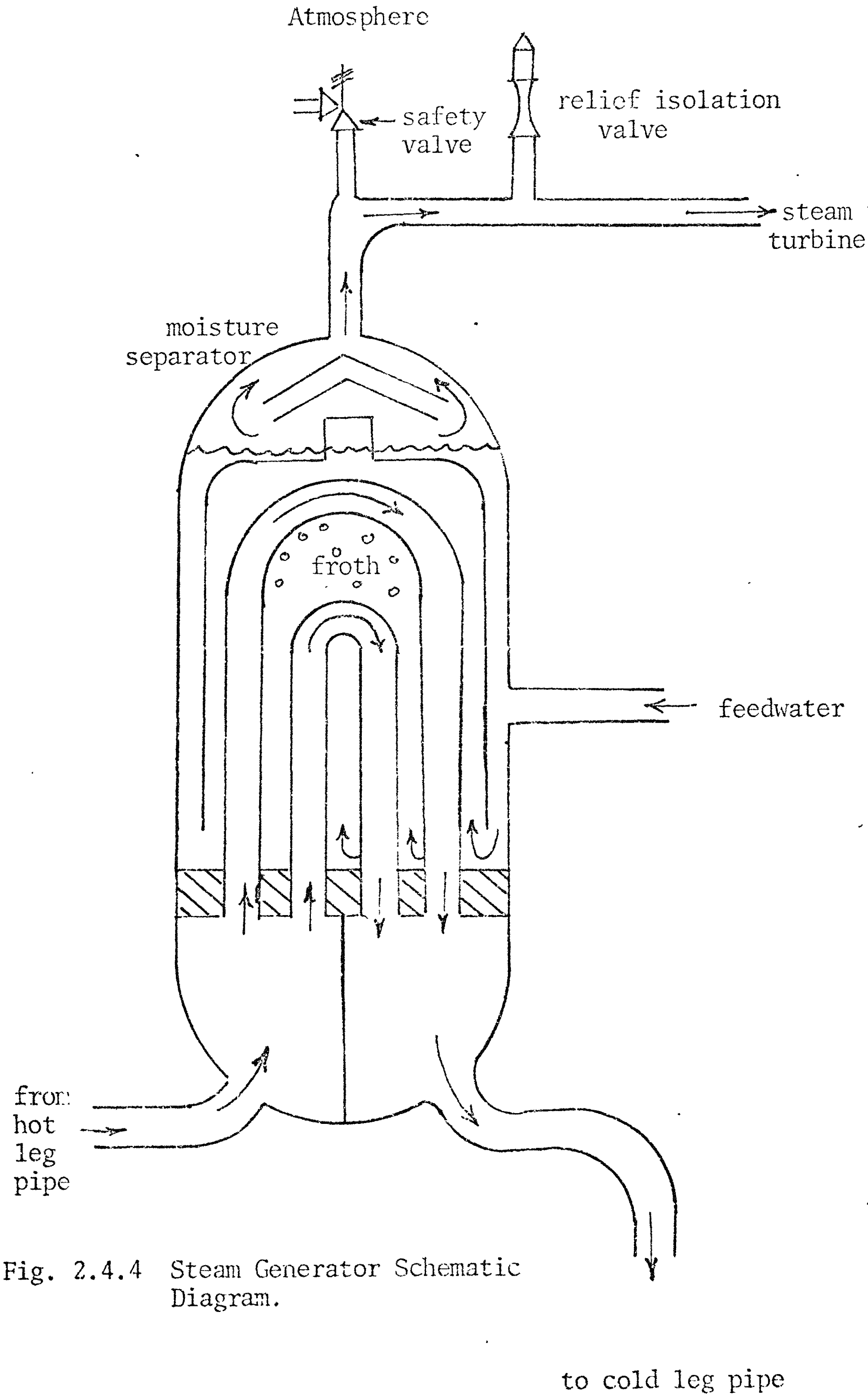

Fig. 2.4.4 Steam Generator Schematic Diagram.

Table 2.4.2

Essential Data for Generating

a Typical UTSG Model

Number of UTSG/plant, NUTSG	4
Primary water mass flow rate, $\dot{m}_p$ (lbm/hr)	3.939×10^7
Specific heat of primary water, C_{pp} (Btu/lbm°F)	1.390
Primary water inlet temperature, T_{pi} (°F)	592.5
Primary water outlet temperature, T_{po} (°F)	542.5
Average density of primary water, ρ_p (lbm/ft^3)	45.710
Primary loop average pressure, P_p (psia)	2250
Steam flow rate, W_s (lbm/hr)	3.731×10^6
Steam pressure, P_s (psig)	832.0
Saturation temperature at steam pressure Tsat (°F)	521.9
Feedwater inlet temperature, T_{FW} (°F)	434.3
Subcooled secondary water average density ρ_s (lbm/ft^3)	52.32
Subcooled secondary water specific heat, C_{PS} (Btu/lbm°F)	1.165
Overall heat transfer coefficient from primary fluid to metal, $(h_{eff})_{pm}$ (Btu/hr ft^2°F)	4150.75
Heat transfer area of primary fluid to metal A_{pm} (ft^2)	45614.3
Overall heat transfer coefficient from metal to secondary fluid, $(h_{eff})_{ms}$ (Btu/hr ft^2°F)	5361.07

Heat transfer area from metal to secondary, A_{ms} (ft^2)	51500.0
Mass of metal tube, m_m (lbm)	8948
Mass of water inside tubes, m_p, (lbm)	4.03974×10^5
Metal heat capacity, C_{pm} (Btu/lbm°F)	0.11
Enthalpy of saturated steam h_s(=hg) (Btu/lbm)	1198.3
Specific volume of saturated steam, V_g (ft^3/lbm)	0.5457
$\partial T_{sat}/\partial P_s$	0.14
$\partial hg/\partial P_s$	-0.35
hot leg piping time constant, τ_{HL}(S)	3.19
col leg piping time constant, τ_{CL} (S)	4.67

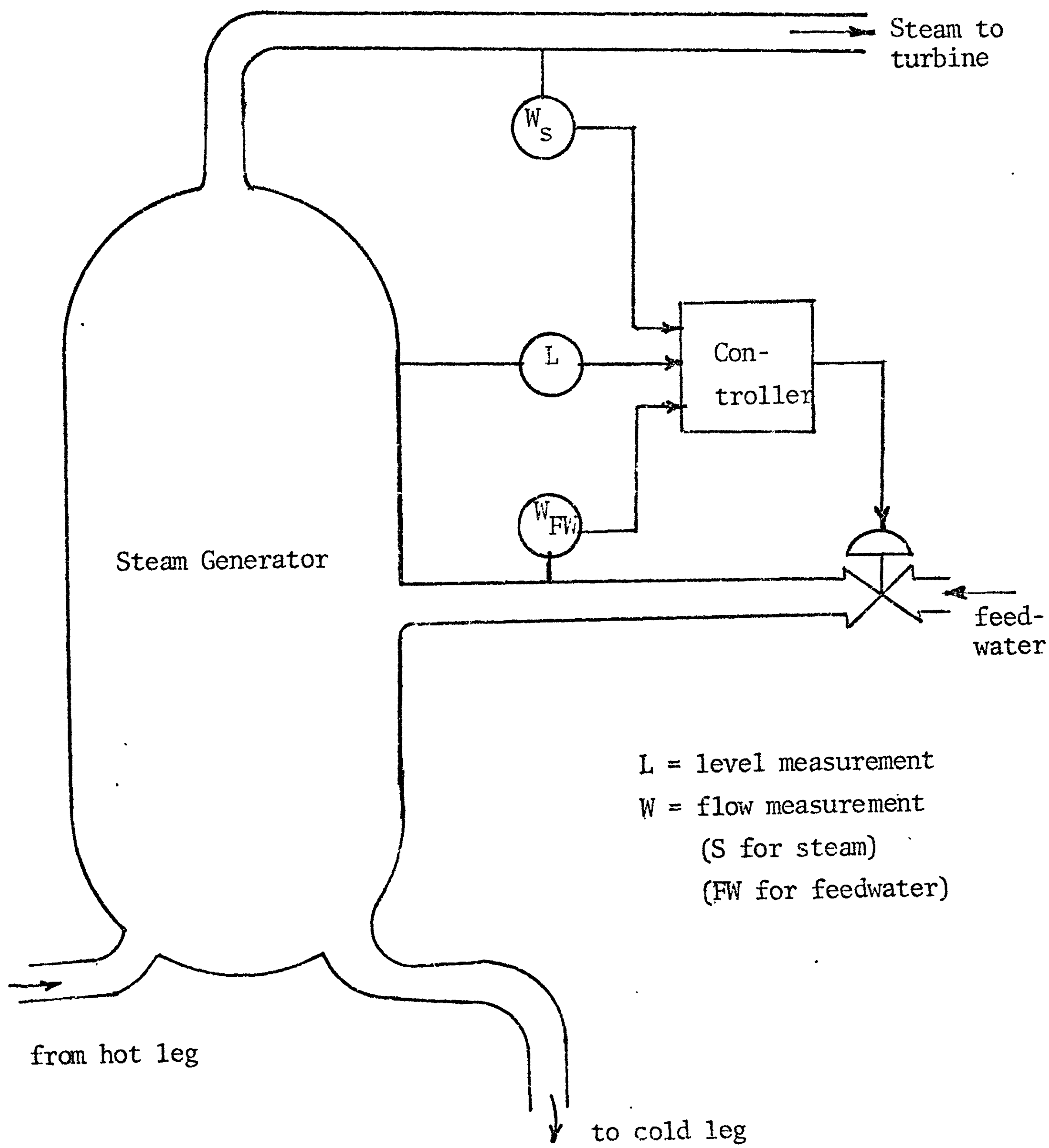

Fig. 2.4.5 Three Element Controller Schematic.

$$\frac{d}{dt}\,\delta P_s = \frac{1}{K}\,\{(h_{eff}A)_{ms}\,\delta T_m - [(h_{eff}A)_{ms}\,\frac{\partial T_{sat}}{\partial P_s} + W_s\,\frac{\partial h_s}{\partial P_s} + \varepsilon_o\,(h_s - h_{FW})]\,\delta P_s + W_s\,C_{p_s}\,\delta T_{FW} - W_s\,(h_s - h_{FW})\,\frac{\delta\varepsilon}{\varepsilon_o}\} \qquad (2.4.14)$$

The steam generator is equipped with a three element feedwater controller as shown in Fig. 2.4.5, which maintains a programmed water level on the secondary side. Details about the steam generator water-level control are given in reference (41). The dynamics of this device may involve six equations (29). But in this study the feedwater flow is assumed to be controlled perfectly and hence the dynamics of the three-element controller are eliminated from the overall system model.

2.4.5 The Turbine and Feedwater Heaters Model

This model is shown schematically in Fig. 2.4.6. The parameters needed to calculate the coefficients are given in Table 2.4.3. It was originally developed by (34) and derived with modifications in (29, 30). The model involves mechanical and heat transfer processes which take place in the secondary side. It is described in Appendix A by an 11th order state variable representation. In this section it is reduced to a 5th order representation.

Eqn. (A.31) which gives the state variable h_c

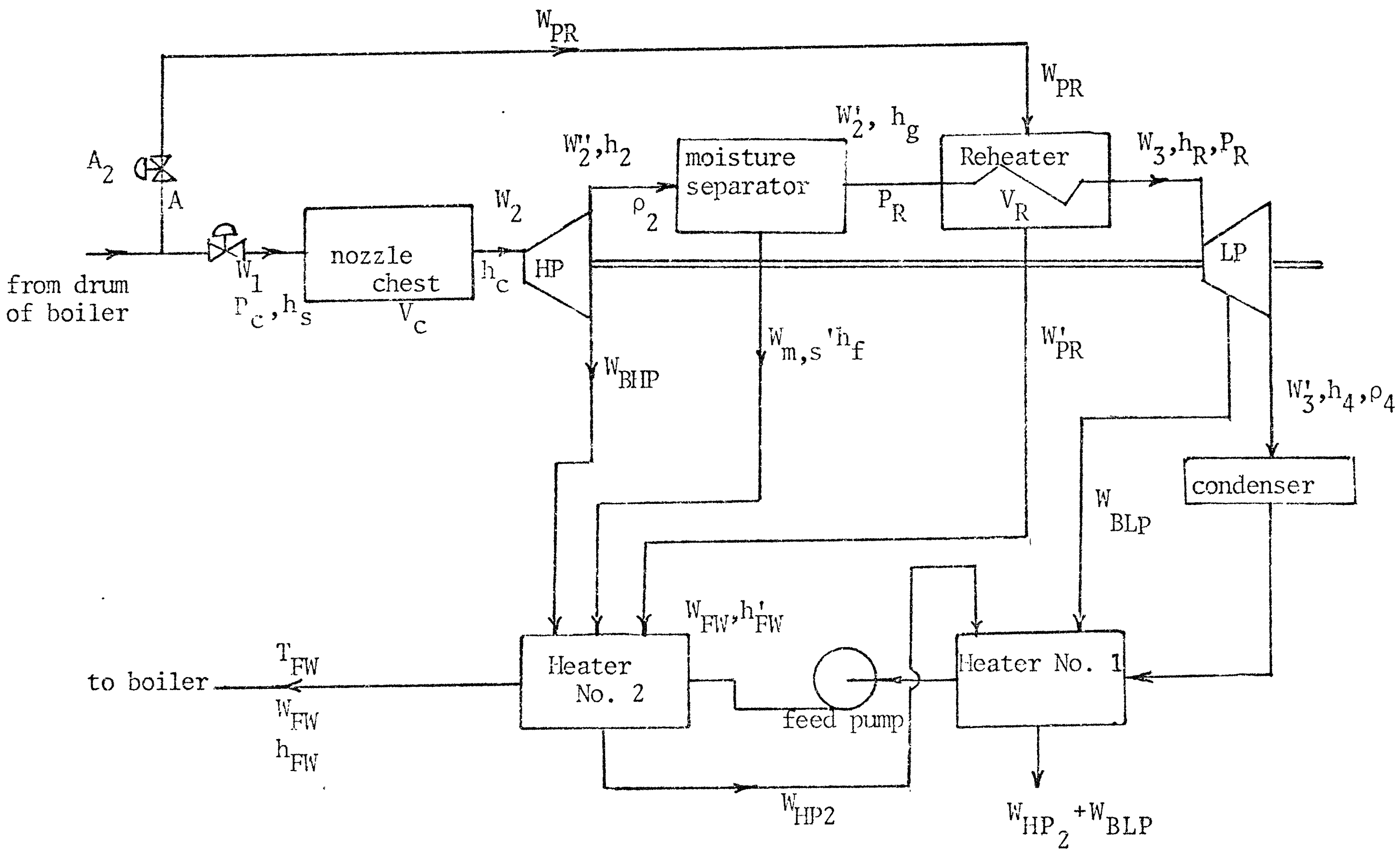

Fig. 2.4.6 Schematic Diagram of the Turbine Feedwater Heaters Model.

Table 2.4.3

Essential Data for the Turbine

Feedwater Heaters Model

Flow rate of steam in and out of the nozzle chest, W_1, W_2 (lbm/sec)	3959.5
Flow rate of steam in and out of the reheater shell side, W_2, W_3 (lbm/sec)	2852.8
Flow rate of steam in and out of the reheater tube side W_{PR}, $\dot{W}_{PR}$ (lbm/sec)	182.36
The flow rate of the drain from the moisture separator W_{MS}, (lbm/sec)	385.03
The flow rate of the main steam and feedwater at initial conditions from all UTSG's, W_s, W_{FW} (lbm/sec)	4145.9
Flow of steam leaving HP turbine to the mositure separator, W_2'' (lbm/sec)	3210.86
Flow of steam leaving the LP turbine to the condenser W_3' (lbm/sec)	2232.6
Flow of fluid from feedwater heater 2 to feedwater heater 1, W_{HP2} (lbm/sec)	1217.8
Fraction of steam entering the HP turbine that is extracted to feedwater heater 2, K_{BHP}	0.1634
Fraction of steam entering the LP turbine that is extracted to feedwater heater 1, $K_{B_{PL}}$	0.2174

Table(2.4.3) continued

Time constant for feedwater heater 1 heat transfer τ_H, (sec)	100.0
Time constant for feedwater heater 2 heat transfer, τ_{H2}, (sec)	40.0
Time constant for feedwater heater 2 shell side, τ_{HP2} (sec)	10.0
Time constant for flow in LP turbine, τ_{R2} (sec)	4.0
Time constant for flow in reheater τ_{W2} (sec)	2.0
Enthalpy of steam leaving reheater h_R(B/lbm)	1270.8
Enthalpy of steam leaving HP turbine to moisture separator h_2 (B/lbm)	1100.3
Enthalpy of steam entering and leaving the nozzle chest h_s, h_c (B/lbm)	1196.1
Enthalpy of saturated water in the moisture separater, h_f (B/lbm)	338.75
Latent heat of vaporization in the moisture separater, h_{fg} (B/lbm)	857.7
Density of steam leaving HP turbine to the moisture separator, ρ_2 (lbm/ft^3)	1.8281
Density of steam leaving the nozzle chest, ρ_c (lbm/ft^3)	2.1263
Density of steam leaving the reheater, ρ_R (lbm/ft^3)	0.3566
Pressure of the steam leaving the nozzle chest, P_c (psig)	756.363

(Table 2.4.3) continued

Specific heat of the feedwater, C_{PFW} (B/lbm-°F)	1.14
Volume of the reheater shell side, V_R (ft^3)	20000.0
Volume of the nozzle chest, V_c (ft^3)	200.0
Assumed constant enthalpy of shell side in heater 2, H_{FW} (B/lbm)	475.0
Assumed specific heat of steam in reheater, H_R (MW)	21.6
Initial heat transfer in reheater, Q_R (MW)	226.43
Valve coefficient of bypass steam, ε_2 (lbm/sec-psi)	0.21918
Valve coefficient of main steam, ε (lbm/sec-psi)	1.2458
Area used in empirical relationship for steam flow out of the nozzle chest, A_{k2} (ft^2)	207.82
Area used in empirical relationship for steam flow out of the reheater shell side, K_3 (ft^2)	798.7
Constant used in Callender's relationship, K_1	7.415
Constant used in Callender's relationship, k_2	149670.0
Constant used in ideal gas law, R (ft-lbf/lbm-°R)	85.78

represents an energy balance done on the nozzle chest. Fig. 2.4.7 (30) shows the enthalpy versus the entropy for the turbine and reheater part only. It is clear that the enthalpy does not change appreciably across the nozzle chest and therefore h_c may be assumed to be equal to the inlet enthalpy h_s. The quality of the steam generated in the boiler is around 99.75%. We assume that the quality of the steam entering the nozzle chest is approximately 1.0, therefore

$$\delta h_s = \frac{\partial hg}{\partial P_s} \delta P_s \qquad (2.4.15)$$

where $\frac{\partial hg}{\partial P_s}$ is the gradient of steam enthalpy to steam pressure in the main steam line. This quantity can be easily evaluated from the steam tables.

The differential equation (A.31) can be eliminated and the state variables δh_c is substituted in the state-variable representation by Eqn. (2.4.15).

The other approximation is that all the equations which involve a simple time constant are eliminated by assuming that the fluid enters the system and leaves it almost instantaneously. The time constants are assumed very small and can be neglected. The equations under this case are (A.40), (A.45), (A.49) and (A.52).

The sixth equation to be eliminated is that of the

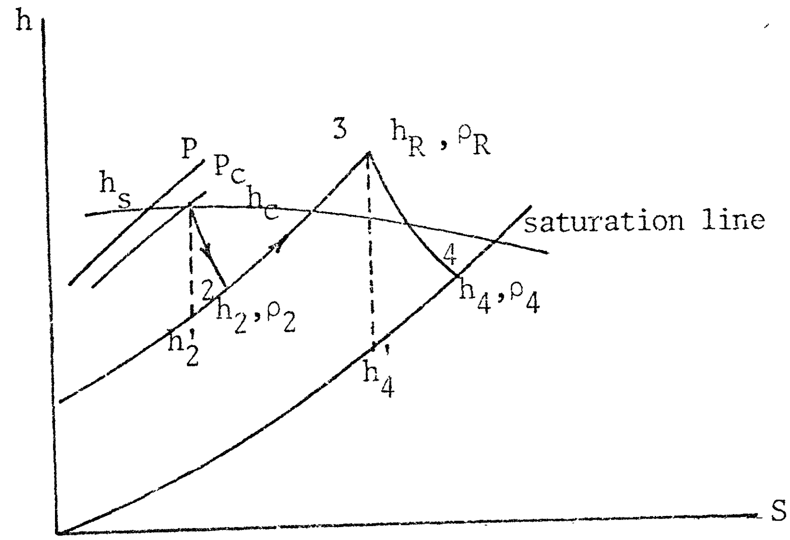

Fig. 2.4.7 Rankine Cycle: turbine and Reheater Part Only.

state variable h'_{FW} which is the enthalpy of the feedwater leaving heater 1 and entering heater 2. This is done by combining the two heaters into one control volume as shown in Fig. 2.4.8. The resulting governing equation of the feedwater temperature is given by

$$\frac{d}{dt}\,\delta T_{FW} = \frac{1}{C_{p_2}\tau_H}\Big[\frac{H_{FW}}{W_{FW}}\,(2K_{BHP}\delta W_2 + 2\delta W_{ms} + 2\delta W'_{PR} + K_{BLP}\delta W_3)$$

$$- \frac{H_{FW}}{W^2_{FW}}\,(2K_{BHP}W_2 + 2W_{ms} + 2W'_{PR} + K_{BLP}W_3)\,\delta W_{FW}\Big]$$

$$- \frac{1}{\tau_H}\,\delta T_{FW} - \frac{h_{FW}}{C_{p_2}W_{FW}}\,\frac{d}{dt}\,\delta W_{FW} \qquad (2.4.16)$$

where $\tau_H = \tau_{H1} + \tau_{H2}$.

The rest of the equations representing the turbine and feedwater heaters are (A.30),(A.41),(A.42) and (A.48) namely

$$\frac{d}{dt}\,\delta\rho_c = \frac{1}{V_c}[\delta W_1 - \delta W_2] \qquad (2.4.17)$$

where δW_1 and δW_2 are substituted by (A.32) and (A.33)

$$\frac{d}{dt}\,\delta\rho_R = \frac{1}{V_R}[\delta W'_2 - \delta W_3] \qquad (2.4.18)$$

where $\delta W'_2$ and δW_3 are substituted by (A.43) and (A.44).

$$\frac{d}{dt}\,\frac{\delta h_R}{h_{Ro}} = \eta_5\delta W'_2 + \eta_6\delta h_g + \eta_7\delta W_3 + \eta_8\,\frac{\delta h_R}{h_{Ro}} + \eta_9\delta Q_R \qquad (2.4.19)$$

$$\frac{d}{dt}\,\delta Q_R = \frac{1}{\tau_{R2}}\Big[\frac{1}{2}H_R(T_s - T_R)(\delta W_{PR} + \delta W'_{PR})$$

$$+ \frac{1}{2}\,H_R(W_{PR} + W'_{PR})(\delta T_s - \delta T_R) - \delta Q_R\Big] \qquad (2.4.20)$$

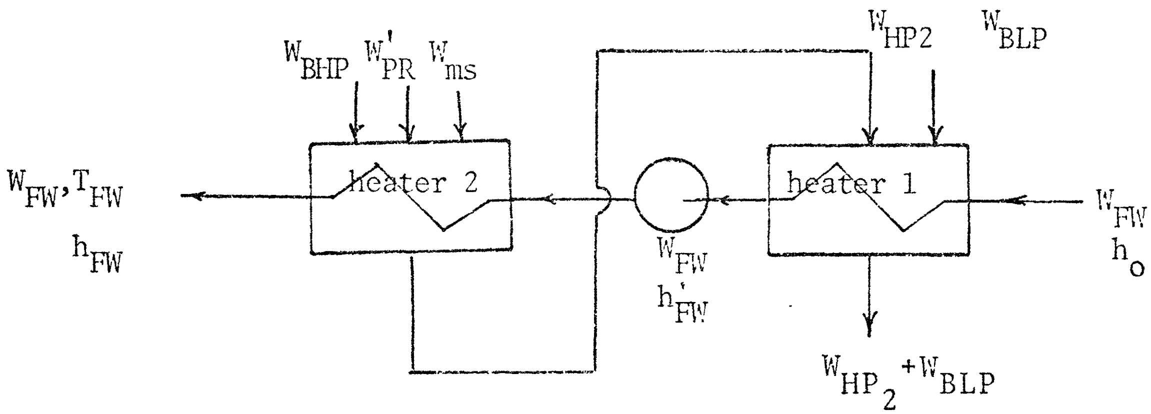

Old Configuration

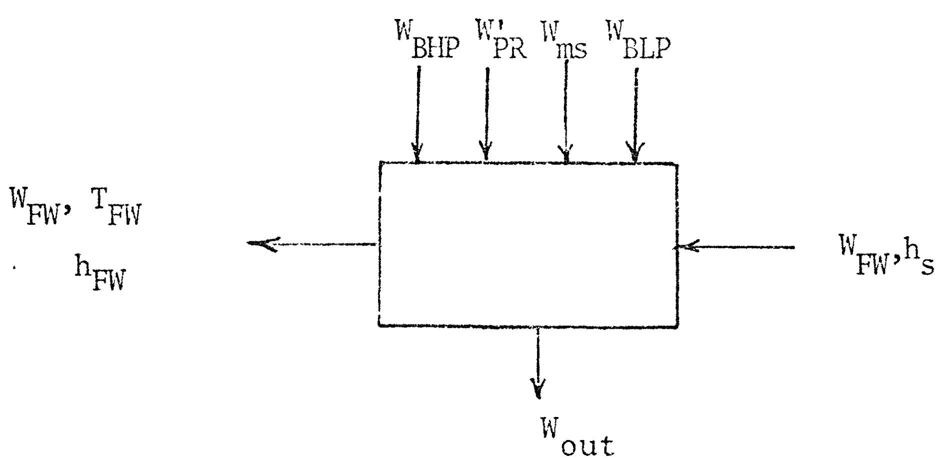

New Configuration

Fig. 2.4.8 Control Volume Combining Heater 1 and Heater 2.

2.4.6 A Reduced Order Model

So far, the reduction process followed in this section has resulted in reducing the set of equations presented in Appendix A from 31 equations to 14 equations. Table 2.4.4 gives a list of the 14 state variables. In this relatively low order model the turbine and the feedwater heaters are approximated by a mathematical model of five equations, Eqns. (2.4.16) - (2.4.20), instead of eleven equations given in Appendix A. Another representation of the turbine and the feedwater heaters system is given by two equations only involving an appropriate time constant (18). In this approximation, the detailed dynamics of the HP and LP turbines, the moisture separators, the reheater, the feedwater heaters, etc., are thus all lumped into this single time constant. In this representation, the turbine power L_T is considered as a state variable. The fractional change in the turbine power output is given in linearized form as

$$\frac{d}{dt} \frac{\delta L_T}{L_{TO}} = \frac{1}{\tau_T} \left(\frac{\delta P_c}{P_{CO}} - \frac{\delta L_T}{L_{TO}}\right) \tag{2.4.21}$$

where

P_C = pressure in front of the nozzle chest

τ_T = 5.5 sec

An equation giving $\frac{\delta P_c}{P_{CO}}$ is needed to predict the turbine

Table 2.4.4

The State Variables of

the 14th Order Model

δC	fractional change in delayed neutron precursor group
δT_f	change in average fuel temperature of the core (°F)
δT_{c1}	change in coolant node 1 of the reactor core (°F)
δT_{c2}	change in coolant node 2 of the reactor core (°F)
δT_{HL}	change in hot leg temperature
δT_{CL}	change in cold leg temperature
δT_P	change in the average primary coolant temperature in the UTSG (°F)
δT_m	change in the average tube temperature in UTSG (°F)
δP_s	change in the average steam pressure of the UTSG (psi)
$\delta \rho_c$	change in the density of the steam in the nozzle chest (lbm/ft^3)
$\delta \rho_R$	change in the density in the reheater tube side (lbm/ft^3)
$\frac{\delta h_R}{h_{Ro}}$	fractional change in enthalpy of reheater tube side
δQ_R	change in the heat transfer in the reheater sheel to tube (MW-hr/sec)
δT_{FW}	change in feedwater temperature leaving heater 2

power output. The differential equation describing the nozzle chest pressure is given by

$$\frac{d}{dt}\frac{\delta P_c}{P_{co}} = \frac{1}{\tau_c}\left[\frac{P_{so}}{P_{co}}\frac{\delta P_s}{P_{so}} - \frac{\delta P_c}{P_{co}} - 0.157\frac{\delta\varepsilon_2}{\varepsilon_{20}} + \frac{\delta\varepsilon}{\varepsilon_o}\right] \quad (2.4.22)$$

where,

τ_c = 0.5 sec

$\frac{\delta\varepsilon_2}{\varepsilon_{20}}$ = fractional change in the by-pass valve coefficient

$\frac{\delta\varepsilon}{\varepsilon_o}$ = fractional change in the main valve coefficient

An additional simplification involves the hot leg piping. This is to eliminate T_{HL} by lumping the outlet temperature of the coolant node 2, T_{c2}, with the hot leg temperature, T_{HL}, in a single time constant τ_{c2}

$$\tau_{c2} = \left(\frac{m}{\dot{m}}\right)_{C2} + \tau_{HL} \quad (2.4.23)$$

Equation (2.4.6) becomes

$$\frac{d}{dt}\delta T_{c2} = \frac{(1-f)Po}{(mC_p)_{c2}}\frac{\delta P}{Po} + \frac{A_f h_{eff}}{2(mc_p)_{c2}}[\delta T_f - \delta T_{c1}] - \frac{1}{\tau_{c2}}[\delta T_{c2} - \delta T_{c1}] \quad (2.4.24)$$

Table 2.4.5 gives a list of the 10 state variables. It is this low-order model which is investigated in the application of Chapter 6.

Table 2.4.5

The State Variables

of the 10th Order Model

The first seven state variables:

δC, δT_f, δT_{c1}, δT_{c2}, δT_{CL}, δT_p and δT_m

are as given in Table 2.4.4. The remaining state variables are:

$\frac{\delta P_s}{P_{so}}$ fractional change in the average steam pressure

$\frac{\delta L_T}{L_o}$ fractional change in the turbine output

$\frac{\delta P_c}{P_{co}}$ fractional change in the nozzle chest pressure

Chapter 3
STATE RECONSTRUCTION

3.1 Introduction

Many control system designs are based on state vector feedback, where the input to the system is a function only of the current state vector $\underline{x}(t)$. For the linear-time-invariant dynamic system described in state-space form by the continuous time model:

$$\dot{\underline{x}} = A\underline{x} + B\underline{u} + \underline{G}w \tag{3.1.1}$$

$$\underline{z} = M\underline{x} \tag{3.1.2}$$

$$\underline{y} = H\underline{x} \tag{3.1.3}$$

where,

$\underline{x}$ is an nxl state vector

$\underline{u}$ is an rxl input control vector

w is a scalar input disturbance

$\underline{y}$ is a pxl system output vector

$\underline{z}$ is an mxl measurement output vector

A,B,H and M are matrices and $\underline{G}$ is a vector all with appropriate dimensions.

the hypothesized structure for a linear full-state feedback control takes the form:

$$\underline{u} = K\underline{x} \tag{3.1.4}$$

Such full-state vector feedback designs offer certain advantages with respect to both system performance and analysis (45,46,47). There is, however, one major drawback. In many control problems, the system state vector is not available for direct measurement and so a control law given by Eq. (3.1.4) cannot be used. Thus, a reasonable substitute for the state vector must be found; otherwise the whole control scheme must be abandoned.

This reasonable substitute for the state vector may be approximately reconstructed by using an observer. The observer reconstructs the state vector from the available outputs only. Once the state vector has been reconstructed, we shall be able to use the control law of Eq. (3.1.4), which assumes knowledge of the complete state vector, by replacing the actual state $\underline{x}$ with the reconstructed state, say $\hat{\underline{x}}$ so the control law becomes:

$$\underline{u} = K\hat{\underline{x}} \tag{3.1.5}$$

In this study we will be dealing with the type of observer whose output approaches, as time increases, the state that must be reconstructed but does not explicitly take into account the difficulties that arise because of the presence of noise in the measurements.

This type of observer for purely deterministic continuous-time linear time-invariant systems was first proposed by Luenberger (48, 49, 50). In an earlier work, Kalman and Bucy (51) treated the problem of estimating the state when measurements of the outputs are corrupted by noise.

3.2 Observing a Linear System

Consider, for simplicity, a linear-time invariant system given by:

$$\dot{\underline{x}}(t) = A\underline{x}(t) + \underline{B}(u+w), \qquad \underline{x}(0)=\underline{x}_o \qquad (3.2.1)$$

where $\underline{x}$ is an nxl state vector and u and w are scalar inputs for control and disturbance respectively. A system with no observations at all can be observed by merely copying the original system (49) as shown in Fig. (3.2.1). The inputs u and w to the original system are acting on the system, u is a control supplied to it and w is the process disturbance applied on it and hence they can be applied to the copy as well. The system copy is represented as:

$$\dot{\hat{\underline{q}}}(t) = A\hat{\underline{q}}(t) + \underline{B}(u+w), \qquad \hat{\underline{q}}(0)=\hat{q}_o \qquad (3.2.2)$$

where $\hat{\underline{q}}$ is the state estimate of the copy model which can be easily measured.

It is clear that if $\hat{\underline{q}}(0) = \underline{x}(0)$, the system copy will follow the original system exactly. The reason is that the error vector, $\underline{e}(t)$, which is the difference between the estimate vector $\hat{\underline{q}}$ and the original state vector $\underline{x}$,

$$e(t) = [\hat{\underline{q}}(t) - \underline{x}(t)]$$

will be zero. Note that the solution of $\dot{\underline{e}}(t)$, namely

$$[\dot{\hat{\underline{q}}}(t) - \dot{\underline{x}}(t)] = A[\hat{\underline{q}}(t) - \underline{x}(t)] \qquad (3.2.3)$$

is given by:

$$\underline{e}(t) = [\hat{\underline{q}}(t) - \underline{x}(t)] = e^{At}[\hat{\underline{q}}(0) - \underline{x}(0)] \qquad (3.2.4)$$

consequently with $\hat{q}(0) = x(0)$, the system copy will track the original system exactly, i.e., $\hat{\underline{q}}(t) = \underline{x}(t)$

Now if $\hat{\underline{q}}(0) \neq \underline{x}(0)$, the error $\underline{e}(t)$ given by Eq. (3.2.4) may not die out quickly. It tends to zero only if the original system is stable and then only at a speed determined by the eigenvalues of the original system matrix, A. This is indeed a serious limitation.

Suppose that the original system represented by Eq. (3.2.1) has m observations given by:

$$\underline{z} = M\underline{x} \qquad (3.2.5.)$$

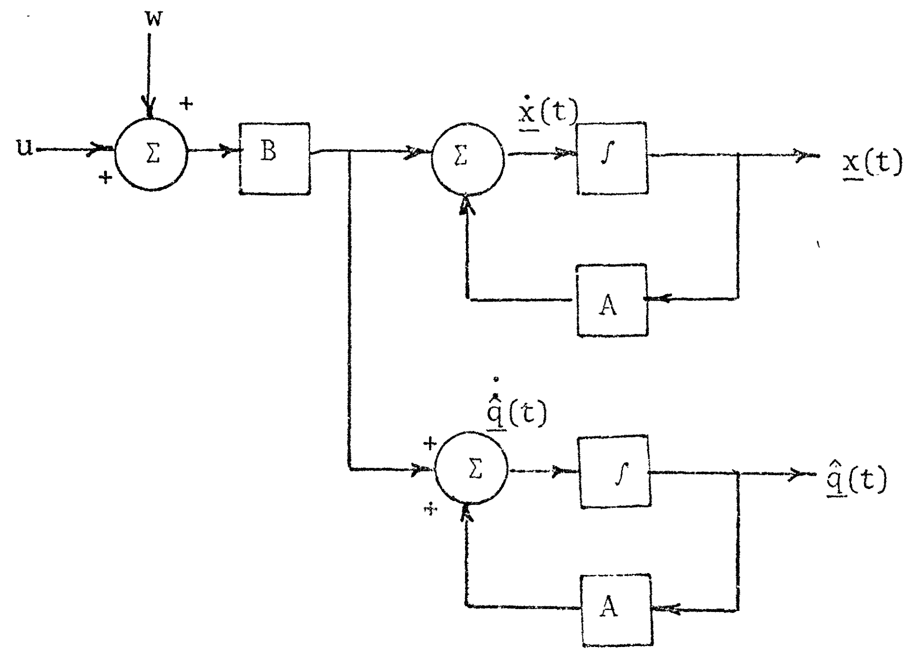

Fig. (3.2.1) An original System Observed by a System Copy

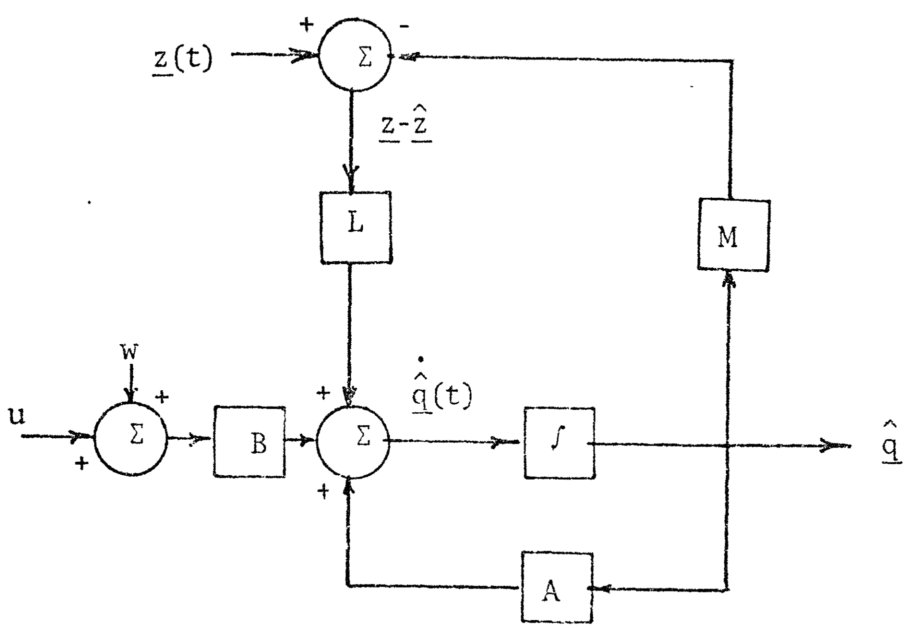

Fig. (3.2.2) A Block Diagram Representing Eqn. (3.2.7).

with m<n. In order to overcome the previous limitation, an extra term that is proportional to the difference $(\underline{z}-\hat{\underline{z}})$ is added to Eq. (3.2.2.) where

$$\hat{\underline{z}} = M\hat{\underline{q}} \tag{3.2.6}$$

$\hat{\underline{z}}$ is the observed variable as reconstructed by the observer. In this case, the estimate of the state vector is given by:

$$\hat{\underline{q}}(t) = A\hat{\underline{q}}(t) + B(u+w) + L[\underline{z}(t)-\hat{\underline{z}}(t)] \tag{3.2.7}$$

where L,a matrix called the gain matrix of the observer, is yet to be determined. Fig. 3.2.2 shows the scheme described by Eq.(3.2.7).

In this scheme, it is clear that:

(i) If $\hat{\underline{z}}(t) = \underline{z}(t)$

the observer will be nothing more than the system copy given in the previous scheme.

(ii) If $\hat{\underline{z}}(t) \neq \underline{z}(t)$

by making the appropriate substitutions, the error dynamics are expressed as:

$$[\dot{\hat{\underline{q}}}(t) - \dot{\underline{x}}(t)] = (A-LM)[\hat{\underline{q}}(t) - \underline{x}(t)] \tag{3.2.8}$$

The difference between this equation and Eqn. (3.2.3) is clear. The solution of Eq. (3.2.8) is given by:

$$\underline{e}(t) = [\hat{\underline{q}}(t)-\underline{x}(t)] = \exp\{(A-LM)t\}[\hat{\underline{q}}(0)-\underline{x}(0)] \tag{3.2.9}$$

Therefore, if the observer is initiated such that $\hat{\underline{q}}(0)=\underline{x}(0)$, it follows that $\hat{\underline{q}}(t) = \underline{x}(t)$ for all $t>0$, i.e., the state of the observer tracks the state of the original system. When $\hat{\underline{q}}(0) \neq \underline{x}(0)$, the error vector, $\underline{e}(t)$, dynamics are governed by the matrix (A-LM) in Eqn. (3.2.8) and Eqn. (3.2.9).

If the system matrix (A-LM) is asymptotically stable, the error vector, $\underline{e}(t)$ tends to zero at a rate determined by the dominant eigenvalue of (A-LM). Here, the gain matrix, L of the observer plays an important role in prescribing the eigenvalues of (A-LM) according to the designer's choice.

In the two examples above, it is clear that the estimate vector $\hat{\underline{q}}(t)$ has the same order as the state vector $\underline{x}(t)$. But is is actually not always necessary that the order of $\hat{\underline{q}}$ be equal to that of $\underline{x}$. This will be the subject of the next section. Once the order of the estimate $\hat{\underline{q}}$ is specified, the order of the gain matrix L is also specified.

3.3 Full and Reduced Order Observers

When the order of this estimate vector $\hat{\underline{q}}(t)$ is equal to the order of the state vector $\underline{x}(t)$, we say that we have a full-order observer. The observer given by Eqn. (3.2.7) is a full-order observer. It is customarily expressed as:

$$\dot{\hat{\underline{x}}}(t) = A\hat{\underline{x}}(t) + B(u+w) + L(\underline{z}(t)-\hat{\underline{z}}(t)) \qquad (3.3.1)$$

where $\hat{x}$ is the estimate. Fig. 3.3.1 shows an original system observed by a full-order observer.

For a system expressed by:

$$\dot{\underline{x}}(t) = A\underline{x} + B\underline{u} + \underline{G}w \qquad (3.3.2)$$

$$\underline{z} = Mx \qquad (3.3.3)$$

where the vectors $\underline{x}$, $\underline{u}$ and $\underline{z}$ as well as the scalar w are as defined by Eqn. (3.1.1) the corresponding full-order observer is given by:

$$\dot{\hat{\underline{x}}}(t) = A\hat{\underline{x}}(t) + B\underline{u} + \underline{G}w + L(\underline{z}-M\hat{\underline{x}}) \qquad (3.3.4)$$

If for some reason the input disturbance, w cannot be observed then the full-order observer will be biased by the term $\underline{G}w$ and, therefore, given by:

$$\dot{\hat{\underline{x}}}(t) = A\hat{\underline{x}}(t) + B\underline{u} + L(\underline{z}-M\hat{\underline{x}}) \qquad (3.3.5)$$

Since there are different types of observers, it is instructive to express the observer in general terms. For a linear time-invariant dynamic system given by Eqns. (3.3.2)

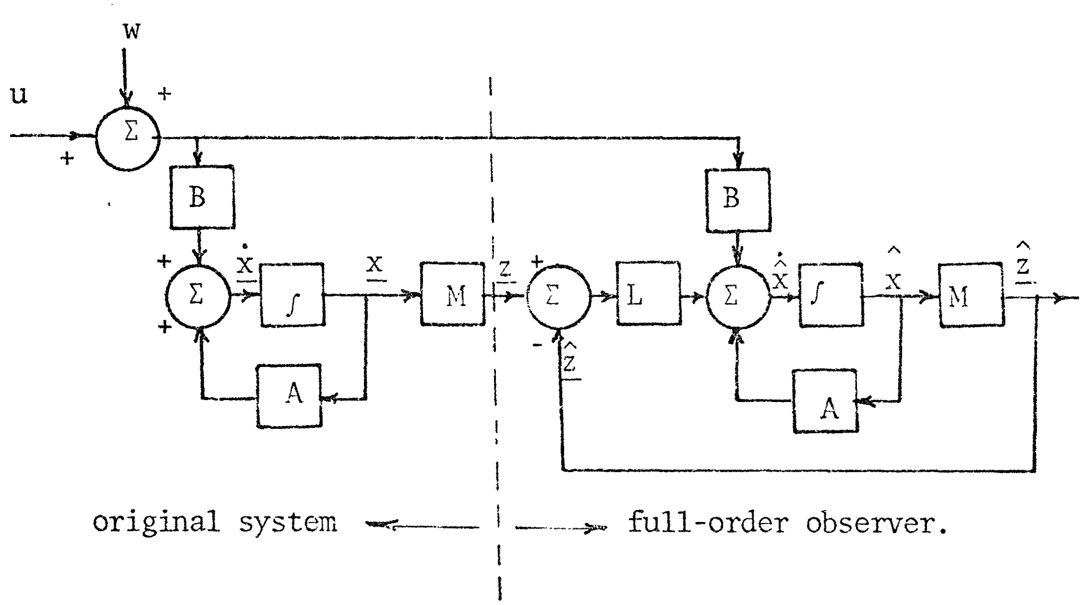

Fig. 3.3.1 An original System Observed by a Full-Order Observer.

and (3.3.3) a general observer design is given by:

$$\dot{\hat{\underline{q}}}(t) = F\hat{\underline{q}} + C\underline{z} + U\underline{u} + \underline{W}w \qquad (3.3.6)$$

where $\hat{\underline{q}}$ is the estimate vector which may have different orders for different observers, and the vectors $\underline{z}$ and $\underline{u}$ as well as the scalar w are as defined by Eqn. (3.1.1). The matrices F, C and U as well as the vector $\underline{W}$ take their particular forms according to the particular observer used. For example, in the case of a full-order observer, these matrices and the vector $\underline{W}$ are determined by comparing the full-order observer equation (3.3.4) with the general equation (3.3.6). This yields:

$$\begin{aligned} F &= A-LM \\ C &= L \\ U &= B \\ \underline{W} &= \underline{G} \end{aligned} \qquad (3.3.7)$$

The inaccessible states of the original system can similarly be expressed in general terms. By adding and subtracting the term $L\underline{z}$ from the right-hand side of Eqn. (3.3.2), the inaccessible state vector $\underline{x}=\underline{q}$ is given by:

$$\dot{\underline{q}}(t) = F\underline{q} + C\underline{z} + U\underline{u} + \underline{W}w \qquad (3.3.8)$$

where the matrices F, C and U and the vector $\underline{W}$ are as defined by Eqn. (3.3.7).

The error dynamics are obtained by subtracting Eqn. (3.3.8) from Eqn. (3.3.6), i.e. similar to Eqn. (3.2.8),

$$\dot{\underline{e}}(t) = (A-LM)\underline{e}(t) \qquad (3.2.8 \text{ bis})$$

As stated in Section 3.2, the gain matrix of the observer L, is chosen by the designer so as to make the matrix (A-LM) asymptotically stable. In this case, the error vector $\underline{e}(t)$ tends to zero at a rate determined by the dominant eigenvalue of (A-LM).

The estimate vector $\hat{\underline{q}}(t)$ in Eq. (3.3.6) takes the order of the particular observer used. Now, if the original system is of order n and the observations, $\underline{z}$, are of order m, then a full-order observer will reconstruct all n state variables of the original system even though m of these variables, already measured, are known precisely. Therefore, a full-order observer possesses a certain degree of redundancy.

The redundancy may be eliminated by reducing the order of the observer to (n-m) only. In this case, the full state of the original system is obtained from the (n-m) state variables of the observer and the m observations. This type of observation is termed a reduced-order observer. The reduced-order observer can consequently be cheaper to design and implement.

In Appendix B, the detailed derivation of the governing equations of a reduced-order observer is shown. The general approach was first considered by Luenberger (48,52), but the derivation in Appendix (B) follows that of Cumming (53).

Consider the original linear time-invariant system described by Eqns. (3.3.2) and (3.3.3), and define first a new state vector $\underline{x}_1$ characterized by the fact that the first m elements are equal to $\underline{z}$

$$\underline{x}_1 = \left[\frac{\underline{z}}{\underline{\eta}}\right] \tag{3.3.9}$$

Here we need a nonsingular transformation relating $\underline{x}$ to the new state vector $\underline{x}_1$.

Assume that the system is observalbe, m<n, and the rows of the matrix M in Eqn. (3.3.3) are linearly independent. In this case an (n-m)xn matrix N is selected such that

$$\underline{\eta} = N\underline{x} \tag{3.3.10}$$

Note that it is possible to find such a matrix N since M has rank m (M is assumed linearly independent).

The new vector is now given by:

$$\underline{x}_1 = [\frac{\underline{z}}{\underline{\eta}}] = [\frac{M}{N}]\underline{x} \tag{3.3.11}$$

Up to this point, the approach of a reduced-order observer requires only a nonsingular transformation:

$$\underline{x} = [\frac{M}{N}]^{-1} [\frac{\underline{z}}{\underline{\eta}}] \tag{3.3.12}$$

and then, like the full-order observer, it follows exactly the line stated earlier in Section 3.2.

Following the derivation in Appendix B, the governing equations of a reduced-order observer is expressed in general form by Eqn. (3.3.6)

$$\dot{\hat{\underline{q}}}(t) = F\hat{\underline{q}} + C\underline{z} + U\underline{u} + \underline{W}w \tag{3.3.6 bis}$$

such that:

$$\begin{aligned} F &= P - LR \\ C &= PL-LRL+V-LJ \\ U &= TB_3 \\ \underline{W} &= T\underline{G}_3 \end{aligned} \tag{3.3.13}$$

where

$$B_3 = [-\frac{M}{N}]B \quad \text{and} \quad \underline{G}_3 = [\frac{M}{N}]\underline{G}$$

and the different matrices are defined in Appendix B.

The inaccessible state vector, $\underline{q}$ is expressed in general form by Eqn. (3.3.8).

$$\dot{\underline{q}}(t) = F\underline{q} + C\underline{z} + U\underline{u} + \underline{W}w \qquad (3.3.8 \text{ bis})$$

where the matrices F,C and U as well as the vector $\underline{W}$ are as defined by Eqns. (3.3.13).

Therefore, the error dynamics are given by:

$$\dot{\underline{e}}(t) = (P-LR)\underline{e}(t) \qquad (3.3.14)$$

Now by appropriately choosing the initial conditions of the estimate vector $\hat{\underline{q}}(t)$ in order to make use of Eqn. (B15) such as

$$\begin{aligned} \hat{\underline{q}}(0) &= T\underline{x}_1(0) \\ &= [-L \; I_\eta][\frac{M}{N}] \; \underline{x}(0) \end{aligned} \qquad (3.3.15)$$

the observer will track the (n-m) nonmeasured state variables, $\underline{q}$, of the original system. But if Eqn. (3.3.15) is not satisfied due to the initial conditions of the estimate vector, $\hat{\underline{q}}(t)$, the error vector, $\underline{e}(t)$ will be governed by Eqn. (3.3.14) and hence given by:

$$\underline{e}(t) = \exp\{(P-LR)t\}\underline{e}(0) \tag{3.3.16}$$

If the system matrix (P-LR) is asymptotically stable, the error vector, $\underline{e}(t)$ tends to zero at a rate determined by the dominant eigenvalue of (P-LR). The role of the designer is then to choose the appropriate observation gain matrix L. A system observed by a reduced-order observer is presented in Fig. (3.3.2).

3.4 Representation of an Observed System in Terms of the State Vector, $\underline{x}(t)$ and Error Vector, $\underline{e}(t)$

It was stated in Section 3.1 that once the state vector has been reconstructed via an appropriate observer, then the control law of Eqn. (3.1.4) which assumes knowledge of the complete state vector can be employed by replacing the actual state $\underline{x}$ with the reconstructed state $\hat{\underline{x}}$

$$\underline{u} = K\hat{\underline{x}} \tag{3.4.1}$$

In case of the reduced-order observer, the reconstructed state vector, $\hat{\underline{x}}$ is obtained, by using Eqn. (3.3.12), from the non-singular transformation as:

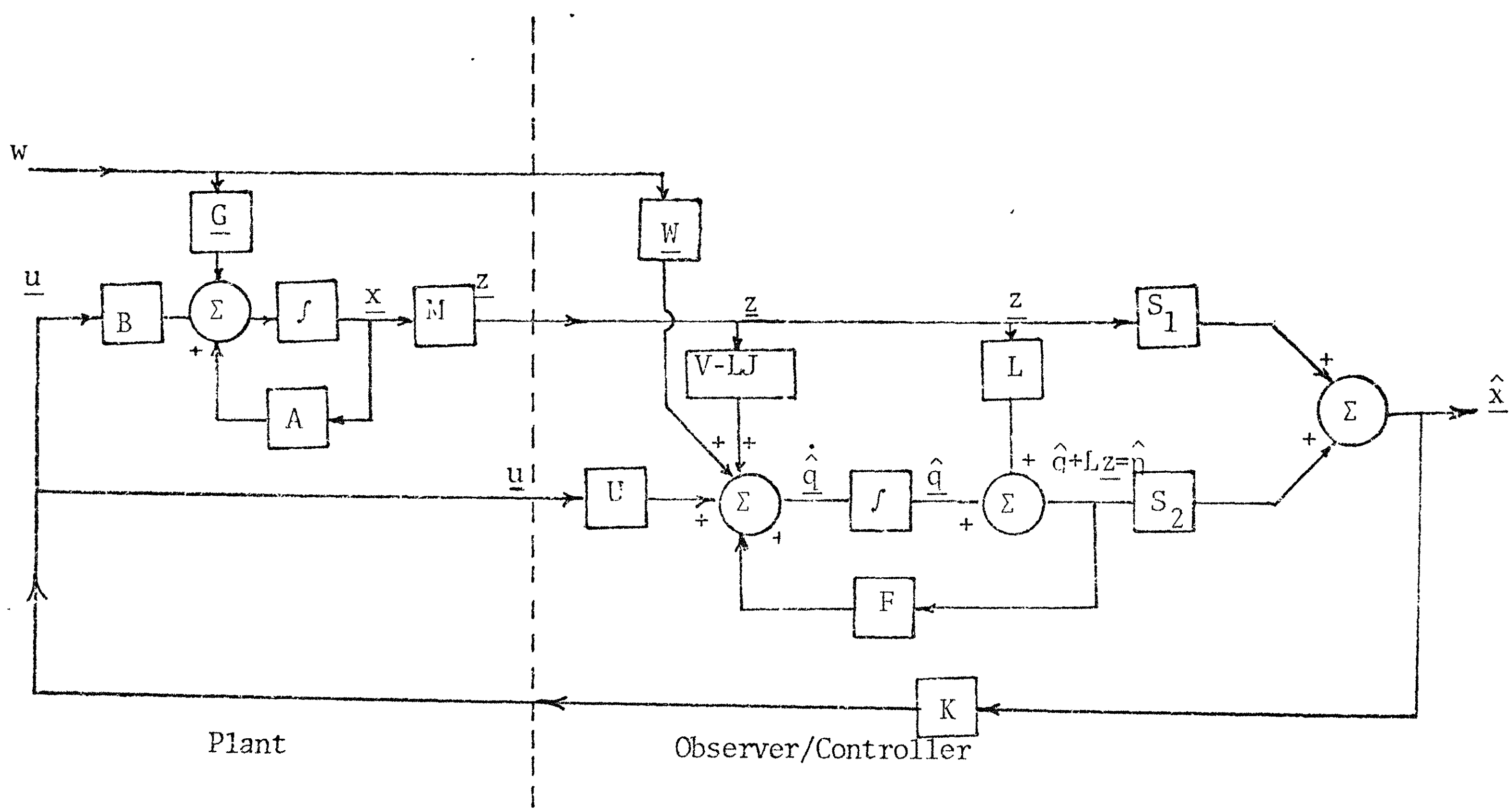

Fig. 3.3.2 Original System Observed by a Reduced-Order Observer.

$$\underline{\hat{x}} = \left[\frac{M}{N}\right]^{-1} \hat{x}_1$$

$$= [S_1 S_2] \left[\frac{\underline{z}}{\underline{\hat{n}}}\right]$$

$$= S_1\underline{z} + S_2\underline{\hat{n}} \tag{3.4.2}$$

Substituting for $\hat{x}$, the control law of Eqn. (3.4.1) becomes

$$\underline{u} = KS_1\underline{z} + KS_2\underline{\hat{n}} \tag{3.4.3}$$

By adding and subtracting the term $KS_2\underline{n}$ in the right hand side of Eqn. (3.4.3), making the appropriate substitutions for $\underline{z}$, Eqn. (3.3.3), and $\underline{n}$ Eqn. (3.3.10), and recognizing that $S_1M+S_2N = I$, an nxn identity matrix, the control law becomes,

$$\underline{u} = K\underline{x} + KS_2\underline{e} \tag{3.4.4.}$$

Substituting for $\underline{u}$ in Eqn. (3.3.2), the linear time-invariant system is expressed in terms of $\underline{x}$ and $\underline{e}$ as:

$$\underline{\dot{x}} = (A+BK)\underline{x} + BKS_2\underline{e} + \underline{G}w \tag{3.4.5}$$

$$\underline{z} = M\underline{x} + 0\underline{e} \tag{3.4.6}$$

Where 0 is a zero matrix of order mx(n-m).

The error dynamics are given by Eqn. (3.3.14), i.e.,

$$\underline{\dot{e}} = (P-LR)\ \underline{e} \tag{3.4.7}$$

Note that if the disturbance were not observed the dynamics of the unmeasured state vector $\underline{q}$ would still be given by Eqn. (3.3.8 bis) while the dynamics of the estimate vector $\underline{\hat{q}}$ would be given by:

$$\underline{\dot{\hat{q}}} = F\underline{\hat{q}} + C\underline{z} + U\underline{u} \tag{3.4.8}$$

where the matrices F, C and U are as defined by Eqn. (3.3.13).

In this case, the error dynamics become

$$\underline{\dot{e}} = (P-LR)\underline{e} - W\underline{w} \tag{3.4.9}$$

The distinction between these two cases was made in order to identify the effect of the disturbance on the behavior of the observer.

In the case of a full order observer, the control law is still given by Eqn. (3.4.1). By adding and subtracting $K\underline{x}$ from the right-hand side of this equation we get

$$\underline{u} = K\underline{x} + K\underline{e} \tag{3.4.10}$$

By substituting for $\underline{u}$ in Eqn. (3.3.2), the linear time-variant system will be expressed in terms of $\underline{x}$ and $\underline{e}$ as:

$$\dot{\underline{x}} = (A+BK)\underline{x} + BK\underline{e} \qquad (3.4.11)$$

$$\underline{z} = M\underline{x} + 0\underline{e} \qquad (3.4.12)$$

where 0 is a zero matrix of order mxn.

The error dynamics are given by Eqn. (3.2.8 bis) as

$$\dot{\underline{e}} = (A-LM)\underline{e} \qquad (3.4.13)$$

Here again, if the disturbance were not observed, the error dynamics would be given by:

$$\underline{e} = (A-LM)\ \underline{e} - G\underline{w} \qquad (3.4.14)$$

The derivation of these equations is useful in expressing the system together with the observer as a composite system in matrix notation in chapters to follow.

3.5 Conditions for the Observability of a LTI System:

In deriving the equations describing the reduced order observer in Section 3.4 it was assumed that the system is observable. In fact, this is not just an assumption but rather a necessary and sufficient condition for the design of an observer (full or reduced). Otherwise, the observation matrix L cannot be chosen and hence the state vector will not be reconstructed.

Consider the observer

$$\dot{\hat{\underline{q}}} = F\hat{\underline{q}} + C\underline{z} + U\underline{u} + W\underline{w} \tag{3.5.1}$$

for the LTI system

$$\dot{\underline{x}} = A\underline{x} + B\underline{u} + G\underline{w}$$

$$\underline{z} = M\underline{x} \tag{3.5.2}$$

where all the matrices, vectors and scalar are as defined in Section (3.3).

Note in particular that:

(i) for a full-order observer F=A-LM

(ii) for a reduced-order observer F=P-LR.

Observer Theorem(a) [47,50]

"The observation gain matrix, L, can be designed or, in either words, the characteristic values of F(=A-LM) can be arbitrarily located in the complex plane by choosing L suitably if and only if the LTI system given by Eqn. (3.5.2) is completely observable".

In (47), it is a complete reconstructibility of the system which is evoked. Note that for LTI systems, complete reconstructibility implies and is implied by complete observability.

The system (3.5.2) is completely observable which means that the pair {A,M} is observable if and only if the rank of the observability matrix is n, i.e.,

$$\text{rank } [M' \ AM' \ A^2M' \ \ldots \ A^{n-1}M'] = n \qquad (3.5.3)$$

where M' = transpose of M

A' = transpose of A.

The structure (A'-M'L') is used to generate a stabilizing L since

$$\det[\lambda I-(A-LM)] = \det\ [\lambda I-(A'-M'L')] \qquad (3.5.4)$$

where λ is the characteristic value.

It is very well known from the structure (A'-M'L') that a stabilizing L' cannot be generated unless the pair {A',M'} is completely controllable. This is in fact dual to saying the pair {A,M} is completely observable.

This result, due to duality, will be of help in generating a stabilizing L as we will see in Chapter (5).

Now concerning F=P-LR, for a reduced-order observer, Gopinath (54) states the following theorem:

Theorem(b)

"If {A,M} is completely observable, then {P,R} is completely observable."

From Eqn. (B.7), our system is partitioned as:

$$\dot{\underline{z}} = J\underline{z} + R\underline{\eta} + B_1\underline{u} + \underline{G}_1 w \tag{3.5.5}$$

$$\dot{\underline{\eta}} = V\underline{z} + P\underline{\eta} + B_2\underline{u} + \underline{G}_2 w. \tag{3.5.6}$$

Where all variables, matrices and vectors are as defined in Section 3.3.

It follows that if w were known, the only information about $\underline{\eta}$ is obtained from Eqn. (3.5.5).

$$R\underline{\eta} = \dot{\underline{z}} - J\underline{z} - B_1\underline{u} - \underline{G}_1 w \tag{3.5.7}$$

which implies that $\underline{P}$ and R should be completely observable in order that {A,M} be completely observable.

Some authors in the literature have relaxed the condition of complete observability to simply detectability (47).

Consider the LTI system given by Eqn. (3.5.2) and its observer given by Eqn. (3.5.1).

Theorem(c) [47):

"An observation gain matrix, L, can be found such that the observer is asymptotically stable if and only if the system given by Eqn. (3.5.2) is detectable".

Consider the system given by Eqn. (3.5.2) to be transformed to:

$$\dot{\tilde{\underline{x}}} = \begin{bmatrix} \tilde{A}_{11} & 0 \\ \tilde{A}_{21} & \tilde{A}_{22} \end{bmatrix} \tilde{\underline{x}} + \tilde{B}\underline{u} + \tilde{G}\underline{w}$$

$$\underline{z} = [\tilde{M}_1 \;\; 0]\, \tilde{\underline{x}} \qquad (3.5.8)$$

where the pair $\{\tilde{A}_{11}, \tilde{M}_1\}$ is completely observable. Then the system is detectable if and only if the matrix $\tilde{A}_{22}$ is asymptotically stable.

We have to first transform the system to the structure given by Eqn. (3.5.8) in order to check for the detectability of the system via $\tilde{A}_{22}$.

Chapter 4

SET-THEORETIC CONTROL

4.1 Introduction

Most practical systems are not completely isolated from their environments and so are constantly subjected to interactions in the form of input disturbances from their environment. In order that the performance of the system be considered acceptable, the system states (or outputs) must be kept within prespecified bounds at all times. This often calls for the use of some form of control which are limited in availability. The effectiveness of many control systems in practice is evaluated in terms of their ability to maintain the system states within prescribed bounds, using only available control effort, in the presence of input disturbances. Set-Theoretic Control is designed to address this class of problems.

Set-Theoretic Control (STC) is characterized by the two following aspects (1).

a) direct treatment of the state and control constraints. (Note that in some other techniques, the emphasis is placed on optimizing certain cost criteria and the satisfaction of the state and control constraints are treated indirectly.

b) the disturbance is treated as an unknown--but bounded process. (In some other techniques, the disturbance is modeled as a stochastic process. Note that, it may be easier in practice to define the bounds of a disturbance than to measure its stochastic properties).

These are really two major departures from existing control design techniques.

Usoro (1) formulated the Set-Theoretic Control problem as follows:

(a) attempt to find the maximum amplitude of the unknown-but-bounded input disturbance which can be tolerated by the system instead of defining a prespecified bound on it.

(b) define a specific class of control systems by hypothesizing a full-state feedback control structure and select the best in this class which yields non-violation of state and control constraints in the presence of the input disturbance.

The hypothesized structure for the control used by Usoro (1) is, therefore, of the form:

$$\underline{u} = K\underline{x} \tag{4.1.1}$$

It is important to note that the full-state feedback control system assumes knowledge of the complete state vector. Unfortunately, in many systems in practice, the complete state vector is not always available for measurement and so the full-state feedback control structure cannot be adopted in its original form; rather, as shown in Chapter 3, it can be adopted in terms of state estimates constructed by employing an observer. In the following sections the formulation of the Set-Theoretic Control problem in the case of some inaccessible states is addressed.

4.2 Observation/Control Problem Statement for an LTI System with Inaccessible States:

Consider the linear time invariant dynamic system given by:

$$\dot{\underline{x}} = A\underline{x} + B\underline{u} + \underline{G}w \tag{4.2.1}$$

$$\underline{y} = H\underline{x} \tag{4.2.2}$$

$$\underline{z} = M\underline{x} \tag{4.2.3}$$

where,

$\underline{x}$ is an nx1 state vector

$\underline{u}$ is an rx1 input vector

w is a scalar input disturbance

$\underline{y}$ is an px1 system output vector

$\underline{z}$ is an mx1 measurement output vector

A,B,H and M are matrices of appropriate dimensions

$\underline{G}$ is an nx1 vector.

In this system, it is assumed that some of the state variables are not available for measurement. Therefore, we have to resort to the observer for the reconstruction of the state. It is important that the state be reconstructed properly and accurately if the use of the same class of controls defined in terms of a linear full-state feedback in Eqn. (4.1.1) is to be appropriate.

Assume that the state vector, $\underline{x}(t)$ has been properly and accurately reconstructed and let its estimate be represented by $\underline{\hat{x}}(t)$. Then the hypothesized structure for the linear full-state feedback control is given in terms of the estimate by:

$$\underline{u} = K\underline{\hat{x}} \tag{4.2.4}$$

It is shown in Chapter 3 that the estimated state vector, $\underline{\hat{q}}(t)$ reconstructed by the observer is given in general form by Eqn. (3.3.6) and (3.3.6 bis) namely

$$\underline{\dot{\hat{q}}} = F\hat{q} + C\underline{z} + U\underline{u} + \underline{W}w$$

and the inaccessible state vector $\underline{q}$ is given by Eqns. (3.3.8), namely

$$\dot{\underline{q}} = F\underline{q} + C\underline{z} + U\underline{u} + \underline{W}w$$

where the matrices F,C,U and the vector $\underline{W}$ are given by Eqn. (3.3.7) in the case of a full reconstruction of the state as

$$F = A - LM$$
$$C = L$$
$$U = B$$
$$\underline{W} = \underline{G}$$

and by Eqn. (3.3.13) in the case of a partial reconstruction of the state as:

$$F = P - LR$$
$$C = PL - LRL + V - LJ$$
$$U = TB_3$$
$$\underline{W} = T\underline{G}_3$$

where all the matrices are as defined in Chapter (3).

Matrix L is the gain matrix for the observer as defined in Chapter 3. It is an arbitrary matrix chosen by the designer, and determines the eigenvalues of the matrix F when we have either full or partial reconstruction of the state.

If the observer is initiated such that $\hat{\underline{q}}(0) = \underline{q}(0)$, it follows that $\hat{\underline{q}}(t) = \underline{q}(t)$ for all $t>0$, i.e., the estimate state vector $\hat{\underline{q}}(t)$ of the observer tracks the state $\underline{q}(t)$

of our system. But if $\underline{\hat{q}}(0) \neq \underline{q}(0)$, the error vector, which is the difference between $\underline{\hat{q}}(t)$ and $\underline{q}(t)$, is governed by:

$$\dot{\underline{e}}(t) = F\underline{e}(t) \tag{4.2.5}$$

where F is as defined earlier in either case and $\underline{e}(t)$ is given by:

$$\underline{e}(t) = \exp[Ft]\underline{e}(0) \tag{4.2.6}$$

In our case, it is practical to express the control law in terms of the state vector $\underline{x}$ and the error vector $\underline{e}$. Following the derivation in section 3.4, Eqn. (4.2.4) becomes

$$\underline{u} = K_x\underline{x} + K_e\underline{e} \tag{4.2.7}$$

where,

- in the case of full-state reconstruction
  $K_x=K_e=K$
- in the case of partial-state reconstruction
  $K_x=K$ and $K_e=KS_2$, see Eqn. (3.4.4).

It is important to compare the hypothesized structure for the state feedback control as given by Eqn. (4.1.1) with the hypothesized structure for the estimate feedback control as given by Eqn. (4.2.7). If we were able to eliminate completely the error vector $\underline{e}$ from Eqn. (4.2.7) or at least to make it die out quickly, we would then be practically feeding back the state vector $\underline{x}(t)$ because then the gain matrix $K_x=K$. Hence it can be stated that part of the control problem for the system defined by Eqns. (4.2.1), (4.2.2) and (4.2.3) is to initiate the observer such that $\hat{\underline{x}}(0) = \underline{x}(0)$ and so $\hat{\underline{x}}(t) = \underline{x}(t)$ for all $t>0$ or at least to cause the error vector $\underline{e}(t)$ die out quickly. In this context we are seeking the estimate feedback control, $u = k\hat{x}$, which can tolerate the maximum input disturbance without violating the state and control constraints.

The state constraints are expressed in terms of the system output constraints by:

$$|y_i| \leq y_{imax} \quad i=1,2,3...,p \tag{4.2.8}$$

with $|y_i| = |Y_i - Y_{oi}|$

where

Y_{oi} are known elements of the output set center $\underline{Y_o}$.

y_{imax} are the prespecified bounds on the amplitudes of the associated outputs and referenced about the center.

It is clear that each of the elements y_i of the system output vector $\underline{y}$ must be kept within its prespecified bounds at all times. Eqn. (4.2.8) defines a hyperparallelopiped given by:

$$\underline{y}\varepsilon\Omega_y = \{\underline{y}: |Y_i - Y_{oi}| \leq y_{imax};\ i\text{-}1,2,...p\}$$

$$= \{\underline{y}: (Y_i - Y_{oi})' S_i^{*-1} (Y_i - Y_{oi}) \leq 1;$$

$$i=1,2,;..p\} \qquad (4.2.9\ )$$

where

$$S_i^* = y_{imax}^2 \qquad (4.2.10)$$

Also, each element u_j of the control vector $\underline{u}$ is constrained to lie within its specified bounds at all times. These constraints are of the form:

$$|u_j| \leq u_{jmax} \qquad j\text{-}1,2...r \qquad (4.2.11)$$

with

$$|u_j| = |U_j - U_{oj}|$$

where

U_{oj} are known elements of the control set center $\underline{U}_o$

u_{jmax} are the prespecified bounds on the amplitudes of the associated controls, referenced about the center.

Equation (4.2.11) defines a hyper-parallelopiped given by

$$\underline{u}\varepsilon\Omega_u = \{\underline{u}: |U_j - U_{oj}| \leq u_{jmax};\ j=1,2,\ldots r\}$$

$$= \{\underline{u}: (U_j - U_{oj})' T_j^{*-1} (U_j - U_{oj}) \leq 1 \quad j=1,2\ldots r\} \tag{4.2.12}$$

where,

$$T_j^* = u_{jmax}^2 \tag{4.2.13}$$

In accordance with the formulation of the STC (1), the next step is to find the control gains that maximizes the amplitude of the unknown-but-bounded disturbance w given by:

$$|w| \leq Q^{1/2} \tag{4.2.14}$$

By substituting for $\underline{u}$ from Eqn. (4.2.7) into Eqn. (4.2.1), the system governing equations in terms of $\underline{x}$ and $\underline{e}$ reduces to:

$$\begin{bmatrix} \dot{\underline{x}} \\ \hline \dot{\underline{e}} \end{bmatrix} = \left[\begin{array}{c|c} A+BK_x & BK_e \\ \hline 0 & F \end{array}\right] \begin{bmatrix} \underline{x} \\ \hline \underline{e} \end{bmatrix} + \begin{bmatrix} G \\ \hline 0 \end{bmatrix} w \tag{4.2.15}$$

It follows from the structure of Eqn. (4.2.15) that the eigenvalues of the composite system (the original system and the observer) are those of the feedback system ($A+BK_X$) and those of the observer (F). This is in accordance with the statement by Luenburger (50) that insertion of an observer in a feedback system to replace unavailable measurements does not affect the eigenvalues of the feedback system; it merely adjoins its own eigenvalues.

4.3 The Synthesis Problem

Due to the redundancy of the full-order observer, let us specialize to the design of an observer/controller for the case of a partial-state reconstruction, i.e., the observer is a reduced-order one. Its derivation is given in Appendix (B).

Consider our LTI dynamic system given by Eqns. (4.2.1), (4.2.2) and (4.2.3). By reconstructing the state vector with the reduced-order observer to obtain the estimate vector $\hat{x}(t)$ and by hypothesizing the structure of the desired control system as given by Eqn. (4.2.4), the feedback system of Eqn. (4.2.15) becomes:

$$\begin{bmatrix} \dot{\underline{x}} \\ \hline \dot{\underline{e}} \end{bmatrix} = \left[\begin{array}{c|c} A+BK & BKS_2 \\ \hline 0 & \bar{P}-L\bar{R} \end{array}\right] \begin{bmatrix} \underline{x} \\ \hline \underline{e} \end{bmatrix} + \begin{bmatrix} G \\ \hline 0 \end{bmatrix} w \qquad (4.3.1)$$

where P,R and S_2 are as defined in Appendix B.

K is the gain matrix of the feedback of order rxn

L is the gain matrix of the observer of order (n-m)xm.

The observation/control problem in a STC prespective thus reduces to finding:

(i) the gain matrix, L, of the observer such that the state vector $\underline{x}(t)$ is properly and accurately reconstructed (i.e., $e(t) \to 0$ as fast as possible).

(ii) the control gain matrix K to maximize the allowable unknown-but-bounded input disturbance amplitude which the system can tolerate without violating the output constraint, Eqn. (4.2.9) and the control constraint, Eqn. (4.2.12), subject to the governing equations, Eqn. (4.3.1).

Note that a sufficient condition for the satisfaction of these constraints at all times is that the sets of possible outputs and controls lie within the hyper-parallelopipeds given by Eqns. (4.2.9) and (4.2.12) respectively.

The state governing equations (4.3.1) can be expressed as follows:

$$\dot{\underline{\bar{x}}} = \bar{A}\,\underline{\bar{x}} + \underline{\bar{G}w} \qquad (4.3.2)$$

where,

$\bar{x}$ is an (2n-m) - dimensional state vector given by

$$\underline{\bar{x}} = \left[\frac{\underline{x}}{\underline{e}}\right]$$

the matrix $\bar{A}$ and the vector $\bar{\underline{G}}$ are as specified.

w is the unknown-but-bounded disturbance.

In STC, the initial state vector $\underline{\bar{x}}(0)$ is uncertain and is regarded as belonging to a set of possible initial state given by $\Omega_{\bar{x}}(0)$ ($\underline{2}$) which can be approximated by an ellipsoid and is given by:

$$\underline{\bar{x}}(0) \ \varepsilon\Omega_{\bar{x}}(0) \ = \ \{\underline{\bar{x}}:(\underline{\bar{X}}-\underline{\bar{X}}_o)'\psi^{-1}(\underline{\bar{X}}-\underline{\bar{X}}_o)\underline{<1}\} \qquad (4.3.3)$$

where,

ψ = a characteristic positive definite matrix describing the ellipsoidal set $\Omega_{\bar{x}}(0)$.

$\underline{\bar{X}}_o$ = (2n-m) - dimensional vector denoting the center $\Omega_{\bar{x}o}$.

It is shown in ($\underline{2}$) that the state vector $\underline{\bar{x}}(t)$, at any time t, is contained within an ellipsoidal set $\Omega_{\bar{x}}(t)$ given by:

$$\underline{\bar{x}}(t)\varepsilon\Omega_{\bar{x}}(t) \ = \ \{\underline{\bar{x}}: \ (\underline{\bar{X}}-\underline{\bar{X}}_o)'\Gamma^{-1}(t)(\underline{\bar{X}}-\underline{\bar{X}}_o)\underline{<1}\} \qquad (4.3.3)$$

where

$\Gamma(t)$ is a positive definite matrix (or a positive semi-definite matrix in the case where the ellipsoids are expressed in terms of support functions--Appendix C) which satisfies the equations: [See Appendix D].

$$\frac{d\Gamma(t)}{dt} = \bar{A}\Gamma + \Gamma\bar{A}' + \beta(t)\Gamma + \frac{\bar{G}Q\bar{G}'}{\beta(t)}$$

$$\Gamma(0) = \psi$$

$\beta(t) \geq 0$, is a free parameter that enters in the construction of the ellipsoid. (4.3.5)

If Eqn. (4.3.5) is solved for $\Gamma(t)$, then the ellipsoids bounding the set of possible states at the corresponding times are defined.

The hypothesized structure for the estimate feedback control, $\underline{u} = k\hat{x}$, is expressed in terms of $\underline{x}$ and $\underline{e}$ in Eqn. (4.2.7), therefore, we can write

$$\underline{u} = [K_x K_e]\left[\frac{x}{\underline{e}}\right]$$

$$= \bar{K}\,\underline{\bar{x}} \qquad (4.3.6)$$

where

$$K_x = K \text{ and } K_e = KS_2$$

It is shown in (1) that if the set of possible states $\Omega_{\bar{x}}$ is bounded, the set of possible controls Ω_u is also bounded and is simply a linear transformation of the set of possible states. This set is bounded by the ellipsoid

$$\Omega_u = \{\underline{u}:(\underline{U}-\bar{K}\underline{X}_o)'[\bar{K}\Gamma\bar{K}']^{-1}(\underline{U}-\bar{K}\underline{X}_o)\underline{<}1\} \qquad (4.3.7)$$

where

$$\bar{K}\underline{X}_o = \underline{U}_o$$

In order to satisfy the control constraint, the bounding ellipsoid for the set of possible controls, Eqn. (4.3.7), must lie within the control constraint hyper-parallelopiped given by Eqn. (4.2.12). Figure 4.3.1 illustrates this condition for a two-dimensional case. This condition is satisfied if:

$$\underline{K}_j\Gamma\underline{K}_j' \leq T_j^* \qquad j=1,2...r \qquad (4.3.8)$$

where $\underline{K}_j$ is the $j^{\underline{th}}$ row vector of the control gain matrix $\bar{K}$.

Eqn. (4.3.8) represents the statement of the control constraint.

In a similar manner, the system output Eqn. (4.2.2) may also be expressed in terms of $\bar{\underline{x}}$ as follows:

$$y = [H \ 0] \ [\frac{x}{\underline{e}}]$$

$$= \bar{H} \ \bar{\underline{x}} \qquad (4.3.9)$$

Since the output given by Eqn. (4.3.9) is just a

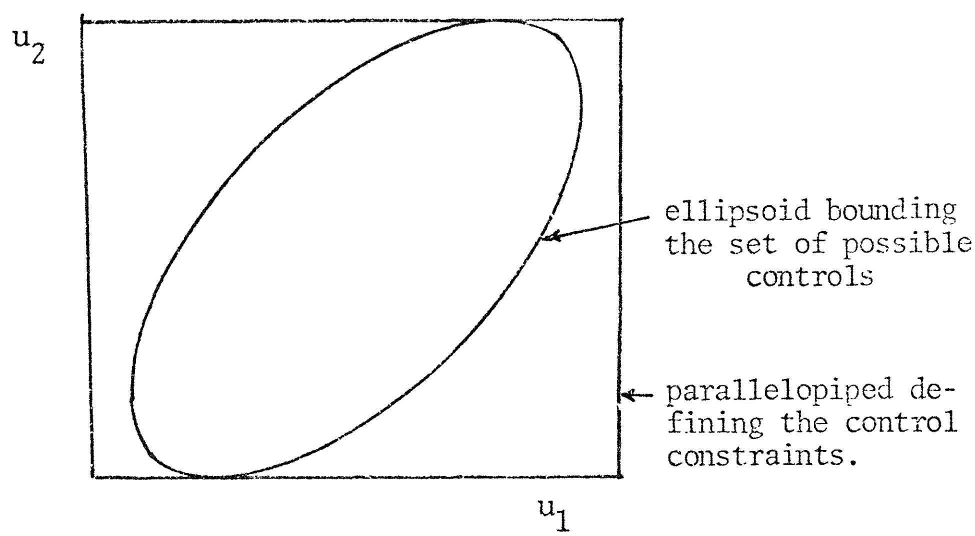

Fig. 4.3.1 Sufficient Condition for the Satisfaction of the Control Constraints.

(the constraints are satisfied if the bounding ellipsoid is contained within the parallelopiped).

linear transformation of the system state $\underline{\overline{x}}$, it follows that with a bounded system state the output is also bounded by the ellipsoid

$$\Omega_y = \{\underline{y}: (\underline{Y}-\overline{H}\underline{X}_o)' [\overline{H}\Gamma\overline{H}']^{-1}(\underline{Y}-\overline{H}\underline{X}_o) \leq 1\} \qquad (4.3.10)$$

where $\overline{H}\underline{X}_o = \underline{Y}_o$.

In order to satisfy the output constraint, the bounding ellipsoid for the set of possible outputs, Eqn; (4.3.10), must lie within the output constraint hyper-parallelopiped given in Eqn. (4.2.9). This condition is satisfied if:

$$\underline{\overline{H}}_i\Gamma\underline{\overline{H}}_i' \leq S_i^* \qquad i=1,2,\ldots p \qquad (4.3.11)$$

where $\underline{\overline{H}}_i$ is the $i^{\underline{th}}$ row vector of the system output matrix $\overline{H}$.

It is shown in (1) that if the system output is given by:

$$\underline{y} = \overline{H}\underline{\overline{x}} + D\underline{u} + \underline{E}w \qquad (4.3.12)$$

then a sufficient condition for the output constraint to be satisfied is

$$\{E_i Q E_i' + (\overline{H}+D\overline{K})_i \; \Gamma (\overline{H}+D\overline{K})_i' ;$$

$$+ 2[E_i Q E_i' \Gamma (\overline{H}+D\overline{K})_i \; \Gamma (H+DK)_i']^{1/2} \} \leq S_i^*$$

$$i=1,2,\ldots,p \quad (4.3.13)$$

where

E_i is the $i^{\underline{th}}$ row of $\underline{E}$

$(\overline{H}+D\overline{K})_i$ is the $i^{\underline{th}}$ row of $(\overline{H}+D\overline{K})$.

Eqn. (4.3.11) or Eqn. (4.3.13) represents the statement of the output constraint.

Now for a constant β, the governing equation (4.3.5) becomes:

$$\frac{d\Gamma(t)}{dt} = (\overline{A} + \frac{1}{2}\beta I)\Gamma + \Gamma \; (\overline{A}+\frac{1}{2}\beta I)' + \frac{\overline{G}Q\overline{G}}{\beta}$$

$$\psi(0)=\psi$$

$$\beta \geq 0 \quad \text{is now a constant} \qquad (4.3.14)$$

Eqn. (4.3.14) reveals that (2) a large β tends to make the system unstable while a small β tends to amplify the effect of the input bound Q.

Hence, by choosing appropriately the free parameter

β and a stable $(\bar{A}+\frac{1}{2}\beta I)$, it is possible to find a steady-state solution. Under the condition of stable $(\bar{A}+\frac{1}{2}\beta I)$ the steady-state solution may be shown to be the unique solution Γ_s of the Lyapunov equation (55)

$$(\bar{A} + \frac{1}{2}\beta I)\Gamma_s + \Gamma_s(\bar{A} + \frac{1}{2}\beta I)' + \frac{1}{\beta}\bar{G}Q\bar{G}' = o \qquad (4.3.15)$$

and

$$\Gamma_s \geq 0 \qquad (4.3.16)$$

Furthermore, if the system is controllable from the disturbance, i.e, if

$$\text{rank } [\bar{G}, \bar{A}\,\bar{G}, \ldots, \bar{A}^{n-1}\bar{G}] = (2n-m) \qquad (4.3.17)$$

then in fact

$$\Gamma_s > 0 \qquad (4.3.18)$$

Therefore, in order for the steady state solution Γ_s to define an ellipsoid, the condition for stable $(\bar{A} + \frac{1}{2}\beta I)$ must first be satisfied. In this case, Γ_s defines a steady state set, Ω_s, in accordance with (4.3.4), with the implication that if system starts with an initial state that is within Ω_s, i.e., $\underline{x}(0)\epsilon\Omega_s$, then the system state will lie within this set at all times.

The synthesis problem is then to find

(i) a positive free parameter β

(ii) a gain matrix for the observer, L

(iii) a gain matrix for the control, K

that yield a stable $(\bar{\Lambda} + \frac{1}{2}\beta I)$ and maximize Q subject to the Lyapunov equation (4.3.15), the output constraint, Eq. (4.3.11) or Eqn. (4.3.13) and the control constraint, Eqn. (4.3.8).

Chapter 5
SOLUTION PROCEDURE

5.1 Introduction

The main goal in this study is to be able to use a full state feedback control but only after the reconstruction of this state is accomplished in the form of a state estimate, $\hat{\underline{x}}$, when a whole or part of this state, $\underline{x}$, is not available. The control law used in this study is:

$$\underline{u} = K\hat{\underline{x}} \tag{5.1.1}$$

After stating our observation/control problem in a STC prespective, the synthesis problem was formulated in Section 4.3 as a constrained non-linear optimization problem of the form:

Determine: β,L and K that yield a maximum Q subject to:

1. Governing equation

$$(\overline{A}+\frac{1}{2}\beta I)\Gamma+\Gamma(\overline{A}+\frac{1}{2}\beta I)'+\frac{1}{\beta}\,\overline{G}Q\overline{G}'= 0 \tag{5.1.2}$$

2. Output constraint

$$\underline{\overline{H}}_i\Gamma\underline{\overline{H}}_i' \leq S_i^* \quad i=1,2,3...p \tag{5.1.3}$$

3. Control constraint

$$\underline{\overline{K}}_j \Gamma \underline{\overline{K}}_j' \leq T_j^* \qquad j=1,2,3,\ldots r \tag{5.1.4}$$

4. Beta constraint

$$\beta \geq 0 \tag{5.1.5}$$

5. Ellipsoidal representability constraint

$$(\overline{A}+\tfrac{1}{2}\beta I) \text{ is stable} \tag{5.1.6}$$

Two main approaches (1) for solving the non-linear constrained optimization problem posed above have been identified as:

(i) The Direct Search approach.

(ii) The Lagrange approach.

Figure 5.1.1 illustrates the different routes that are possible in each approach.

In the Direct Search approach, a search is performed over the independent variables and is restricted to the feasible region where all constraints are satisfied.

Usoro (1) developed a computer program based on the Direct Search approach where the problem was reduced to an unconstrained optimization problem. The control law (a full-state feedback control) used in (1) assumes availability and knowledge of the whole state, i.e.,

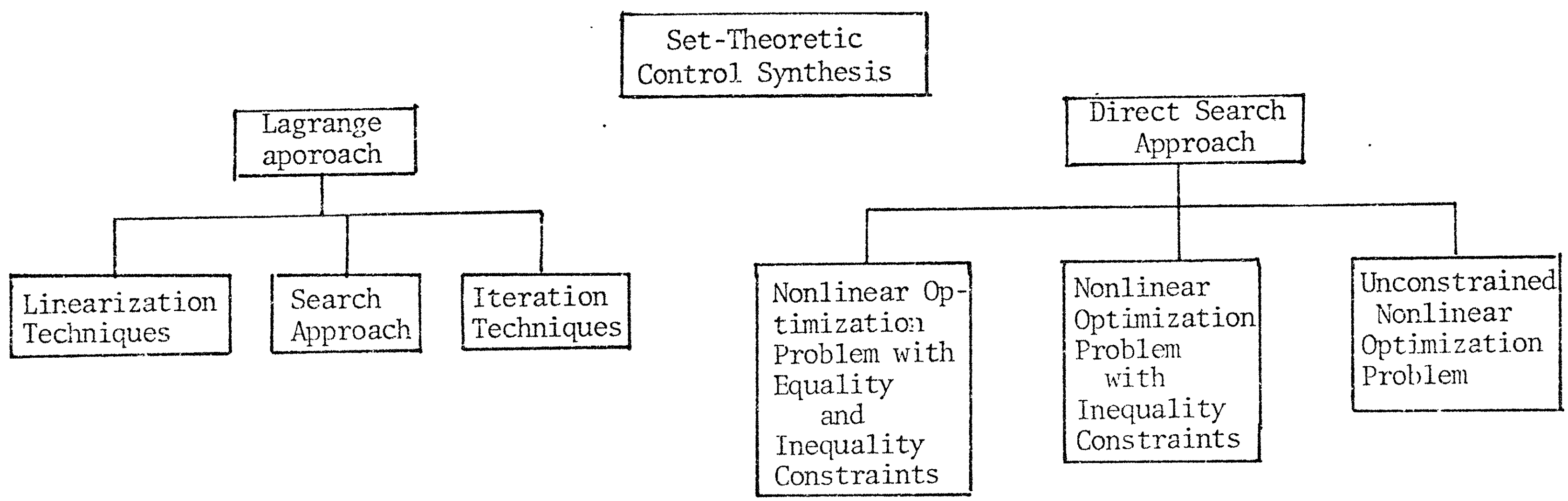

Fig. 5.1.1 Possible Set-Theoretic Control Synthesis Routes.

$$\underline{u} = K\underline{x} \tag{5.1.7}$$

In this study the emphasis is placed on including an extension to the already existing and working program developed in (1) so as to be able to use either the control law given by Eqn. (5.1.1) or the one given by Eqn. (5.1.7) at the choice of the designer. This study allows us to judge the effect on the control when we use a state estimate feedback instead of an original state feedback.

In the Lagrange approach, Lagrange multipliers in conjunction with Kunn-Tucker conditions are used to reduce the constrained nonlinear optimization problem to that of solving a set of simultaneous equations.

Recently, Negahdaripour (56) developed an algorithm based on the Lagrange approach. He asserts that the problem to be solved has been reduced in dimension and the computational time has been decreased in comparison to the Direct Search approach.

5.2 Solution Techniques:

As stated earlier, the synthesis problem is to maximize Q subject to Eqns. (5.1.2), (5.1.3), (5.1.4), (5.1.5) and (5.1.6). The special structure of this problem is exploited in reducing it from a constrained nonlinear optimization problem to an unconstrained optimization problem. To this end, assuming that β, L and K are suitably chosen, the matrix $(\bar{A}+\frac{1}{2}\beta I)$ will be known and then the Lyapunov equation, Eqn. (5.1.2), can be solved for Γ as a function of Q. For a scalar Q, the relationship between Γ and Q is linear and is given by (1):

$$\Gamma = \Theta Q \tag{5.2.1}$$

Substituting for Γ into Eqns. (5.1.2), (5.1.3) and (5.1.4), the governing equation, the output constraint and the control constraint become:

$$(\bar{A}+\tfrac{1}{2}\beta I)\theta + \theta(\bar{A}+\tfrac{1}{2}\beta I)' + \frac{1}{\beta} GG' = o \tag{5.2.2}$$

$$\underline{\bar{H}}_i \theta \underline{\bar{H}}_i' Q \leq S_i^* \qquad i=1,2,\ldots p \tag{5.2.3}$$

$$\underline{\bar{K}}_j \theta \underline{\bar{K}}_j' Q \leq T_j^* \qquad j=1,2\ldots r \tag{5.2.4}$$

It follows from the inequalities, Eqns. (5.2.3) and (5.2.4), that Q should satisfy:

$$Q \leq \frac{S_i^*}{\underline{\bar{H}}_i \theta \underline{\bar{H}}_i'} \qquad i=1,2,\ldots p \tag{5.2.5}$$

$$Q \leq \frac{T_j^*}{\underline{\bar{K}}_j \theta \underline{\bar{K}}_j'} \qquad j=1,2,\ldots r \tag{5.2.6}$$

In order to satisfy the output and control constraints, the objective function, Q, should be less than or equal to the smallest of the right-hand sides of the inequalities, Eqns. (5.2.5) and (5.2.6), that is:

$$Q = \min \left\{ \begin{array}{ll} S_i^*/(\underline{H}_i \theta \underline{H}_i') & i=1,2,\ldots p \\ T_j^*/(\underline{K}_j \theta \underline{K}_j') & j=1,2,\ldots r \end{array} \right. \tag{5.2.7}$$

By defining Q in this way, three of the constraints, Eqns. (5.1.2), (5.1.3) and (5.1.4) have been satisfied.

The two other constraints, non-negativeness of β and stability of $(\bar{A}+\frac{1}{2}\beta I)$, are checked by setting the objective function Q equal to zero whenever any of these constraints are violated, that is

$$\begin{array}{ll} \text{If } \beta < o; & Q = 0 \\ \text{If } (\bar{A}+\frac{1}{2}\beta I) \text{ is unstable;} & Q = 0 \end{array} \tag{5.2.8}$$

It is clear that by exploiting the special structure of the problem, it has been reduced to an unconstrained optimization problem but the starting point for β,L and K, must meet the conditions that $\beta \geq 0$ and $(\bar{A}+\frac{1}{2}\beta I)$ is stable.

The solution procedure is summarized as follows:

(i) Generate feasible starting matrices L and K and parameter β.

(ii) Given β, L and K, solve Eqn. (5.2.2) for θ.

(iii) Compute Q using Eqns. (5.2.7) and (5.2.8)

(iv) Search over L, K and β, and repeat steps (ii) and (iii) until the optimum Q is obtained.

Figure 5.2.1 shows a flow-chart for the solution procedure. It includes the two cases:

Case (i): the full-state $\underline{x}$ is available for feedback control.

Case (ii): a part of the state is not available and then an observer is used to reconstruct a state estimate $\hat{\underline{x}}$.

Note that in the case where the system is not observed, the Lyapunov equation and the objective function are given by:

$$(A+BK+\frac{1}{2}\beta I)\theta + \theta(A+BK+\frac{1}{2}\beta I)'+\frac{1}{\beta} GG'=0 \qquad (5.2.9)$$

$$Q = \begin{cases} S_i^*/(\underline{H}_i\theta\underline{H}_i') & i=1,2,\ldots p \\ T_j^*/(\underline{K}_j\theta\underline{K}_j') & i=1,2,\ldots r \end{cases} \qquad (5.2.10)$$

The difference between Eqn. (5.2.9) and Eqn. (5.2.2) is obvious. Matrix $\overline{A}$ has the form (See Eqn. (4.3.1))

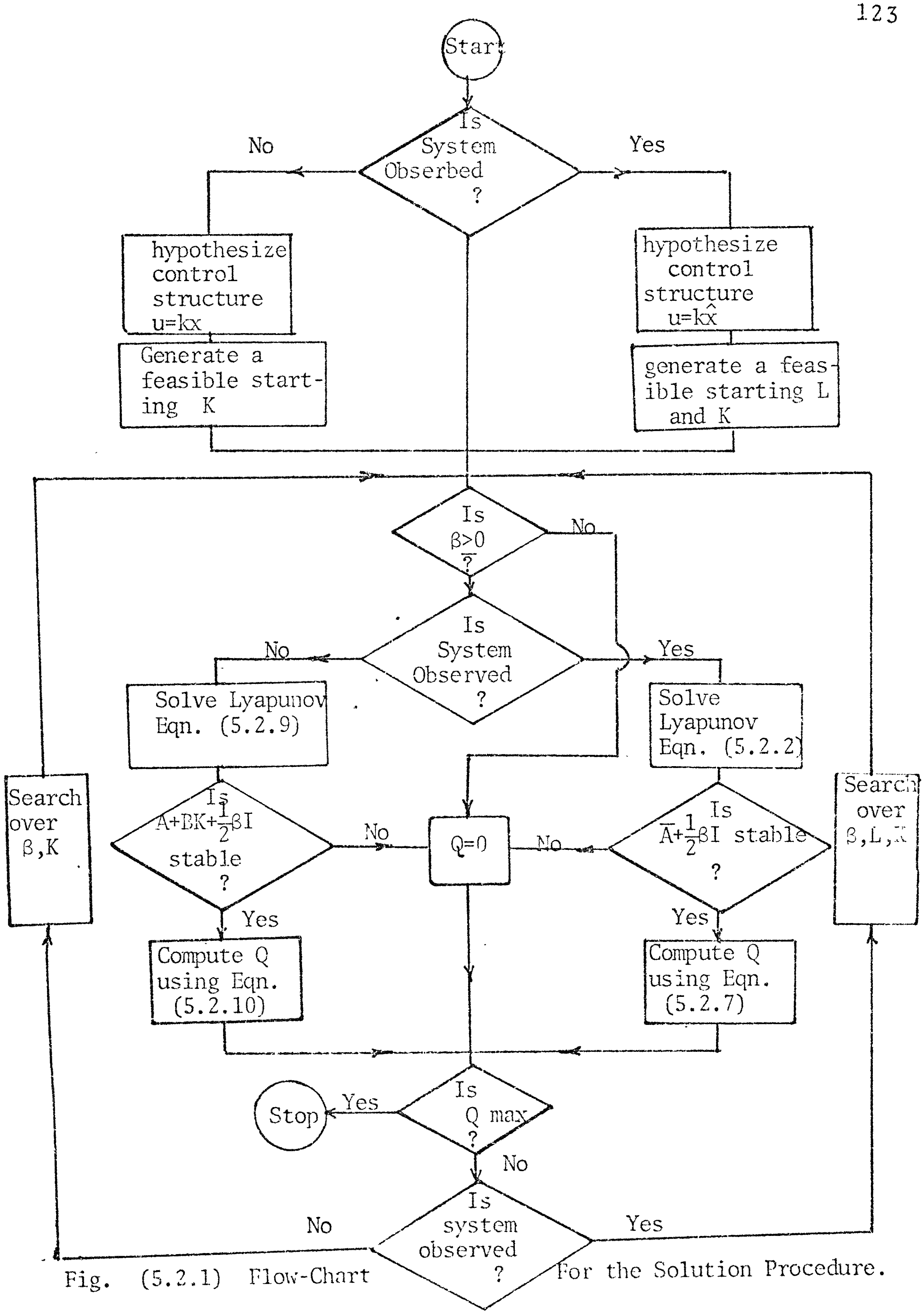

Fig. (5.2.1) Flow-Chart For the Solution Procedure.

$$\bar{A} = \left[\begin{array}{c|c} A+BK & BKS_2 \\ \hline 0 & P-LR \end{array}\right]; \tag{5.2.11a}$$

the relationship between $\bar{H}$ and H is given by Eqn. (4.3.9)

$$\bar{H} = [H\ 0]; \tag{5.2.11b}$$

and that between $\bar{K}$ and K is given by Eqn. (4.3.6)

$$\bar{K} = [K\ KS_2] \tag{5.2.11c}$$

Although the flow-chart in Fig. 5.2.1 defines the solution procedure, certain computational issues require consideration:

- Selecting a non-singular transformation for the case where an observer is used.
- Generating a feasible starting point.
- Solving the Lyapunov equation.
- Searching over the independent variables by using an optimization search method.

5.2.1 Selecting a Nonsingular Transformation:

A reduced-order observer requires a selection of a nonsingular transformation of the form (see Appendix B)

$$S = \begin{bmatrix} M \\ N \end{bmatrix}^{-1} \tag{5.2.12}$$

The nonsingular transformation requires a choice of a matrix N such that the square matrix S is well-conditioned. Matrix M given by Eqn. (4.2.3) is assumed to be linearly independent of rank m. Therefore, it is possible to select the (n-m)xn matrix N satisfying Eqn. (3.3.10), $\underline{\eta} = N\underline{x}$, where n is the order of $\underline{x}$ and m<n.

The nonsingular transformation S is achieved (57) by assigning the maximum value of M_{ij} to the elements of N on the diagonal of S^{-1}. Also the average value of the elements of M is assigned to appropriate locations in S^{-1} such that S becomes non singular. The method was originally implemented in the last version of the computer program OPTSYS of the Mechanical Engineering Department and adopted in this study.

5.2.2 Generating a Feasible Starting Point:

Generating a feasible starting point in the solution procedure means that β,L and K are selected such that

(i) $\beta \geq 0$

(ii) $(\bar{A} + \frac{1}{2}\beta I)$ is stable.

The first condition does not constitute any problem. For the second condition we need to generate a stabilizing K and a stabilizing L in order to make the matrix $(\bar{A} + \frac{1}{2}\beta I)$ stable.

It follows from the special structure of the matrix $\bar{A}$, given by Eqn. (5.2.11a) that the eigenvalues are prescribed by those of (A + BK) and (P-LR).

First for a stabilizing K, we know that the characteristic values of the matrix (A+BK) can be arbitrarily located in the complex plane by choosing K suitably if the pair (A,B) is controllable or at least stabilizable.

Bass (58) showed that for a controllable system described by:

$$\dot{\underline{x}} = A\underline{x} + B\underline{u}$$

$$\underline{u} = k\underline{x}$$

a stabilizing K is given by:

$$K = B'Z^{-1} \tag{5.2.13}$$

where Z = Z'>0 satisfies the Lyapunov equation:

$$[-(A+\gamma I)]Z + Z[-(A+\gamma I)]' = -2BB' \tag{5.2.14}$$

for some $\gamma > ||A||$, where $||A||$ is the norm of the matrix A. The norm is defined as:

$$||A|| = \underset{i}{\text{Max}}\{\sum_{j} A_{ij}\}$$

$$||A|| = \underset{j}{\text{Max}}\{\sum_{i} A_{ij}\} \tag{5.2.15}$$

Armstrong (58) relaxed Bass's requirement from complete controllability to stabilizability.

Second, for a stabilizing L, we know that the characteristic values of the matrix (P-LR) are identical to those of (P'-R'L') since:

$$\det[\lambda I-(P-LR)] = \det[\lambda I-(P'-R'L')] \qquad (5.2.16)$$

Matrix (P'-R'L') has the same structure as the matrix (A+BK). Therefore, the characteristic values of (P'-R'L') can be arbitrarily located by choosing L' appropriately if the pair (P',R') is completely controllable. From Chapter 3, we know that the pair (P',R') is completely controllable if (P,R) is reconstructible. If this condition were satisfied the generation of a stabilizing L' becomes similar to that of a stabilizing K by using Bass algorithm.

The Bass algorithm was originally implemented in Usoro's work (1) for the generation of a stabilizing K and it is adopted in this study to generate both K and L.

5.2.3 Solving the Lyapunov Equation

In the solution of this problem, the Lyapunov Equation appears two times. It is the governing equation: (5.2.2) if the system is observed and (5.2.9) if it is not and the second time in Bass subroutine for the generation of stabilizing K and L. There are several methods for solving the Lyapunov equation. These are (59):

(i) Direct Solution Methods

(ii) Iterative Solution Methods

(iii) Transformation Solution Methods.

In transformation solution methods, the Lyapunov equation is reduced by similarity transformations to some structure easier to solve. For example in the Bartels-Stewart algorithm (60), the system is reduced to a real Schur form by orthogonal similarity transformations. The Bartels-Stewart algorithm was adopted in Usoro's work (1) because of its computational speed and because it does generate eigenvalues as by-products. This algorithm is retained in this study.

5.2.4 Optimization Search Method:

The search over the independent variables (β, the elements of the gain matrix K, and the elements of the observation matrix L) is performed by Powell method (61). The method is illustrated in the flow-chart presented in Fig. 5.2.2 (61). In this method, the iterative procedure involves carrying out a succession of single variable searches in each of "n" sets of independent directions beginning initially with the coordinate directions where "n" is the order of the problem. Powell search method was adopted originally by Usoro (1) is retained in this study

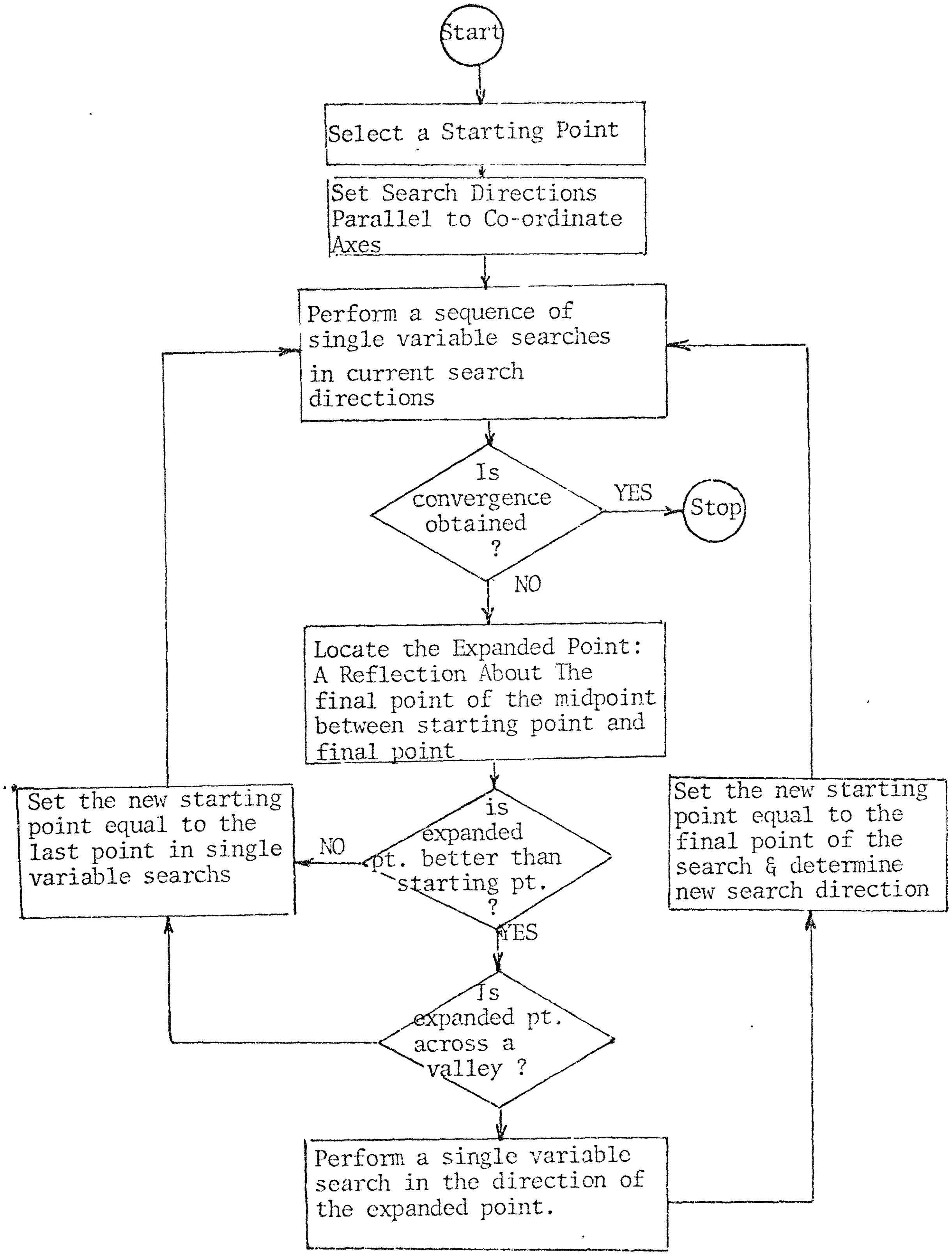

Fig. 5.2.2 A flowchart of the Powell's method.

because it has been reported by others (62) as effective in related fields. Note that Powell's method assume unimodel objective functions and so in order to obtain global optima for multi-modal functions the use of several starting points is recommended.

5.3 Description of the Computer Program

Two programs for solving the problem posed in this study have been developed based on the techniques discussed in Section 5.2. The structures of these programs are similar in all points of view except in the nonsingular transformation. One of the two programs contains the nonsingular transformation as discussed in Section 5.2.1. In this case the input system matrices are: A, B, $\underline{G}$, H, D, $\underline{E}$ and M. The program select a matrix N such that the nonsingular matrix S given by Eqn. (5.2.12) is well conditioned. The matrices P and R are computed directly according to the partitioning of the system matrix given by Eqn.(B7). The second program does not contain this option. Therefore, the partitioning of the system matrix is performed externally and then the matrices P and R are supplied to the input data in addition to A, B, $\underline{G}$, H, D, $\underline{E}$ and M.

For a starting point, a positive "β" is supplied by the designer and stabilizing K and L are generated using

Bass algorithm. Another option exists that a starting point is selected by the designer using any suitable method. It should be noted that the condition on γ_1 that is $(\gamma_1 \geq ||A+\frac{1}{2}\beta I||)$ and on γ_2 that is $(\gamma_2 \geq ||P'+\frac{1}{2}\beta I||)$ in the Bass Algorithm is not a necessary condition and so $\gamma_1 \leq ||A+\frac{1}{2}\beta I||$ and $\gamma_2 \leq ||P'+\frac{1}{2}\beta I||$ may be tried and this may in some cases yield good starting points. When the option is to use Bass algorithm to generate a starting point, the designer must scan the search region by suitably varying β, γ_1 and γ_2 and decide on the "best" starting point to adopt. This procedure greatly improves the chances of obtaining a global optimum for a multi-modal function, and may reduce the computation time required to obtain the solution. When the other option is used, the best parameter β is that is less than twice the smallest eigenvalue of the closed loop system in absolute value (β must be positive).

The objective function value is computed as described in Section 5.2 and illustrated in Fig. 5.2.1. The search over the independent variables is performed using Powell method as illustrated in Fig. 5.2.2. Although Powell method is adopted in this study, any suitable nonlinear optimization method can in fact be employed in place of Powell method.

Both of the two programs contain the two options for solving the Set-theoretic control problem at the choice of the designer as shown in Fig. 5.2.3.

- Option (i): the case where the full-state $\underline{x}$ is available or assumed available for a feedback control. This constitutes the original program developed by Usoro (1).

- Option (ii): the case where a part of the state $\underline{x}$ is not available and then a reduced-order observer is used to reconstruct a state estimate $\hat{\underline{x}}$. This constitutes an extension developed in this study.

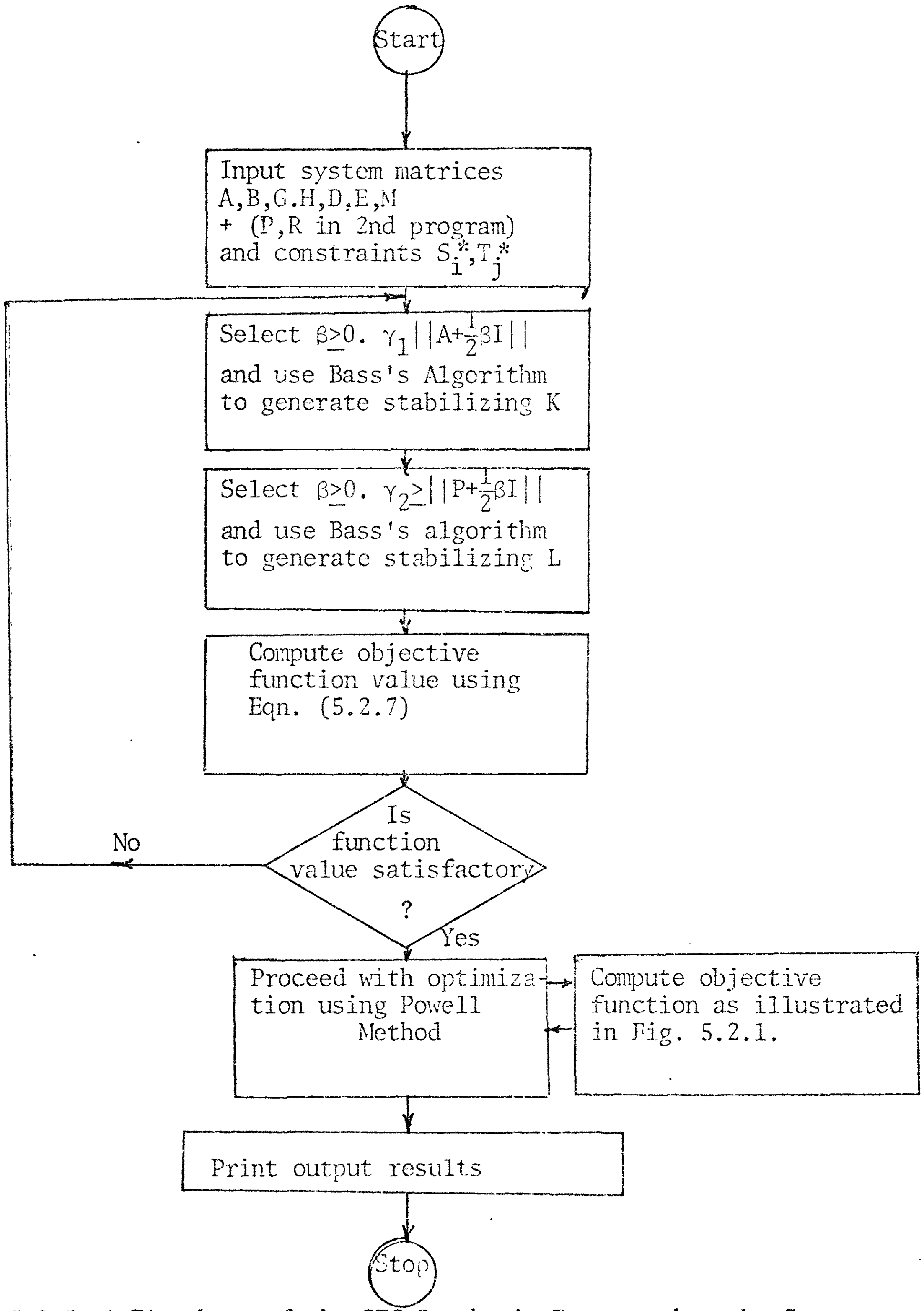

Fig. 5.2.3 A Flowchart of the STC Synthesis Program when the System is Observed.

Chapter 6

APPLICATIONS AND RESULTS

6.1 Introduction

The need to adequately control the PWR power plant was emphasized in Chapter 2. It was stated that the goal is to coordinate the reactor control rods and the turbine throttle valves so as to avoid large deviations in plant variables. Keeping the plant variables within prespecified bounds at all times is a major requirement for the acceptability of the performance of the system. In Chapter 4, it was shown that this class of problems is better addressed by using Set-Theoretic Control technique. The application in this Chapter consists of:

(i) constructing a full-state feedback control system which employes an observer to reconstruct the state estimate when not all the components of the state vector are available for measurement.

(ii) determining the maximum input disturbance amplitude which the system can tolerate without violation of the state and control constraints following the solution procedure presented in Chapter 5.

(iii) Simulating time responses of potential system states and controls in presence of input disturbances. The simulations are obtained from time integration of the associated governing dynamic equations using a fourth-order Runge-Kutta integration routine, DYSYS (63).

Before we proceed to the application to the power plant, the solution procedure is illustrated with a 3rd order system in order to give an insight into the steps to follow.

6.2 Illustrative Example

Consider a third-order marginally stable system described by

$$\begin{bmatrix} \dot{x}_1 \\ \dot{x}_2 \\ \dot{x}_3 \end{bmatrix} = \begin{bmatrix} 0 & 1 & 0 \\ 0 & 0 & 1 \\ 0 & -1 & 0 \end{bmatrix} \begin{bmatrix} x_1 \\ x_2 \\ x_3 \end{bmatrix} + \begin{bmatrix} 0 \\ 0 \\ 1 \end{bmatrix} u + \begin{bmatrix} 1 \\ 1 \\ 1 \end{bmatrix} w \tag{6.2.1}$$

$$z = x_1 = [1 \;\; 0 \;\; 0] \begin{bmatrix} x_1 \\ x_2 \\ x_3 \end{bmatrix} \tag{6.2.2}$$

$$\underline{y} = \begin{bmatrix} x_1 \\ x_3 \end{bmatrix} = \begin{bmatrix} 1 & 0 & 0 \\ 0 & 0 & 1 \end{bmatrix} \begin{bmatrix} x_1 \\ x_2 \\ x_3 \end{bmatrix} \tag{6.2.3}$$

where,

z is the measurement output

$\underline{y}$ is the system output vector.

The constraints imposed on the state variables and the control are given as:

$$|x_1| \leq 1.0$$

$$|x_3| \leq 1.0$$

$$|u| \leq 1.0$$

The problem is to find a control u to keep the system state and control within constraint limits in the presence of the input disturbance w.

It is clear from Eqn. (6.2.2) that we have two inaccessible state variables: x_2 and x_3. In this case we need to use an observer to reconstruct the whole state vector $\underline{x}$. The observer reconstructs a state estimate $\hat{\underline{x}}$ from the measured output z. A hypothesized structure for a full-state feedback control is

$$u = K\hat{\underline{x}} \tag{6.2.4}$$

We shall design a reduced-order observer since it is cheaper to design and implement. A sufficient condition for the existence of the reduced order observer is the observability of the system.

The observability matrix is:

$$[M' \quad A'M' \quad A'^2M'] = \begin{bmatrix} 1 & 0 & 0 \\ 0 & 1 & 0 \\ 0 & 0 & 1 \end{bmatrix}$$

Since the rank of the observability matrix is 3, the system is observable.

Let us define a new state vector $\underline{x}_1$ given by:

$$\underline{x}_1 = \left[\frac{z}{\underline{\eta}}\right] = \begin{bmatrix} x_1 \\ \hline x_2 \\ x_3 \end{bmatrix} \tag{6.2.5}$$

The non-singular transformation relating the state vector $\underline{x}$ to the new state vector $\underline{x}_1$ is given by

$$\underline{x}_1 = \left[\frac{z}{\underline{\eta}}\right] = \left[\frac{M}{N}\right] \underline{x} \tag{6.2.6}$$

where,

$$z = M\underline{x}$$

$$\underline{\eta} = N\underline{x}.$$

The matrix M is known and given by Eqn. (6.2.2). A good choice of the matrix N is

$$N = \begin{bmatrix} 0 & 1 & 0 \\ 0 & 0 & 1 \end{bmatrix} \tag{6.2.7}$$

Eqn. (6.2.6) becomes

$$\underline{x}_1 = \begin{bmatrix} 1 & 0 & 0 \\ \hline 0 & 1 & 0 \\ 0 & 0 & 1 \end{bmatrix} \underline{x}$$

$$\text{i.e., } \underline{x}_1 = \underline{x} \tag{6.2.8}$$

It happens in this example that the non-singular transformation is an identity matrix but this is not always the case. The inverse of this matrix is:

$$\left[\frac{M}{N}\right]^{-1} = [S_1 \; S_2]$$

i.e.,

$$S_2 = \begin{bmatrix} 0 & 0 \\ 1 & 0 \\ 0 & 1 \end{bmatrix} \tag{6.2.9}$$

From Eqn. (6.2.6) we get

$$\underline{x} = \left[\frac{M}{N}\right]^{-1} \left[\frac{z}{\underline{\eta}}\right] = [S_1 \; S_2] \left[\frac{z}{\underline{\eta}}\right]$$

$$\underline{x} = S_1 z + S_2 \underline{\eta} \tag{6.2.10}$$

and similarly

$$\hat{\underline{x}} = S_1 z + S_2 \hat{\underline{n}} \qquad (6.2.11)$$

It is preferable to express $\hat{\underline{x}}$ in terms of $\underline{x}$ and the error vector $\underline{e}$ where,

$$\underline{e} = \hat{\underline{n}} - \underline{n} \qquad (6.2.12)$$

Eqn. (6.2.11) becomes

$$\begin{aligned}\hat{\underline{x}} &= S_1 z + S_2\hat{\underline{n}} - S_2\underline{n} + S_2\underline{n} \\ &= S_1 M\underline{x} + S_2 N\underline{x} + S_2(\hat{\underline{n}}-\underline{n}) \\ &= (S_1 M + S_2 N)\underline{x} + S_2\underline{e} \\ &= \underline{x} + S_2\underline{e} \qquad (6.2.13)\end{aligned}$$

where $(S_1 M + S_2 N) = I(3x3)$.

Substituting for $\hat{\underline{x}}$ in Eqn. (6.2.4), the control law becomes

$$\begin{aligned}u &= K\underline{x} + KS_2\underline{e} \\ &= [K \quad KS_2] \begin{bmatrix}\underline{x} \\ \underline{e}\end{bmatrix} \\ &= \overline{K}\,\overline{\underline{x}} \qquad (6.2.14)\end{aligned}$$

By following the remaining steps from Appendix B, we find that the error dynamics are given by:

$$\dot{\underline{e}} = (A_{22}-LA_{12})\ \underline{e}(t) \tag{6.2.15}$$

where,

$$A_{22} = \begin{bmatrix} 0 & 0 \\ -1 & 0 \end{bmatrix}, \quad A_{12} = [1 \quad 0]$$

It becomes clear from Eqn. (6.2.14) that if we were able to eliminate completely the error vector $\underline{e}$ or at least to make it die out quickly by an appropriate choice of L, we would then be practically feeding back the original state vector $\underline{x}$.

Combining Eqns. (6.2.1), (6.2.14) and (6.2.15), we get

$$\begin{bmatrix} \dot{x}_1 \\ \dot{x}_2 \\ \dot{x}_3 \\ \hline \dot{e}_1 \\ \dot{e}_2 \end{bmatrix} = \left[\begin{array}{ccc|c} & A+BK & & BKS_2 \\ \hline 0 & 0 & 0 & A_{22}-LA_{12} \\ 0 & 0 & 0 & \end{array}\right] \begin{bmatrix} x_1 \\ x_2 \\ x_3 \\ \hline e_1 \\ e_2 \end{bmatrix} + \begin{bmatrix} 1 \\ 1 \\ 1 \\ \hline 0 \\ 0 \end{bmatrix} w \tag{6.2.16}$$

Note that if the disturbance were not observed, the error dynamics will be governed by (see Appendix B).

$$\dot{\underline{e}}(t) = (A_{22} - LA_{12})e(t) - T\underline{G}w \tag{6.2.17}$$

where

$$T = [-L \ \ I_\eta]$$

In order to compute the maximum allowable input disturbance, the constraints on the state variables and the control are translated into the form given by Eqns. (4.2.10) and (4.2.13) as follows:

$$S_1^* = (1.0)^2 = 1.0; \quad S_1^* \text{ is a number}$$
$$S_2^* = (1.0)^2 = 1.0; \quad S_2^* \text{ is a number}$$
$$T_1^* = (1.0)^2 = 1.0$$

The maximum allowable input disturbance is computed by using Eqn. (5.2.7)

$$Q = \min \begin{cases} S_i^*/(\bar{H}_i \theta \bar{H}_i') & i=1,2 \\ T_j^*/(\bar{K}_j \theta \bar{K}_j) & j=1 \end{cases} \qquad (6.2.18)$$

where,

$$\bar{H} = \begin{bmatrix} 1 & 0 & 0 & 0 & 0 \\ 0 & 0 & 1 & 0 & 0 \end{bmatrix}$$

$$\bar{K} = [K \quad KS_2]; \qquad S_2 \text{ is a matrix.}$$

The problem is solved by using the computer program described in Chapter (5) for the following three cases:

(i) assuming a full-state feedback of the structure $\underline{u} = k\underline{x}$ where all the states are assumed known. In this case:

$$\dot{\underline{x}} = (A+BK)\underline{x} + \underline{G}w$$

and $$Q = \min \begin{array}{ll} S_i^*/(H_i \theta H_i') & i=1,2 \\ T_j^*/(K_j \theta k_j') & j=1 \end{array}$$

(ii) using a reduced order-observer. In this case the governing equations are given by Eqn. (6.2.16) and Q is computed from Eqn. (6.2.18).

(iii) using a reduced order-observer but we assume that the disturbance is not observed. In this case we substitute Eqn. (6.2.17) for Eqn. (6.2.15) in the governing equations and then use Eqn. (6.2.18) for the computation of Q.

The results are summarized in Table 6.2.1 .

It is clear that Case 2 is very close to Case 1, whereas Case 3 does not represent the right picture since an input is not fed to the observer. We, therefore, deduce that in order to have a true state reconstruction all inputs supplied to the original system must be supplied to the observer.

TABLE (6.2.1)

Results of the Illustrative Example

		System Not Observed	System Observed	
			Disturbance Observed	Disturbance Not Observed
Free Parameter	β	0.5863	0.5837	0.59456
Maximum tolerable amplitude of the disturbance	$Q^{\frac{1}{2}}$	0.21118	0.21113	0.198348
Control Gains	K_{11}	-1.4994	-1.4808	-4.8232
	K_{12}	-1.9507	-1.9055	-3.1222
	K_{13}	-2.2526	-2.1983	-3.7592
Observation Gains	L_{11}		6.1135	1.3702
	L_{21}		5.3298	-0.031811
Closed-loop Eigenvalues	λ_1	-0.85365	-0.83894	-0.42338+j1.2152
	λ_2	-0.6995+j1.1257	-0.67969+j1.1415	-0.42338-j1.2152
	λ_3	-0.6995-j1.1257	-0.67969-j1.1415	-2.9124
	λ_4		-4.7928	-0.68512+j0.70626
	λ_5		-1.3207	-0.68512-j0.70626

Case 2 shows that by an appropriate design of the observer, i.e., a good selection of the observation gain matrix L, we can obtain virtually the same control gain matrix K as with a full-state feedback.

The response characteristics of the three cases were investigated by simulation studies of their transient responses to a step input. In each case the step input is the maximum tolerable amplitude of the disturbance. The cases were run at zero steady state conditions for two seconds before being subjected to the disturbance as shown in the figures. In these figures, the numbers stand for the different variables as indicated in Table 6.2.2. Figure 6.2.1 shows the disturbance $Q^{\frac{1}{2}}$ for each case where the values are given in Table 6.2.1. The time responses of the states x_1,x_2, and x_3 and the control u are illustrated in Fig. 6.2.2, 6.2.3, 6.2.4, and 6.2.5 respectively. The observer was subjected to a severe condition since the errors on the non-measured states x_2 and x_3 were given an initial value of 10% of the maximum deviation of x_2 and x_3 respectively as shown in Fig. 6.2.6 and 6.2.7. The observer is designed such that the errors die out quickly. For case 2, errors do in fact die out rapidly whereas for case 3, they do not. Even under this severe condition the similarity between cases (1) and

Table 6.2.2

Indication of the Different Variables
of the Marginal System

Variables	Case (1)	Case (2)	Case (3)
*<u>States</u>			
x_1	1	4	9
x_2	2	5	10
x_3	3	6	11
*<u>Errors</u>			
e_1 in x_2		7	12
e_2 in x_3		8	13
*<u>Control</u>			
u	14	15	16
*<u>Disturbance</u>			
w	17	18	19

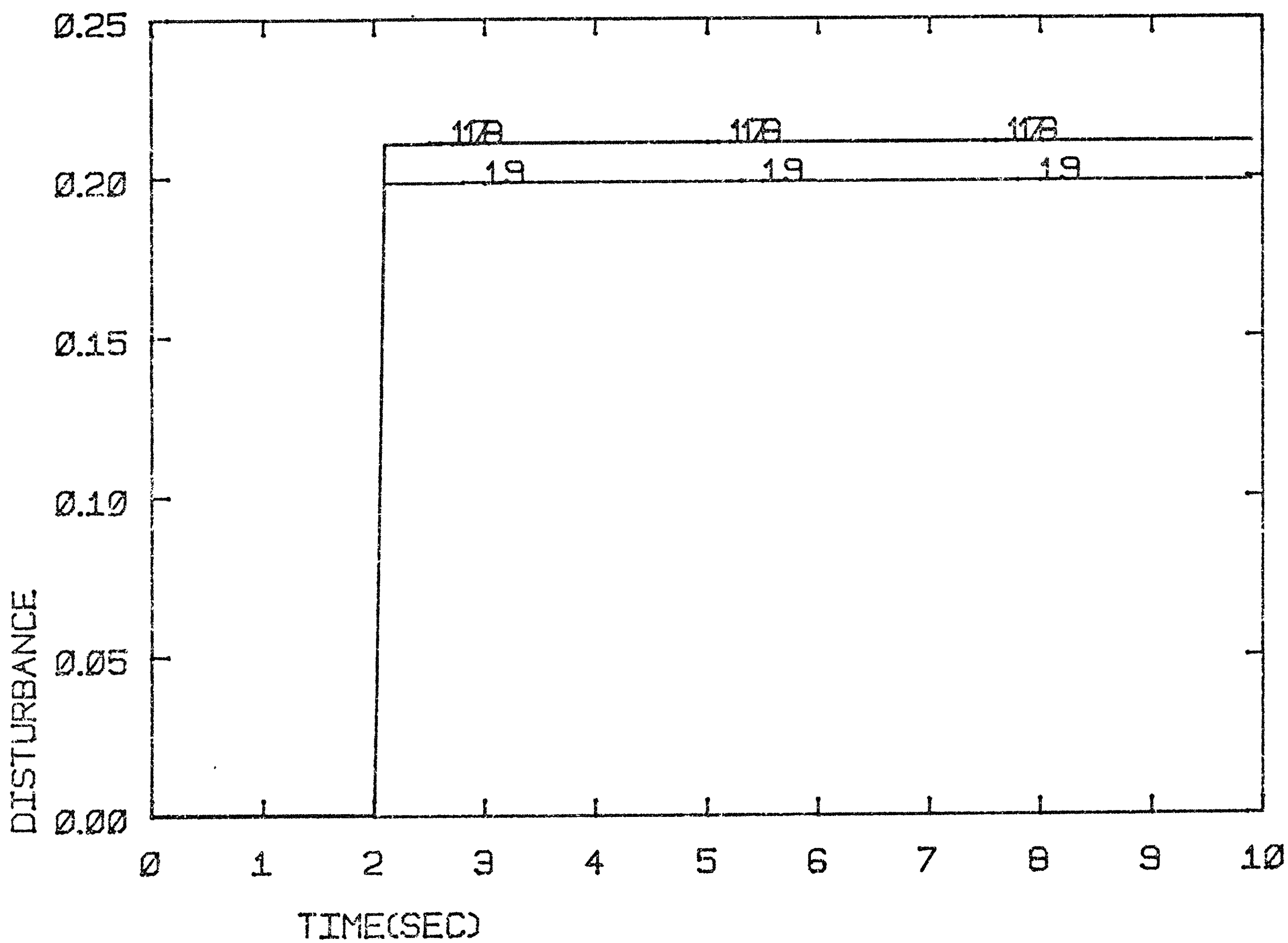

Fig. 6.2.1. Maximum Tolerable Disturbance Amplitude

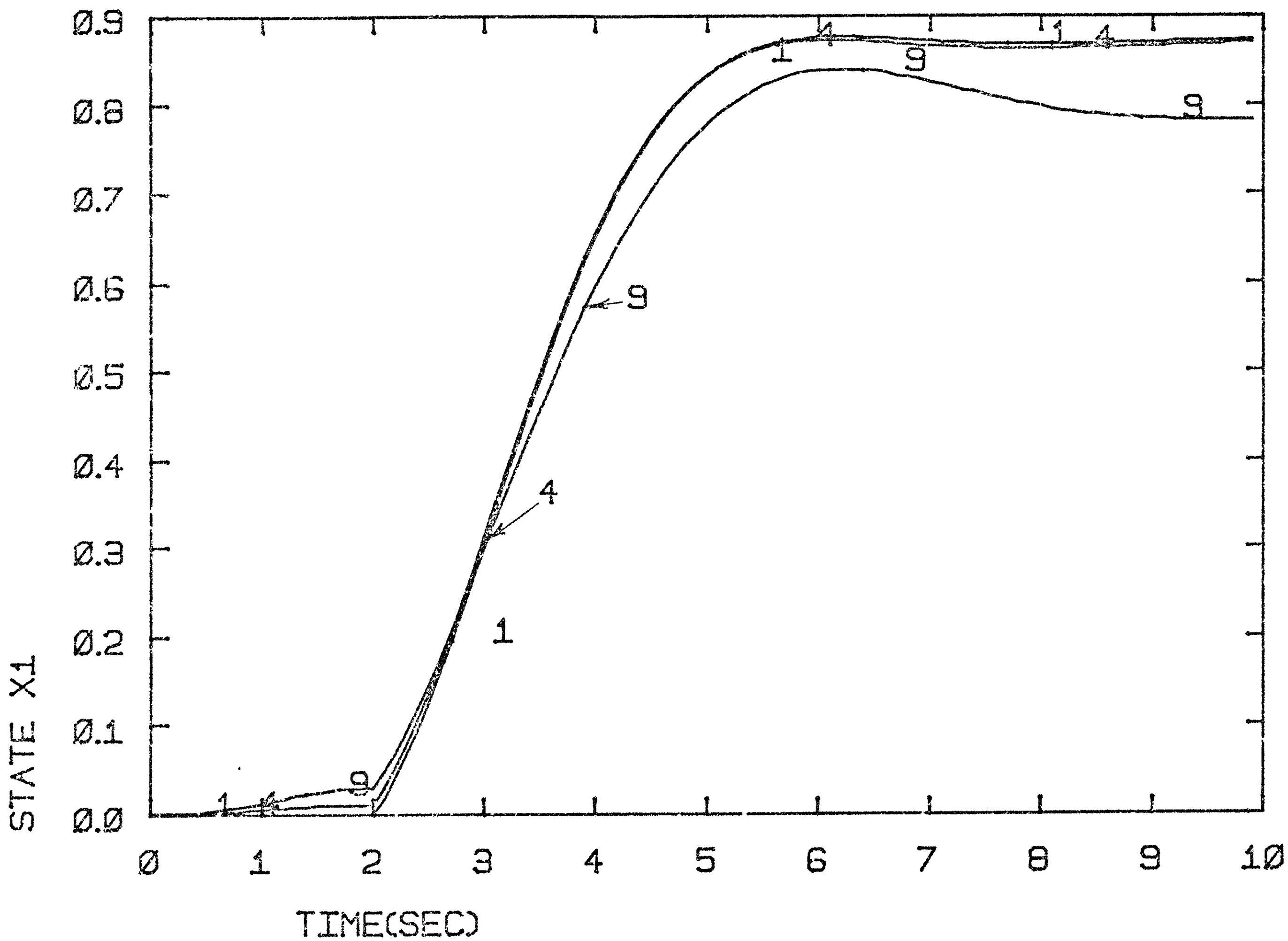

Fig. 6.2.2 Step Response of State x_1.

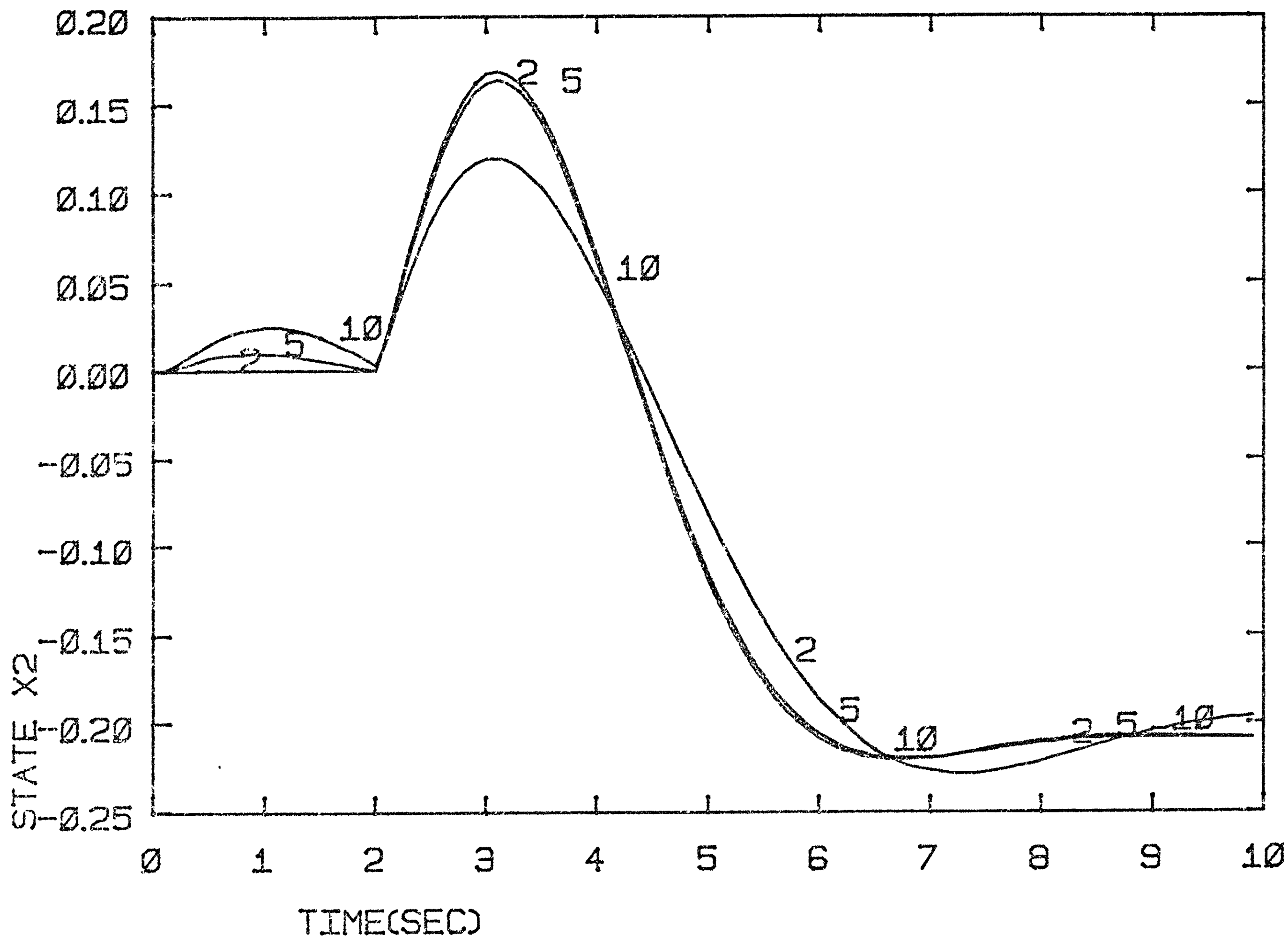

Fig. 6.2.3 Step Response of State x_2.

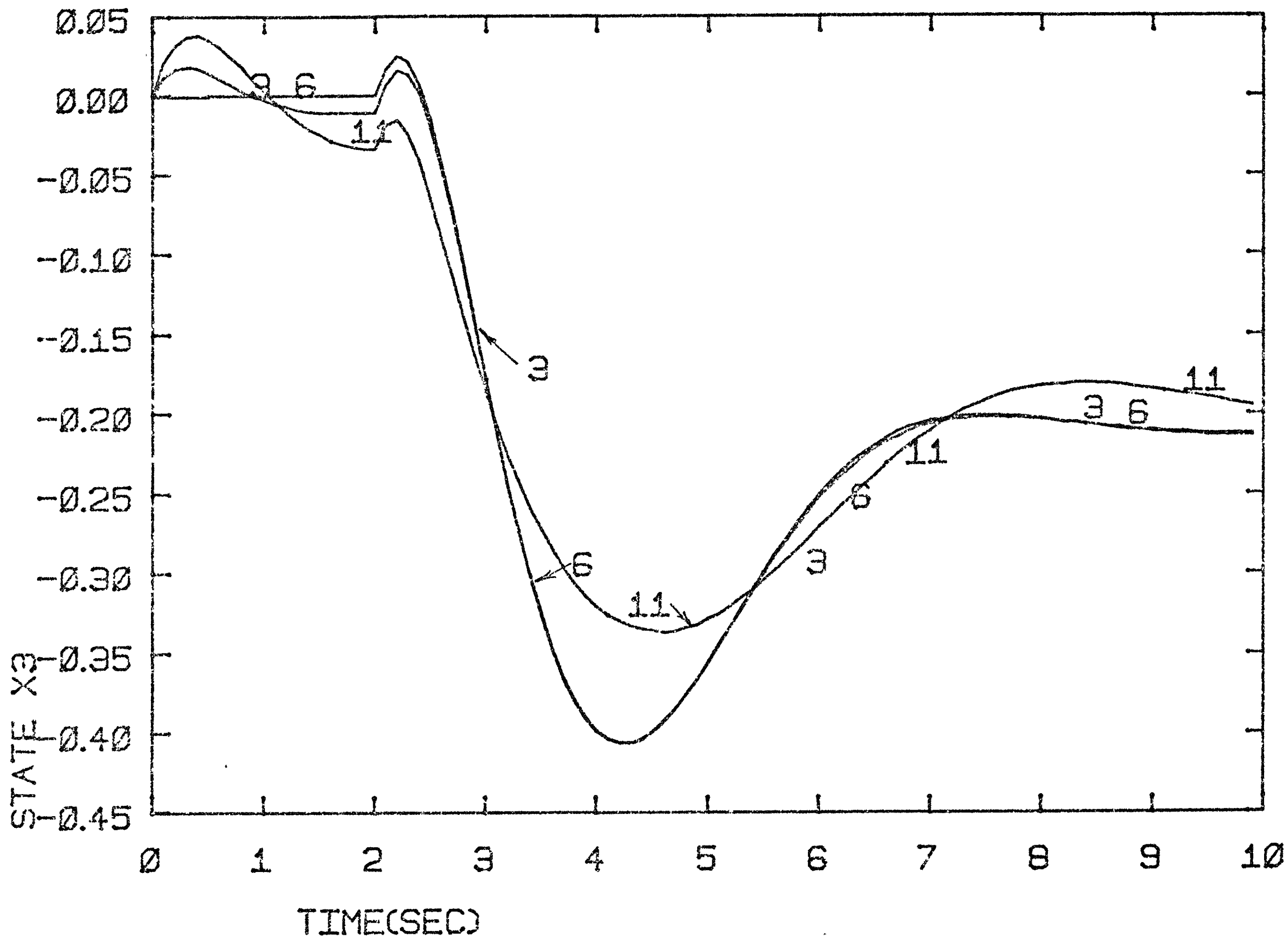

Fig. 6.2.4 Step Response of State x_3.

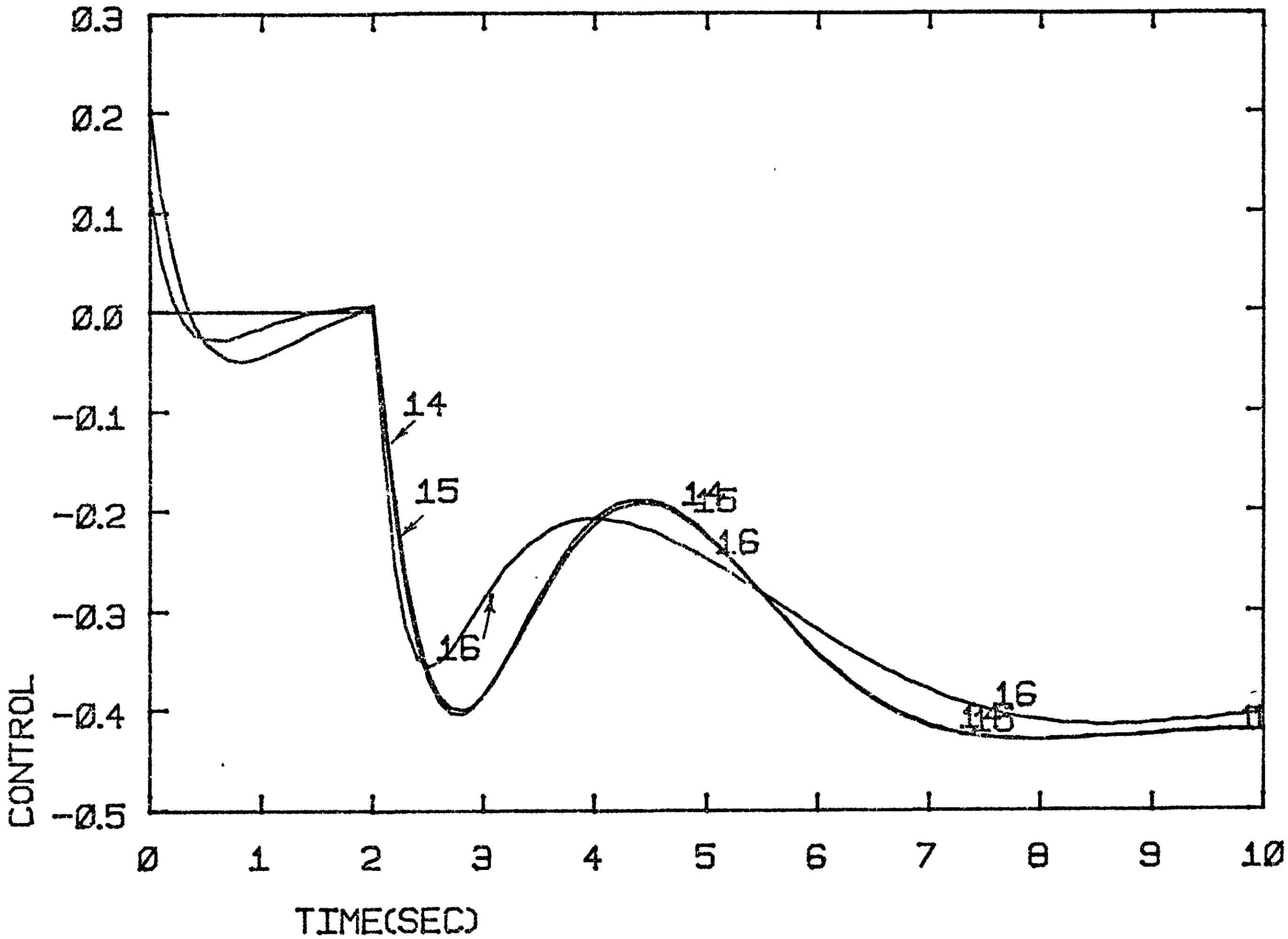

Fig. 6.2.5 Step Response of Control u.

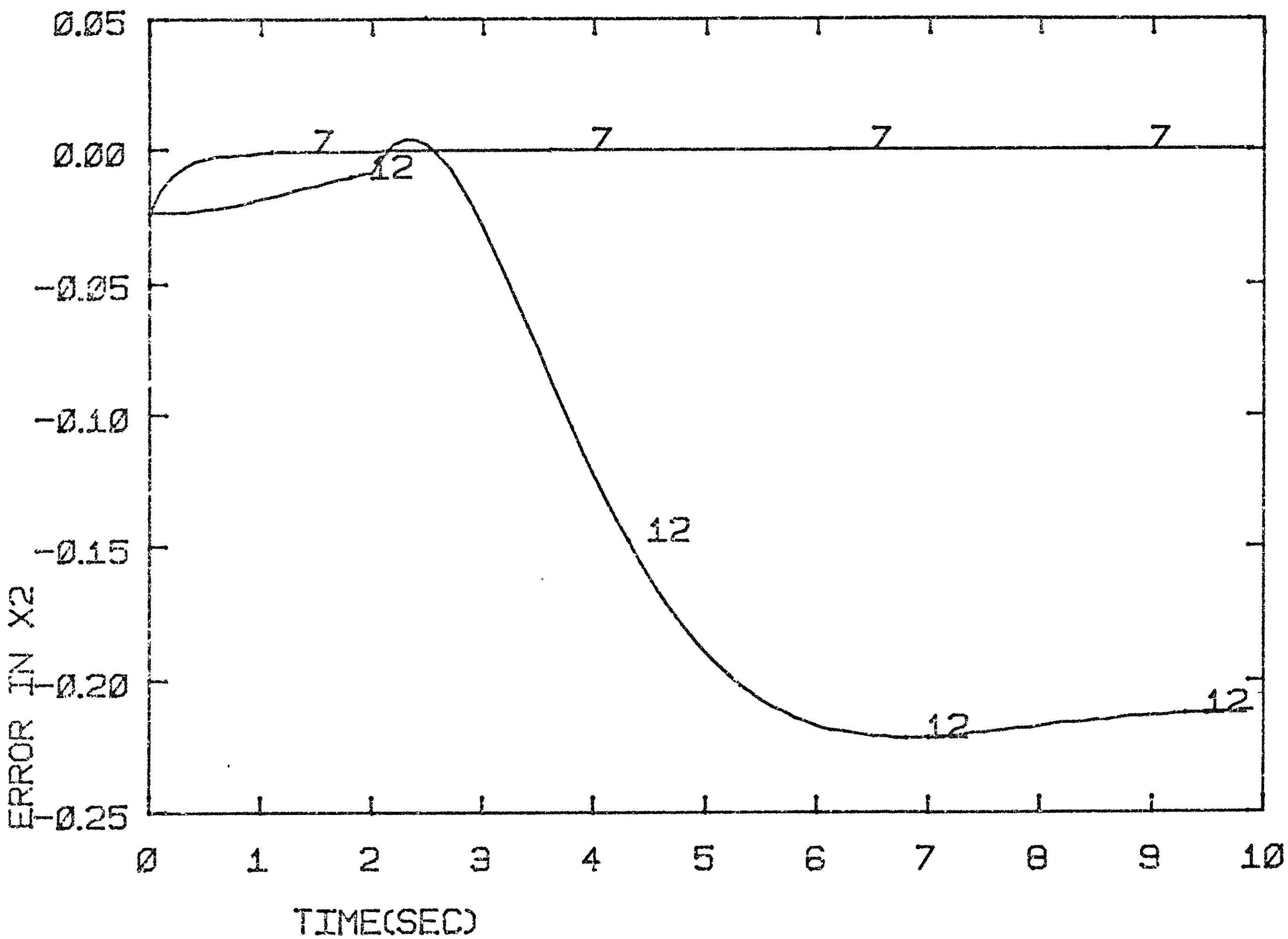

Fig. 6.2.6 Time Response of Error in x_2.

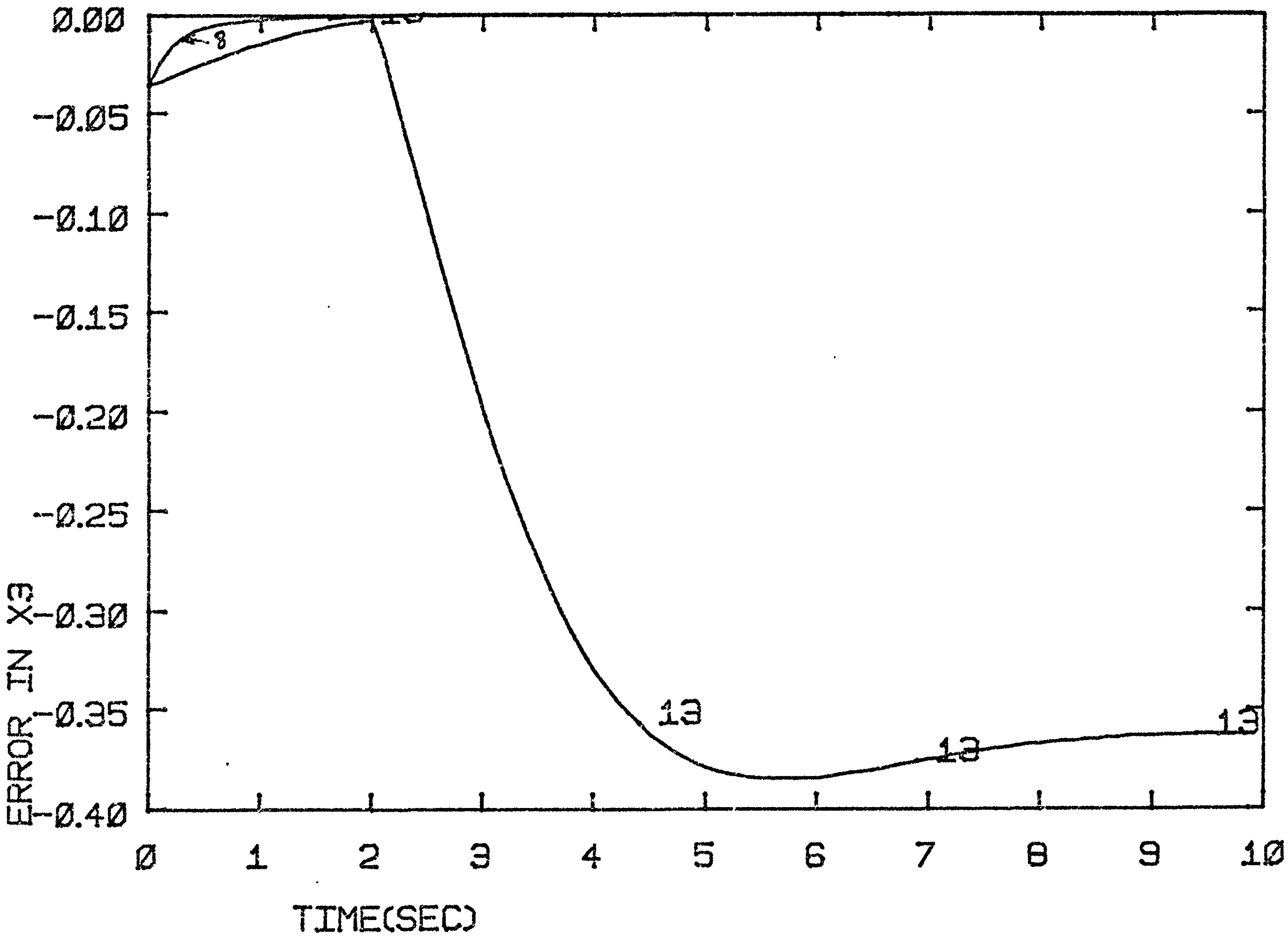

Fig. 6.2.7 Time Response of Error in x_3.

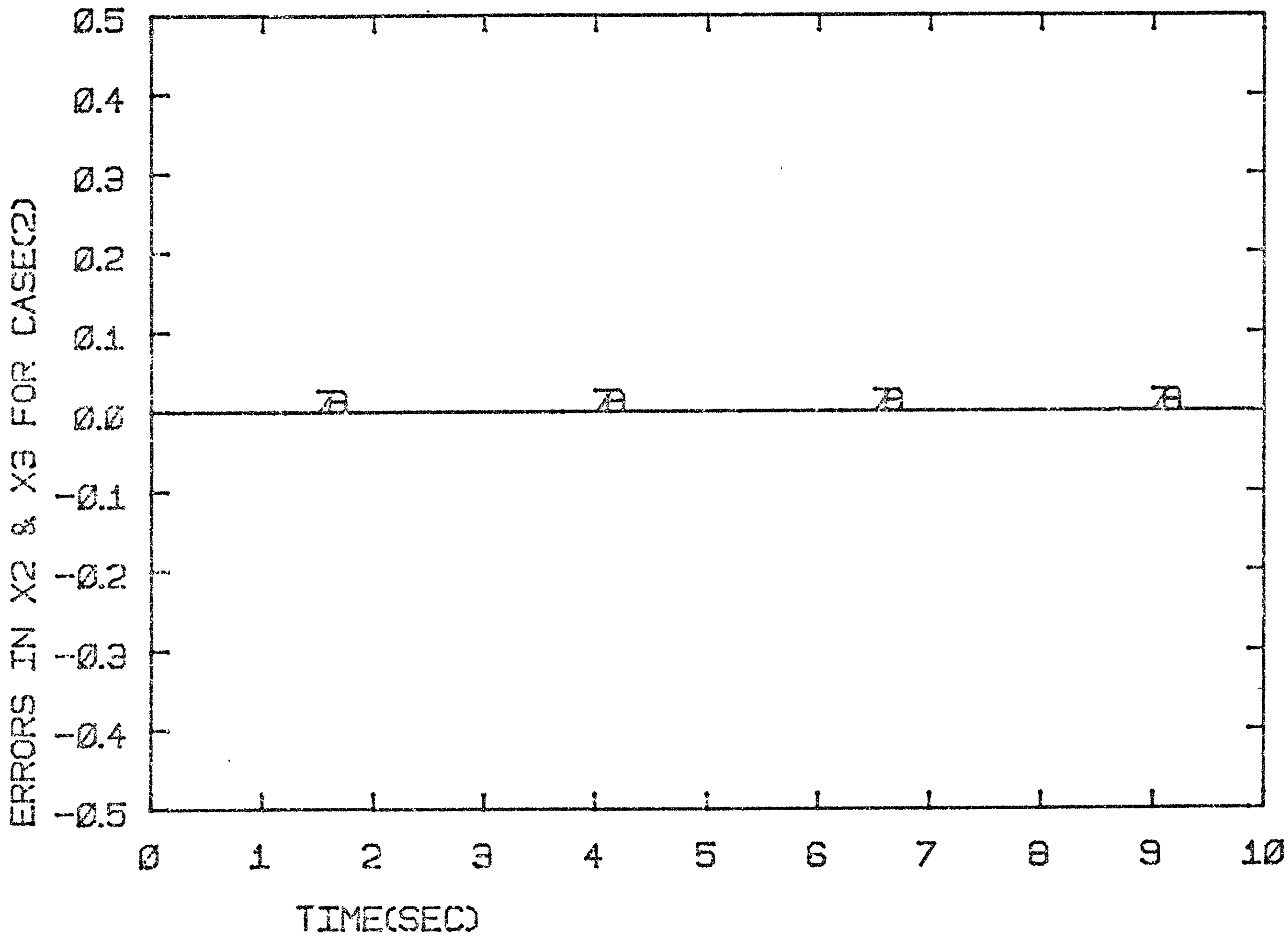

Fig. 6.2.8 Time Response of Errors When $\underline{e}(o)=o$.

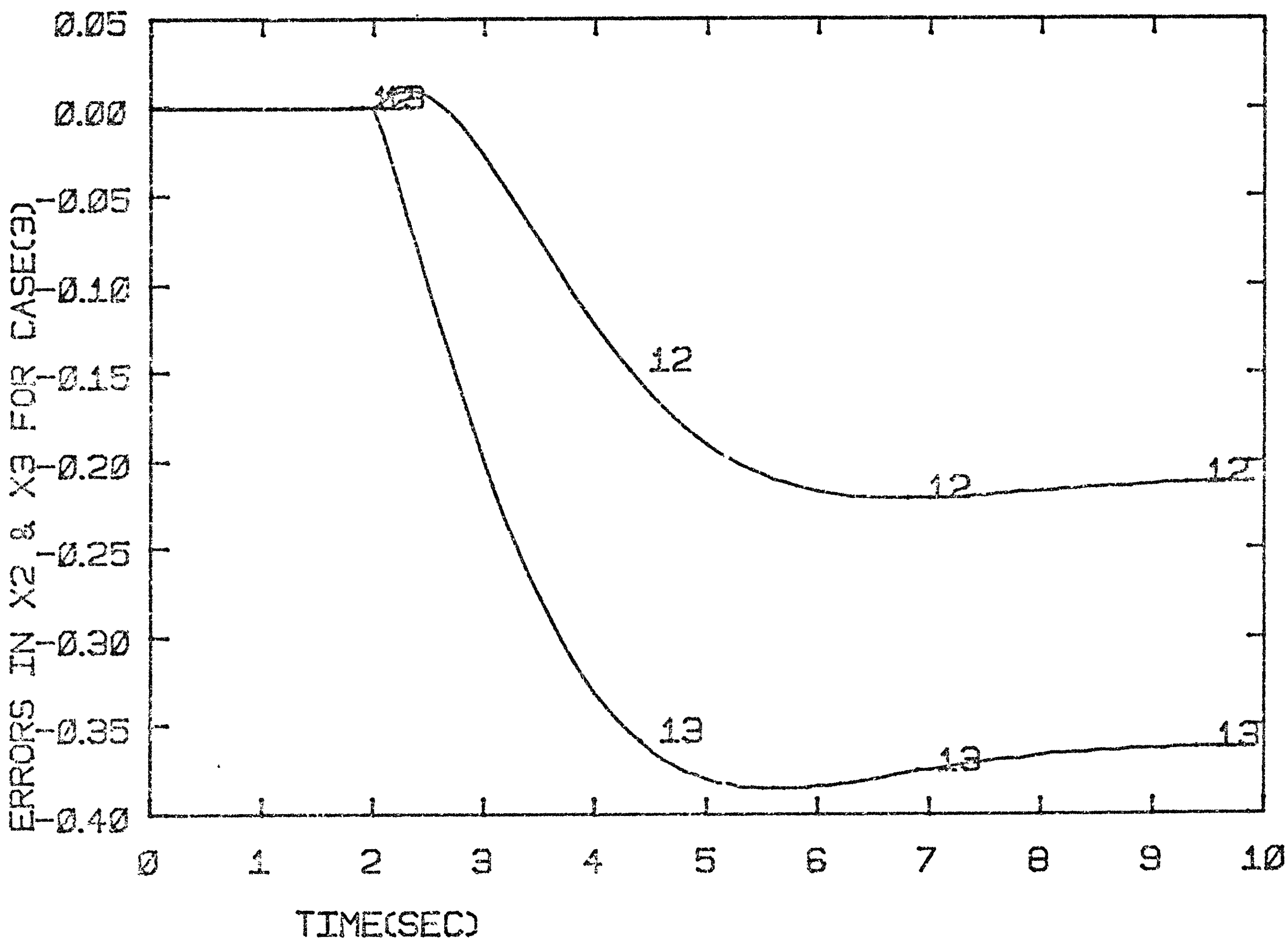

Fig. 6.2.9 Time Response of Errors When $\underline{e}(o)=o$.

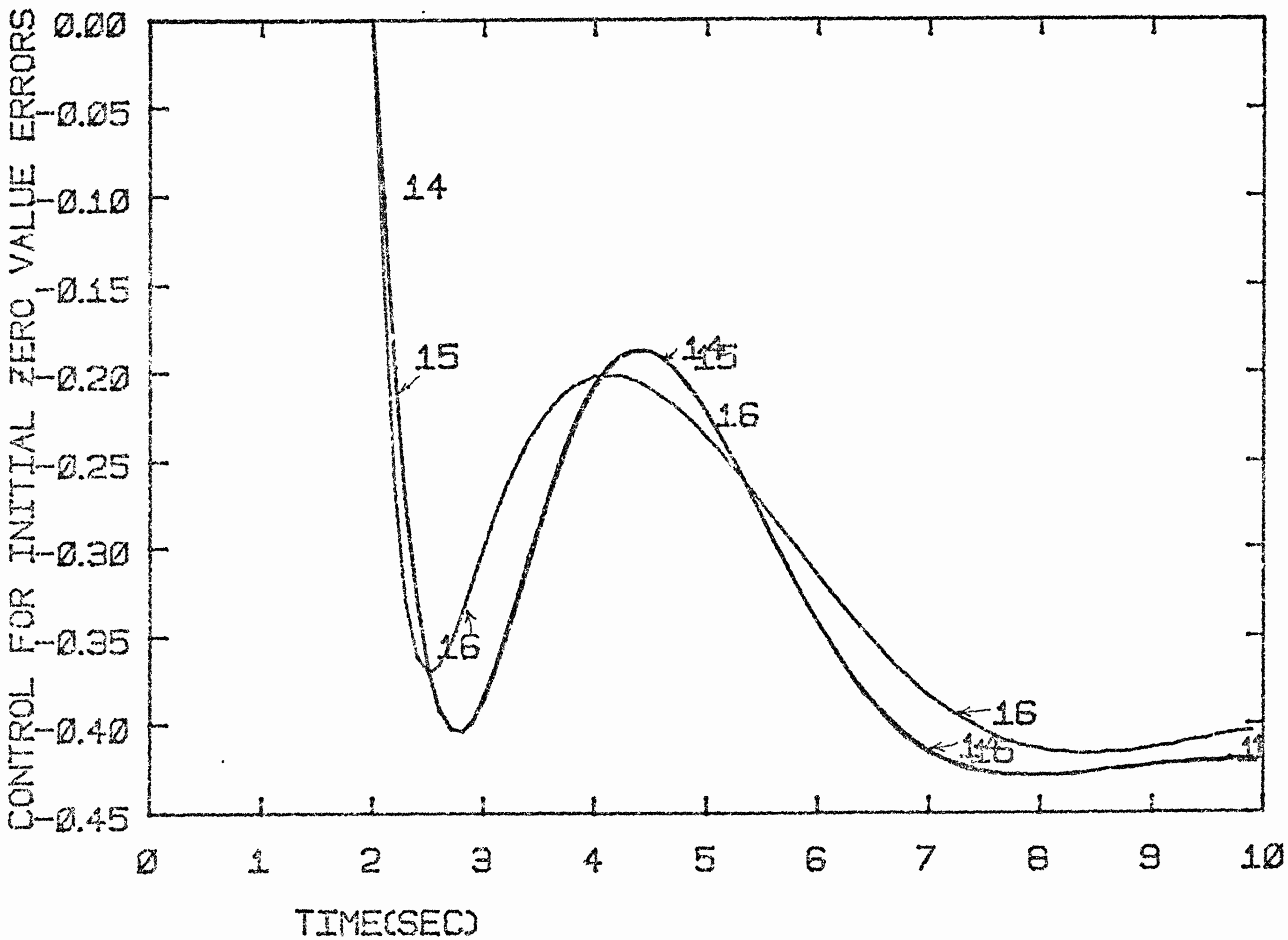

Fig. 6.2.10. Step Response of Control When $\underline{e}(o)=o$.

(2) is clear according to the transient responses of the states and control as shown in the corresponding figures.

The observer may be initiated such that $\underline{\hat{x}}(0)=\underline{x}(0)$ which means $\underline{e}(0)=0$. This situation is illustrated by Fig. 6.2.8 and 6.2.9. In Fig. 6.2.8, the errors start with zero initial value and stay with zero value whereas for case 3 shown in Fig. 6.2.9, even though the errors start with zero initial value, they persist as time goes on. It follows from the assumption $\underline{e}=0$ that $\underline{\hat{x}}(t)=\underline{x}(t)$ for all $t>0$, i.e., the state of the observer tracks exactly the state of the original system. Figure 6.2.10 shows the control of the three cases for this particular situation. Figure 6.2.10 is different from Fig. 6.2.5 in that the controls 14 and 15 for case 1 and case 2 respectively are completely identical if the assumption $\underline{e}=0$ where considered.

6.3 Application to the PWR Power Plant

As stated in the introduction, one of the objectives of this application is to reconstruct the state estimate by using an observer. In order to reconstruct the state estimate as accurately as possible, the input disturbance is considered observed by the reduced-order observer. It was shown in the illustrative example of Section 6.2 that the case where the disturbance is assumed not to be observed is not a realistic situation. Therefore, in this application, the following two cases are considered:

(i) the case where the full-state $\underline{x}$ is assumed available for a feedback control $\underline{u}=k\underline{x}$.

(ii) the case where a part of the state $\underline{x}$ is not available and then a reduced-order observer is used to reconstruct the state estimate $\hat{\underline{x}}$ for a feedback control $u=k\hat{\underline{x}}$. The input disturbance is observed.

6.3.1 The Linear Time-Invariant System

In Section 2.4.6, a linearized model of the power plant was developed. A set of 10 first order differential equations represent the entire PWR power plant as follows:

$$\frac{d}{dt}\delta C = -0.61452\delta T_f -5.58660\ \delta T_{C1} - 5.58660\ \delta T_{C2} + 385.36\ \delta\rho_{ext} \quad (6.3.1)$$

$$\frac{d}{dt}\delta T_f = 5.15147.10^{-2}\delta C -0.63812\delta T_f -3.24600\ \delta T_{C1} -3.49920\ \delta T_{C2} + 241.37\ \delta\rho_{ext} \quad (6.3.2)$$

$$\frac{d}{dt}\delta T_{C1} = 5.5888.10^{-4}\delta C + 9.8744.10^{-2}\delta T_f -3.68720\ \delta T_{C1} -3.7962.10^{-2}\ \delta T_{C2} + 3.54620\ \delta T_{CL} + 2.61860\delta\rho_{ext} \quad (6.3.3)$$

$$\frac{d}{dt}\,\delta T_{C2} = 5.5889.10^{-4}\delta C + 9.8744.10^{-2}\delta T_f + 0.14691\;\delta T_{C1}$$
$$-0.32575\;\delta T_{C2} + 2.61860\;\delta\rho_{ext} \qquad (6.3.4)$$

$$\frac{d}{dt}\,\delta T_{CL} = -0.21411\;\delta T_{CL} + 0.21411\;\delta T_P \qquad (6.3.5)$$

$$\frac{d}{dt}\,\delta T_P = 0.32502\;\delta T_{C2} - 1.60550\;\delta T_P + 1.28050\;\delta T_m \qquad (6.3.6)$$

$$\frac{d}{dt}\,\delta T_m = 4.78740\;\delta T_P - 7.78180\;\delta T_m + 354.95357\;\frac{\delta P_s}{P_{so}} \qquad (6.3.7)$$

$$\frac{d}{dt}\,\frac{\delta P_s}{P_{so}} = 6.61226.10^{-3}\;\delta T_m - 0.93331\;\frac{\delta P_s}{P_{so}} - 0.14572\;\frac{\delta\varepsilon}{\varepsilon_o} \qquad (6.3.8)$$

$$\frac{d}{dt}\,\frac{\delta L_T}{L_{TO}} = 0.18200\;\frac{\delta P_c}{P_{co}} - 0.18200\;\frac{\delta L_T}{L_{TO}} \qquad (6.3.9)$$

$$\frac{d}{dt}\,\frac{\delta P_c}{P_{co}} = 2.20000\;\frac{\delta P_s}{P_{so}} - 2.00000\;\frac{\delta P_c}{P_{co}} - 0.31400\;\frac{\delta\varepsilon_2}{\varepsilon_{20}}$$
$$+ 2.00000\;\frac{\delta\varepsilon}{\varepsilon_o} \qquad (6.3.10)$$

Equation (6.3.8) is further approximated from Eqn. (2.4.14) by assuming that the change in the feedwater temperature δT_{FW} is small and can be neglected. In matrix notation, the system can be described in state space form by:

$$\underline{\dot{x}} = A\underline{x} + B\underline{u} + \underline{G}w \qquad (6.3.11)$$

where,

$\underline{x}$ = a 10^{th}-dimensional state vector having the state variables of the power plant as components (Table 2.4.5).

$\underline{u}$ = a second-dimensional control vector. Its two components are:

$u_1 = \delta\rho_{ext}$ which is the external reactivity of the reactor control rods.

$u_2 = \frac{\delta\varepsilon_2}{\varepsilon_{20}}$ which is the fractional change in the steam by-pass valve coefficient (position).

w = a scalar input disturbance. It is the fractional change in the main steam valve coefficient (position) $\frac{\delta\varepsilon}{\varepsilon_o}$.

A and B are matrices, and $\underline{G}$ is a vector. All are of appropriate dimensions.

In this study, the variable $\delta\varepsilon/\varepsilon_o$ is considered the input disturbance because it is seen as representing the load demand. It is desired to find the maximum amplitude of the input disturbance which the system can tolerate without violation of the potential system state constraints and control constraints.

The potential system state and output are:

(i) the core average coolant temperature, T_{c1}.

(ii) the hot leg coolant temperature, T_{c2}. In the model, T_{c2} represents the core outlet temperature, but in the model reduction, it has been lumped with the hot leg temperature T_{HL} with a single time constant as given by Eqn. (2.4.23).

(iii) the steam pressure in the steam generator P_s

(iv) the steam pressure in front of the nozzle chest of the HP turbine, P_c

(v) the reactor power level P.

The reactor power level P is a system output which is expressed in terms of the state variables by Eqn. (2.4.2)

$$\frac{\delta P}{P_o} = 2.1343.10^{-3}\,\delta C - 1.5947.10^{-3}\,\delta T_f - 1.4497.10^{-2}\delta T_{C1} - 1.4497.10^{-2}\delta T_{c2} + \delta\rho_{ext} \quad (6.3.12)$$

The turbine power output L_T is an important system output but no constraint bounds were considered on the excursions of this variable since it is considered to be directly controlled by $\delta\varepsilon/\varepsilon_o$ which is treated as the input disturbance.

The fuel temperature T_f is a critical state variable but no constraint bounds were considered on this variable because, with a maximum tolerance of more than 8% as shown in Table 6.3.2, it was found that the same results are obtained with or without the constraint bounds on the excursions of T_f.

In matrix notation, the system outputs are given by:

$$\underline{y} = H\underline{x} + D\underline{u} + \underline{E}w \qquad (6.3.13)$$

where,

$\underline{y}$ = a fifth-dimensional system output vector

H,D are matrices and $\underline{E}$ is a vector. All are of appropriate dimensions.

The control problem is to find a control vector $\underline{u}$ such that

$$\underline{u} = K\hat{\underline{x}} \qquad (6.3.14)$$

where,

$\hat{\underline{x}}$ is the state estimate vector of the state vector $\underline{x}$

K is a control gain matrix of appropriate dimensions.

In order to be able to use a full-state estimate feedback control given by Eqn. (6.3.14), the non-measurable state variables are first reconstructed via an "observer".

The inaccessible state variables considered here are:

(i) the delayed neutron precursor concentration C.

(ii) the average fuel temperature T_f.

(iii) the average coolant temperature T_{c1}.

The remaining seven state variables of the vector $\underline{x}$ are assumed measured. In matrix notation, the measurement output vector, $\underline{z}$ is given by:

$$\underline{z} = M\underline{x} \tag{6.3-15}$$

where,

$\underline{z}$ = a seventh-dimensional measurement output vector.

M = a 7x10 measurement matrix.

Equations (6.3.11), (6.3.13) and (6.3.15) constitute the linear time-invariant dynamic system of the PWR power plant described in state-space form. The system matrices are given in Table 6.3.1. The matrix coefficients are obtained upon substitution from the parameter values for a typical 1200 MWe plant at 100% power. The parameter values are given in the tables of Chapter 2.

Table 6.3.1

System Matrices

$$
A=\begin{bmatrix}
0.0 & -.61452 & -5.5855 & -5.5866 & & & & & & \\
5.15147\times10^{-2} & -.63812 & -3.246 & -3.4992 & & & & & & \\
5.5888\times10^{-4} & 9.8744 & -3.6872 & -3.7962\times10^{-2} & 3.5462 & & & & & \\
5.5888\times10^{-4} & 9.8744\times10^{-2} & .1491 & -.32575 & & & & & & \\
 & & & & -.21411 & .21411 & & & & \\
 & & & .32502 & & -1.6055 & 1.2805 & & & \\
 & & & & & 4.7874 & -7.7818 & 354.9536 & & \\
 & & & & & & 6.1226\times10^{-3} & -.9333 & & \\
 & & & & & & & & -.182 & .182 \\
 & & & & & & & 2.2 & & -2.0
\end{bmatrix},\;
B=\begin{bmatrix}
385.36 & \\
241.37 & \\
2.6186 & \\
2.6186 & \\
 & \\
 & \\
 & \\
 & \\
 & \\
 & -.314
\end{bmatrix},\;
G=\begin{bmatrix}
 \\
 \\
 \\
 \\
 \\
 \\
 \\
-.14572 \\
 \\
+2.0
\end{bmatrix}
$$

Table 6.3.1 (cont'd)

$$H=\begin{bmatrix} 2.13426\ 10^{-4} & -1.5947\ 10^{-3} & -1.4497\ 10^{-2} & -1.4497\ 10^{-2} & & & & & & \\ & & 1.0 & & & & & & & \\ & & & 1.0 & & & & & & \\ & & & & & & & 1.0 & & \\ & & & & & & & & & 1.0 \end{bmatrix}, \quad D=\begin{bmatrix} 1.0 & \\ & \\ & \\ & \\ & \end{bmatrix}, \quad \underline{E}=\begin{bmatrix} 0. \\ 0. \\ 0. \\ 0. \\ 0. \end{bmatrix}$$

$$M=\begin{bmatrix} & & & 1.0 & & & & & & \\ & & & & 1.0 & & & & & \\ & & & & & 1.0 & & & & \\ & & & & & & 1.0 & & & \\ & & & & & & & 1.0 & & \\ & & & & & & & & 1.0 & \\ & & & & & & & & & 1.0 \end{bmatrix}$$

6.3.2 System Output and Control Constraint Bounds:

In the presence of load demand changes, the control objective is to find a control $\underline{u}$ given by Eqn. (6.3.14) such that:

$$|y_i| \leq y_{i\max} \qquad i=1,2,\ldots 5 \qquad (6.3.16)$$

$$|u_j| \leq u_{j\max} \qquad j=1,2 \qquad (6.3.17)$$

at all times.

The constraint bounds on the excursions of the system output and control are given in Table 6.3.2. Some of the maximum percent changes from steady state value are obtained from references (64,65).

The bounds on the reactor control rods reactivity are calculated from Eqn. (2.4.7) as follows:

$$(\delta\rho)_{max} = (\delta\rho_{ext})_{max} + \frac{1}{\beta^*}[\alpha_f(\delta T_f)_{max} + \frac{1}{2}\alpha_c (\delta T_{c1\ max} + \delta T_{c2\ max})]$$

where

$(\delta\rho)_{max}$ = \$1 which is the maximum reactivity that a reactor is allowed to reach. In this case the reactor is prompt critical.

Table 6.3.2

Output System and Control Constraint Bounds

output variable	steady-state value at 100% power	maximum possible value (% of 100% value)	constraint bounds	$S_i^* = y_{imax}^2$
$\delta P/P_o$	P_o=3436 MW_t	110%	$\lvert 0.10 \rvert$	0.010
δT_f	T_{fo}=1600 °F	108.2%	$\lvert 131.2 \rvert$	17213.44
δT_{c1}	T_{c1o}=578°F	100.85%	$\lvert 4.913 \rvert$	24.137569
δT_{c2}	T_{c20}=610°F	101.57%	$\lvert 9.577 \rvert$	91.719
$\delta P_s/P_{so}$	P_{so}=847 psia	110.00%	$\lvert 0.10 \rvert$	0.010
$\delta L_T/L_{TO}$	L_{TO}=1183.MWe	none		
$\delta P_c/P_{co}$	P_{co}=762.3 psia	110.00%	$\lvert 0.10 \rvert$	0.010
Control variable	steady-state value at 100% power	maximum % change from steady-state value	constraint bounds	$T_j^* = u_{jimax}^2$
$\delta\rho_{ext}$	$\rho_{ext\ o}$=0.4204 $\delta\rho$ = $1		$\lvert 1.0 \rvert$	1.0
$\delta\varepsilon_2/\varepsilon_{20}$	ε_{20}=0.21918 lbm/sec·psi	50%	$\lvert 0.5 \rvert$	0.25

$(\delta T_f)_{max}$, $(\delta T_{c1})_{max}$ and $(\delta T_{c2})_{max}$ are given in Table 6.3.2.

β^* = fraction of delayed neutron

α_f and α_c = fuel and coolant temperature coefficients.

At the 100% operating load level, about which the plant was linearized, the core reactivity $\delta\rho$ is equal to zero, so the maximum possible external reactivity $\delta\rho_{ext}$ which is induced by the reactor control rods at steady state is equal to the reactor inherent feedback reactivity of \$0.4204 induced by fuel and coolant temperature changes. It follows that $(\delta\rho_{ext})_{max}$ must lie between $\pm$\$1.0 prompt critical reactivity. These are the constraint bounds on the excursions of the control rods reactivity considered in this study.

At the operating load level, the steam by-pass control valve position ε_2 is equal to 0.21918 lb_m/sec.psi. At 110% overpower, the maximum possible ε_2 is equal to 0.2411 lb_m/sec.psi. It follows that ε_2 must lie between zero (completely closed) and 0.2411 (completely open). So at 100% power level, the possible perturbation in ε_2 becomes: $-0.21918 \leq \delta\varepsilon \leq +0.02192$. In order to prevent an over-estimation or an under-estimation, we consider a possible perturbation in ε_2 to occur at 50% power level. In this case we have: $-0.12055 \leq \delta\varepsilon_2 \leq +0.12055$.

Note that the maximum percent changes in the pressures P_s and P_c from steady-state values given in Table 6.3.2 are assumed.

6.3.3 Set-Theoretic Control Results and Transient Response Simulations

In applying Set-Theoretic control to the power plant control problem, the input disturbance $\delta\varepsilon/\varepsilon_o$ is modeled by an unknown-but-bounded uncertainty and the control objective is to find the control that maximizes the tolerable disturbance amplitude, subject to output and control constraints. In this procedure, the constraints on the outputs and controls are translated into parameters S_i^* and T_j^* defined in Chapter 4 as follows:

$$S_i^* = (y_{imax})^2 \qquad i=1,2,\ldots 5 \qquad (6.3.18)$$

$$T_j^* = (u_{jmax})^2 \qquad j=1,2 \qquad (6.3.19)$$

For the constraints specified, the corresponding values of S_i^* and T_j^* are given in Table 6.3.2.

This problem is solved, as described in Chapter 5, using the computer program discussed in Chapter 5. The results are obtained for the two cases:

(i) the case where the full-state vector $\underline{x}$ is assumed available for measurement.

(ii) the case where only the measurement output vector $\underline{z}$ is available.

The resultant control gain matrix K_1 for the first case, the resultant control gain matrix K_2 and the observation gain matrix L for the second case are given in Table 6.3.3. By comparing the two matrices K_1 and K_2, we find that the only difference resides in the two elements: K_{19} and K_{29}. From these results, it is clear that from the measurement output vector $\underline{z}$, the reconstructed state vector $\hat{\underline{x}}$ yields virtually the same control gain matrix: $K_1 \approx K_2$.

The maximum tolerable disturbance amplitude is 5.53579% and 5.53498% for the first and second case respectively. The system eigenvalues for the two cases are given in Table 6.3.4. The bounds on possible variable excursions are given in Table 6.3.5.

The Set-Theoretic control system is further tested by studying the transient responses of the power plant for the two cases. By implementing on the power plant model the control $\underline{u}=K_1\underline{x}$ for the first case and $\underline{u}=K_2\hat{\underline{x}}$ for the second case, we are simulating the time responses of the closed loop systems. In the set of simulations, the system was run at steady state conditions corresponding to the 100% operating load level for few seconds before being subjected to a step down change in main steam control valve position as follows:

Table 6.3.3

Set-Theoretic Control Matrices

$$K_1 = \begin{bmatrix} -0.9797.10^{-3} & -0.011881 & -0.044452 & -0.13279 & -1.295 & -0.12033 & -0.028558 & -10.603 & 0.89492 & 0.38749 \\ 0.26748.10^{-8} & 0.93966.10^{-6} & -0.13648.10^{-5} & 0.10032.10^{-3} & -0.23252.10^{-4} & 0.14367.10^{-2} & 0.1606.10^{-2} & 2.7171 & 0.49665 & 5.2887 \end{bmatrix}$$

$$K_2 = \begin{bmatrix} -0.19797.10^{-3} & -0.011881 & -0.044452 & -0.13279 & -1.295 & -0.12033 & -0.028558 & -10.603 & 0.39355 & 0.38749 \\ 0.26748.10^{-8} & 0.93966.10^{-6} & -0.13648.10^{-5} & 0.10032.10^{-3} & -0.23252.10^{-4} & 0.14367.10^{-2} & 0.1606.10^{-2} & 2.7171 & 0.34726 & 5.2887 \end{bmatrix}$$

$$L = \begin{bmatrix} 0.31664.10^{5} & 0.0 & 0.0 & 0.0 & 0.0 & 0.0 & 0.0 \\ -0.12093.10^{3} & 0.0 & 0.0 & 0.0 & 0.0 & 0.0 & 0.0 \\ 0.58399.10^{2} & 0.0 & 0.0 & 0.0 & 0.0 & 0.2 & 0.2 \end{bmatrix}$$

Table 6.3.4

Eigenvalues of the Closed Loop System

		Case (1) System Not Observed	Case (2) System Observed
Free Parameter β		0.164	0.164
Maximum Tolerable Disturbance Amplitude		5.53579 %	5.53498%
Closed-Loop Eigenvalues	λ_1	-0.19014	-0.1877
	λ_2	-0.68849	-0.68918
	λ_3	-0.082251	-0.082251
	λ_4	-0.30022 - j0.61136	-0.30001-j0.61129
	λ_5	-0.30022 + j0.61163	-0.30001+j0.61129
	λ_6	-1.9698	-1.9694
	λ_7	-3.6526	-3.6551
	λ_8	-3.177 - j1.0527	-3.1771-j1.0527
	λ_9	-3.177 j 1.0527	-3.1771+j1.0527
	λ_{10}	-8.8956	-8.8956
	λ_{11}		-6.2627-j8.1353
	λ_{12}		-6.2627+j8.1353
	λ_{13}		-6.2625

Table 6.3.5

Bounds on Possible Variable Excursions

Variable (units)	Pre-specified Bounds	Bounds on Possible Variable Excursions	
		System Not Observed	System Observed
Nozzle Chest Pressure (fractional change)	$\lvert 0.10 \rvert$	$\lvert 0.10 \rvert^{\dagger}$	$\lvert 0.10 \rvert^{\dagger}$
Steam Pressure in SG	$\lvert 0.10 \rvert$	$\lvert 0.019667 \rvert$	$\lvert 0.019684 \rvert$
Hot Leg Temperature (°F)	$\lvert 9.577 \rvert$	$\lvert 3.0073 \rvert$	$\lvert 2.9885 \rvert$
Average Coolant Temperature (°F)	$\lvert 4.913 \rvert$	$\lvert 0.3954 \rvert$	$\lvert 0.39264 \rvert$
Reactor Power Level (fractional change)	$\lvert 0.10 \rvert$	$\lvert 0.099844 \rvert$	$\lvert 0.098976 \rvert$
Control Rods Reactivity ($)	$\lvert 1.0 \rvert$	$\lvert 0.0789649 \rvert$	$\lvert 0.0784324 \rvert$
By-Pass Control Valve Position (fraction change)	$\lvert 0.50 \rvert$	$\lvert 0.49994 \rvert$	$\lvert 0.49954 \rvert$

†Binding Constraints

(i) in case 1, $\frac{\delta\varepsilon}{\varepsilon_o} = -0.0553579$

(ii) in case 2, $\frac{\delta\varepsilon}{\varepsilon_o} = -0.0553498$

The results for corresponding variables in the two cases are plotted on the same graph for ease of comparison. The labels for the variables in each case are given in Table 6.3.6. The time respones of representative variables are presented in Figure 6.3.1. The sudden closing of the main steam control valve causes an instantaneous decrease in the main steam flow rate and a consequent decrease in nozzle chest pressure accompanied by decrease in turbine power output. The load reduction is accompanied by an increase in the steam pressure inside the steam generator. This response is in good agreement with the "Average-Temperature Program" assigned to the PWR power plant shown in Fig. 2.2.5. The sudden increase in the secondary pressure inside the U-tube steam generator causes a sudden change in the heat removal rate and hence a consequent increase in the primary coolant temperature. The tube metal temperature increases in consequence. Since the temperature of the primary fluid increased inside the UTSG, it follows that the cold leg temperature increases. With the sudden increase in the primary coolant temperature, the control action taken is such that the average coolant

Table 6.3.6

Labels to the Variables of the PWR Power Plant

Variables	System Observed	System Not Observed
*States		
δC	1	11
δT_f	2	12
δT_{c1}	3	13
δT_{c2}	4	14
δT_{CL}	5	15
δT_p	6	16
δT_m	7	17
$\delta P_s/P_{so}$	8	18
$\delta L_T/L_{To}$	9	19
$\delta P_c/P_{co}$	10	20
*Errors		
error in δC, e_1		21
error in δT_f, e_2		22
error in δT_u, e_3		23
*Controls		
$\delta \rho_{ext}$	24	25
$\delta \varepsilon_2/\varepsilon_{20}$	26	27
*System Output		
$\delta P/P_o$	28	29
*Disturbance		
$\delta \varepsilon/\varepsilon_o$	30	

temperature decreases due to:

(i) the reactor inherent feedbacks which are the moderator temperature and Doppler feedbacks.

(ii) a negative reactivity induced externally by the reactor control rods which are manipulated by the reactor control system according to the "Average-Temperature Program".

This control action is accompanied by a decrease in reactor power level.

Note that the Set-Theoretic control system causes a closing of the steam by-pass control valve in order to minimize excursions of the state variables.

The time responses of the errors in the three inaccessible state variables are shown in Fig. 6.3.2. The errors were allocated a 10% of the maximum deviations of the corresponding state variables as initial values in order to use the reduced order observer under a severe condition. The designed observation gain matrix L given in Table 6.3.3 was able to cause the errors to die out rapidly as shown in corresponding figures in less than a half second. Some of the state variables as well as controls are affected by the errors associated with the state reconstruction as shown in the time responses. The average coolant temperature at the core is the most affected state variable. The difference of the time response for the 2nd case from that of the 1st case is considerable. The difference in time responses can be considered to give a measure of performance of the state reconstruction.

It must be emphasized that since the implemented controls $\underline{u} = K_1\underline{x}$ or $\underline{u} = K_2\hat{x}$ are of the proportional feedback type without integral control action, the steady state values of the variables are non-zero as evident in the corresponding figures.

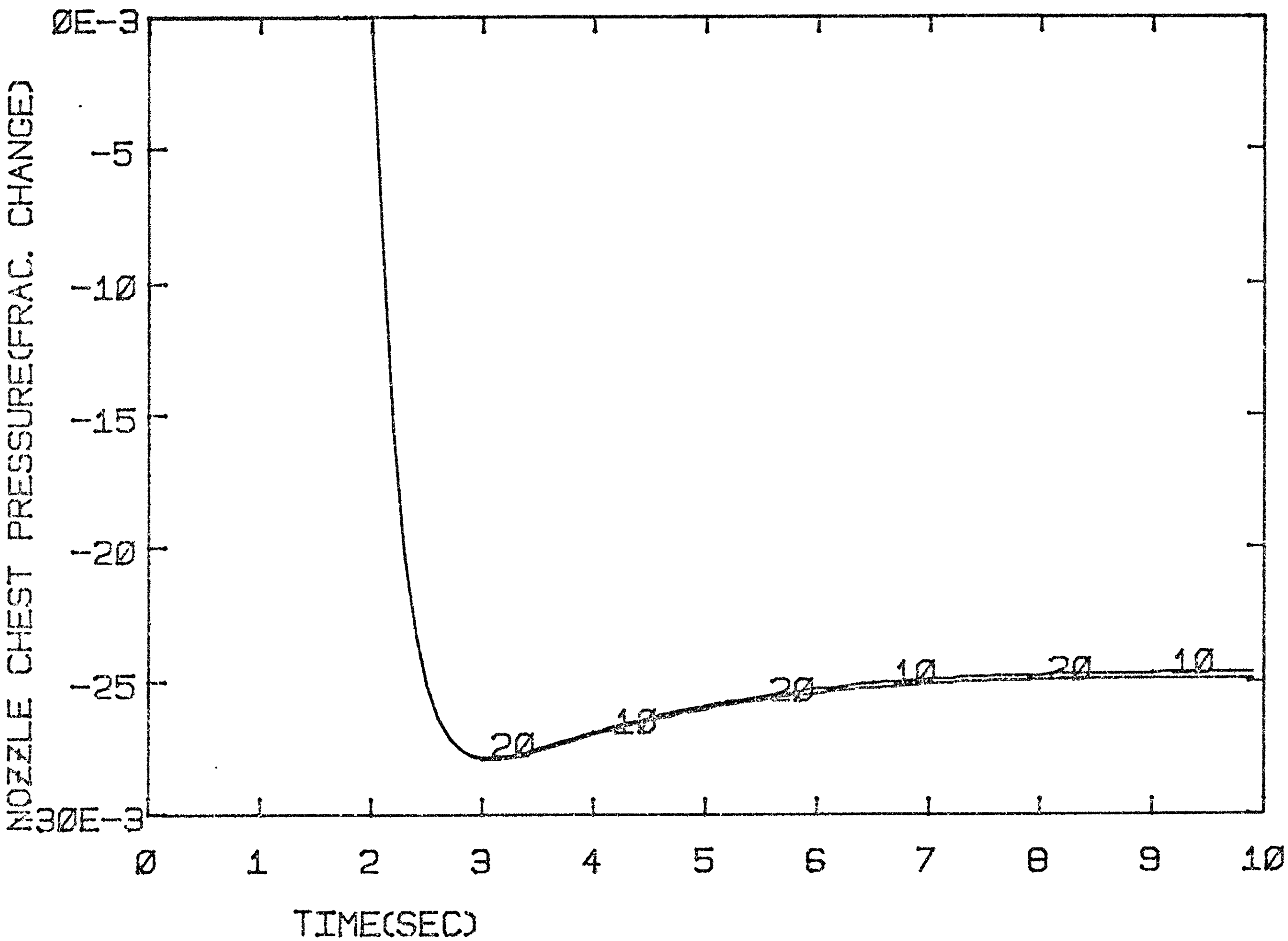

Fig. 6.3.1 (a) Step Responses of the PWR Power Plant.

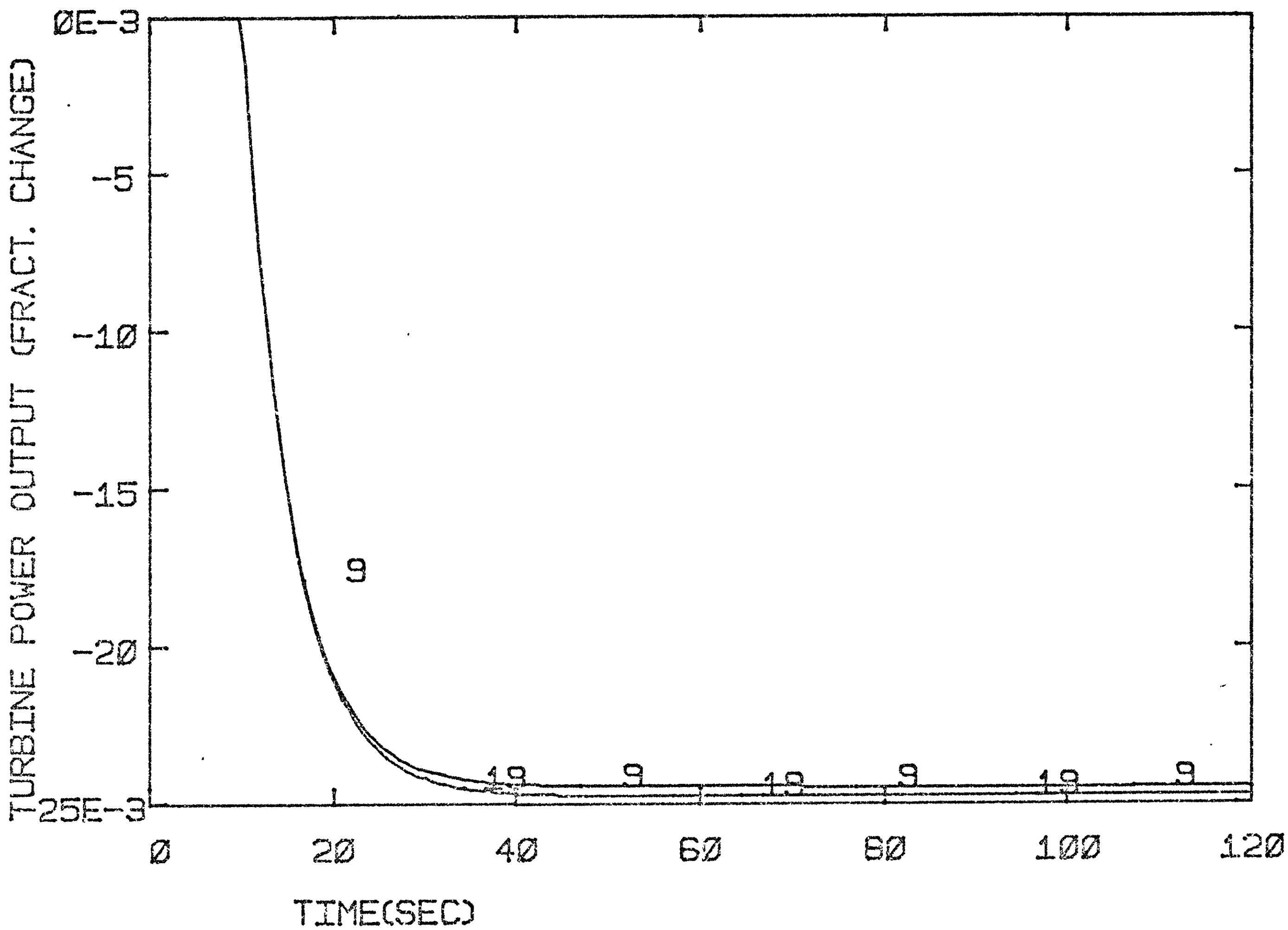

Fig. 6.3.1 (b) Step Responses of the PWR Power Plant.

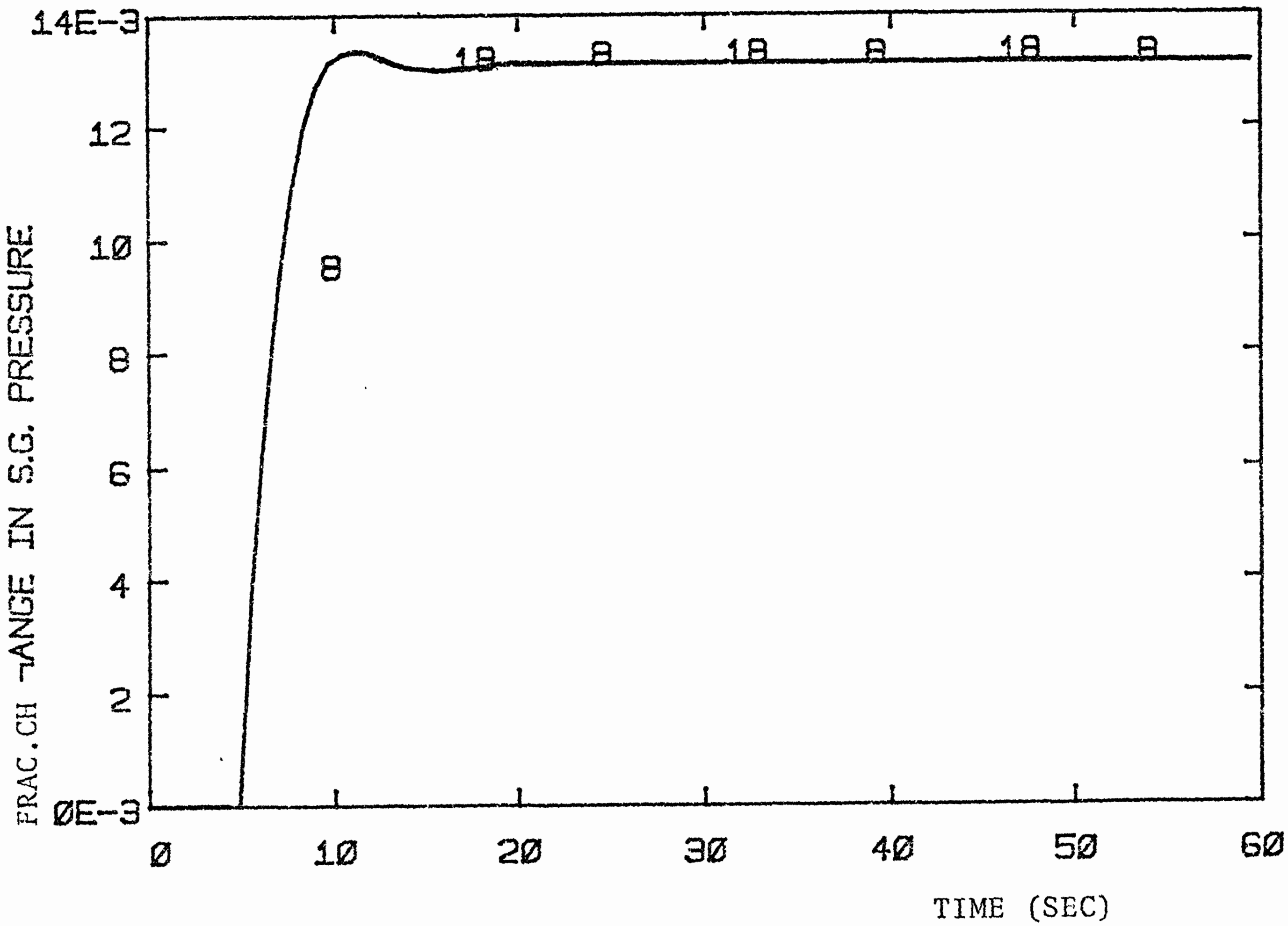

Fig. 6.3.1 (c) Step Responses of the PWR Power Plant.

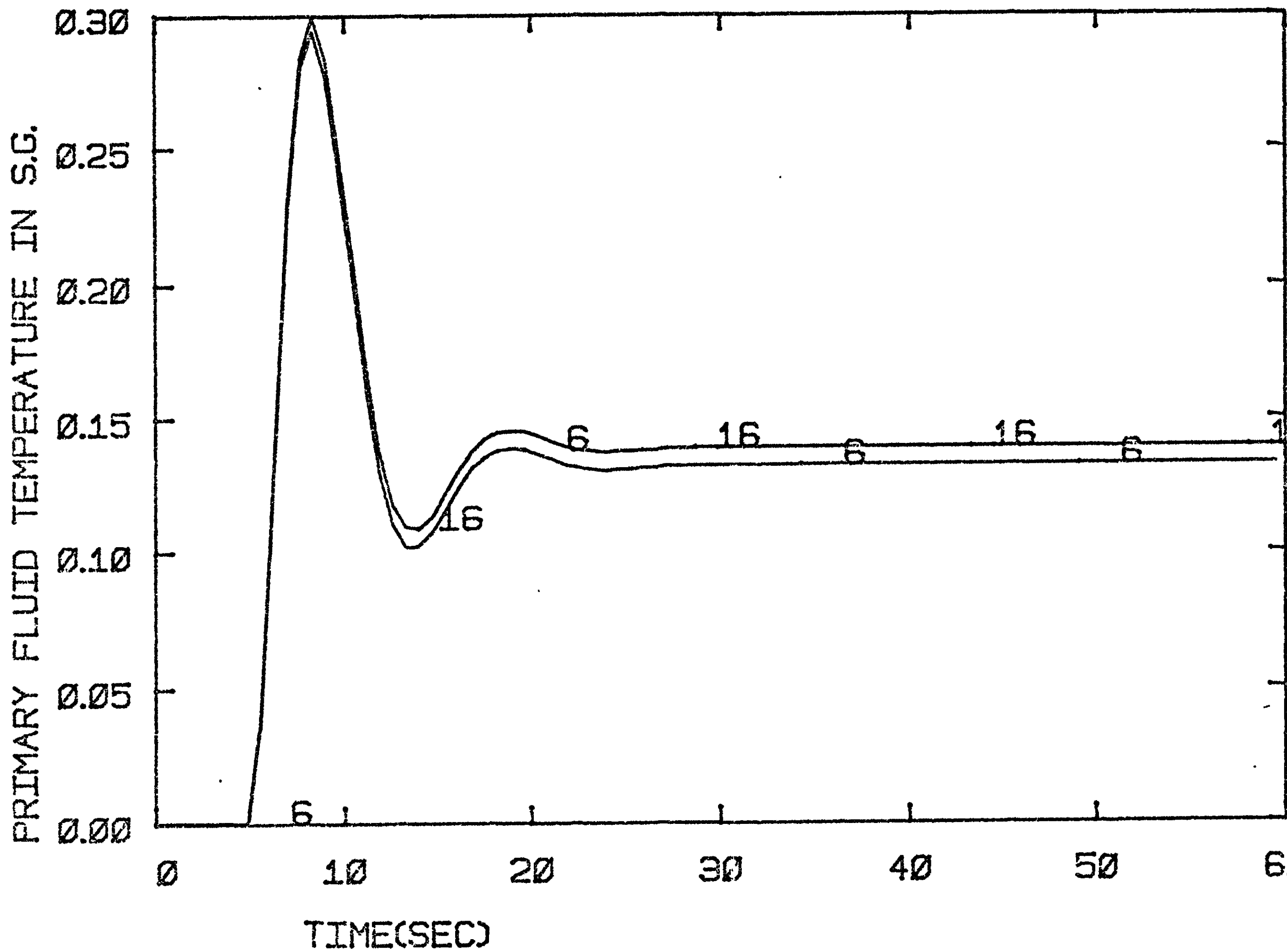

Fig. 6.3.1 (d) Step Responses of the PWR Power Plant.

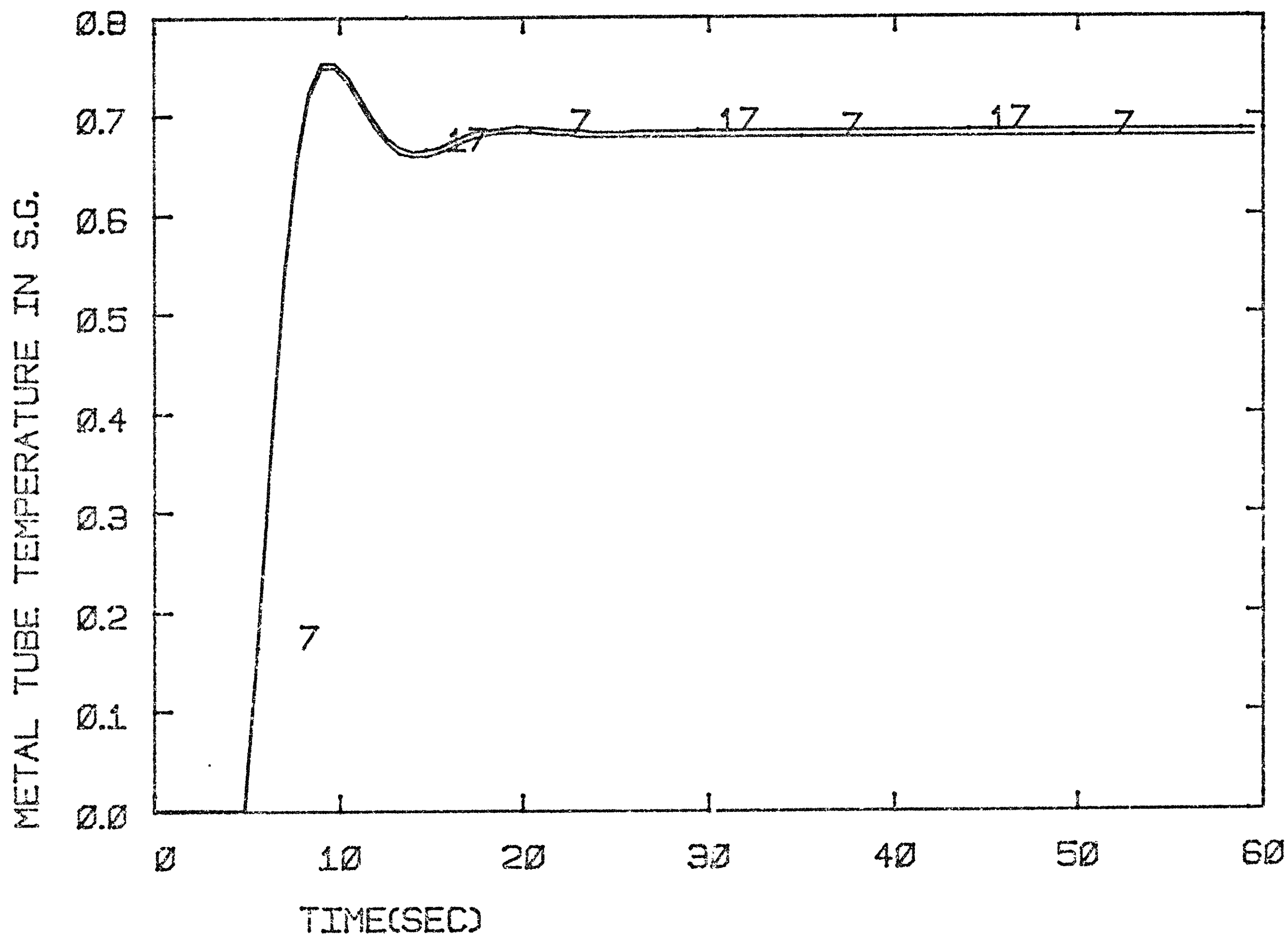

Fig. 6.3.1 (e) Step Res;onses of the PWR Power Plant.

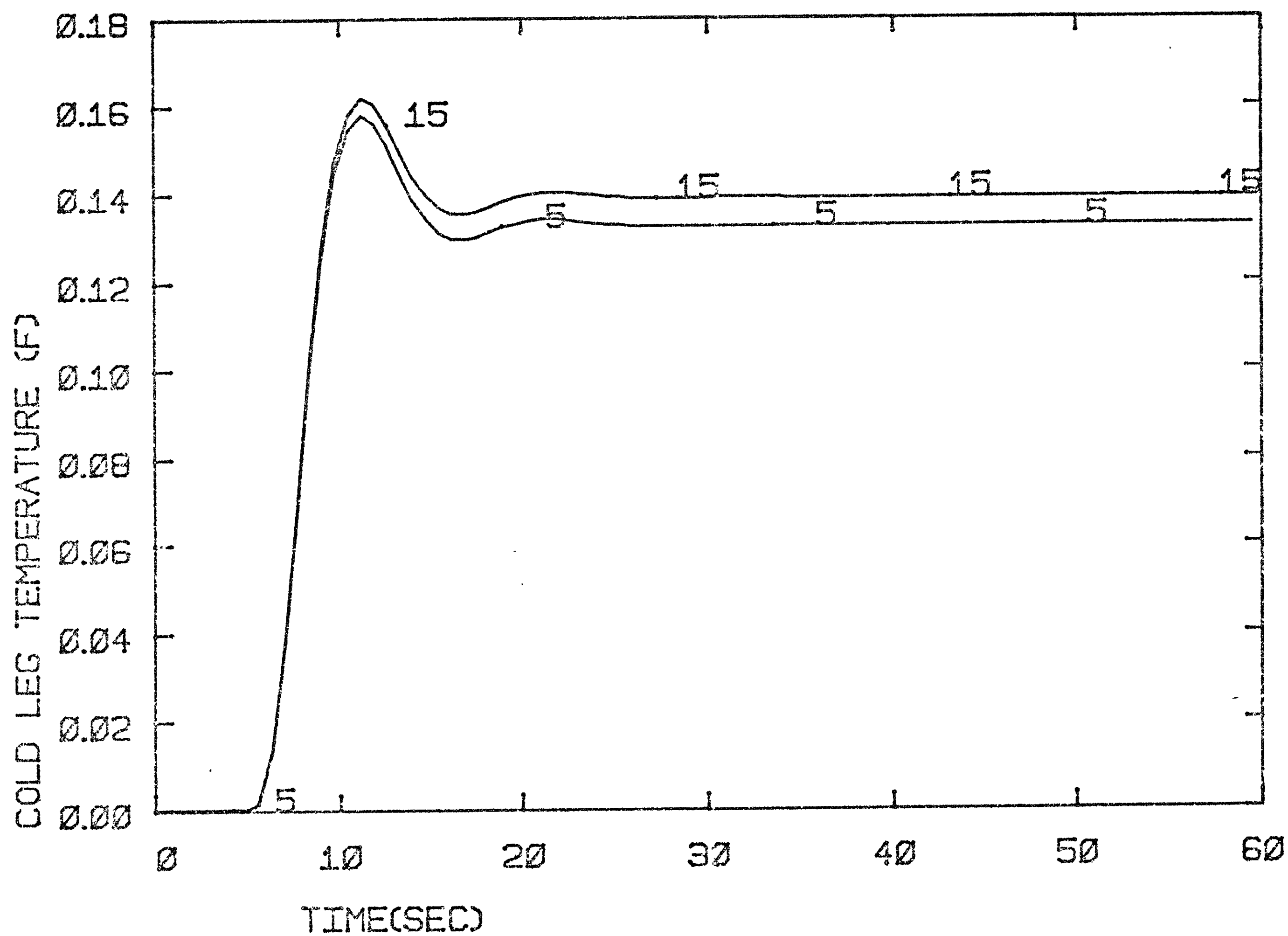

Fig. 6.3.1 (f) Step Responses of the PWR Power Plant.

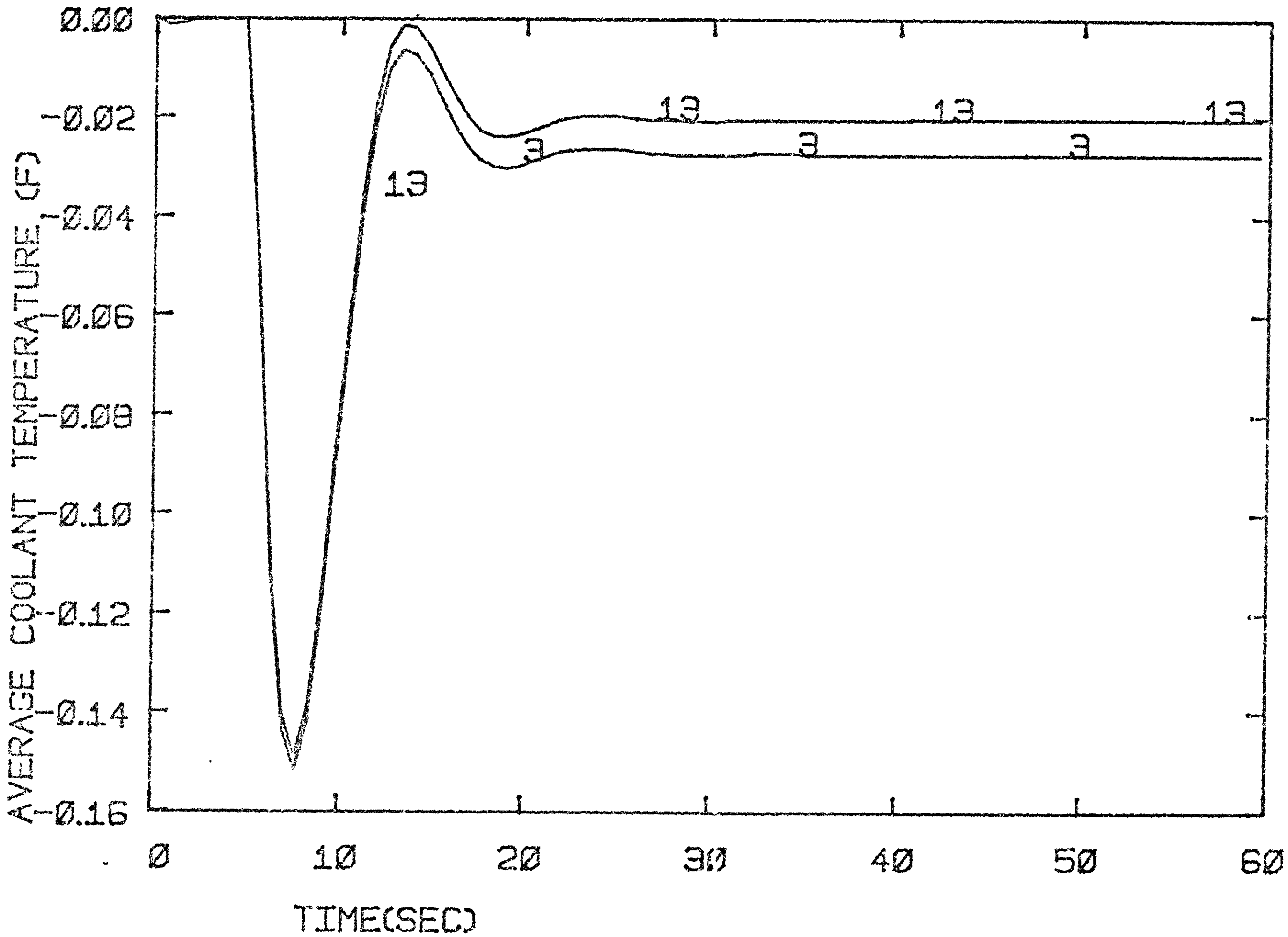

Fig. 6.3.1 (g) Step Responses of the PWR Power Plant.

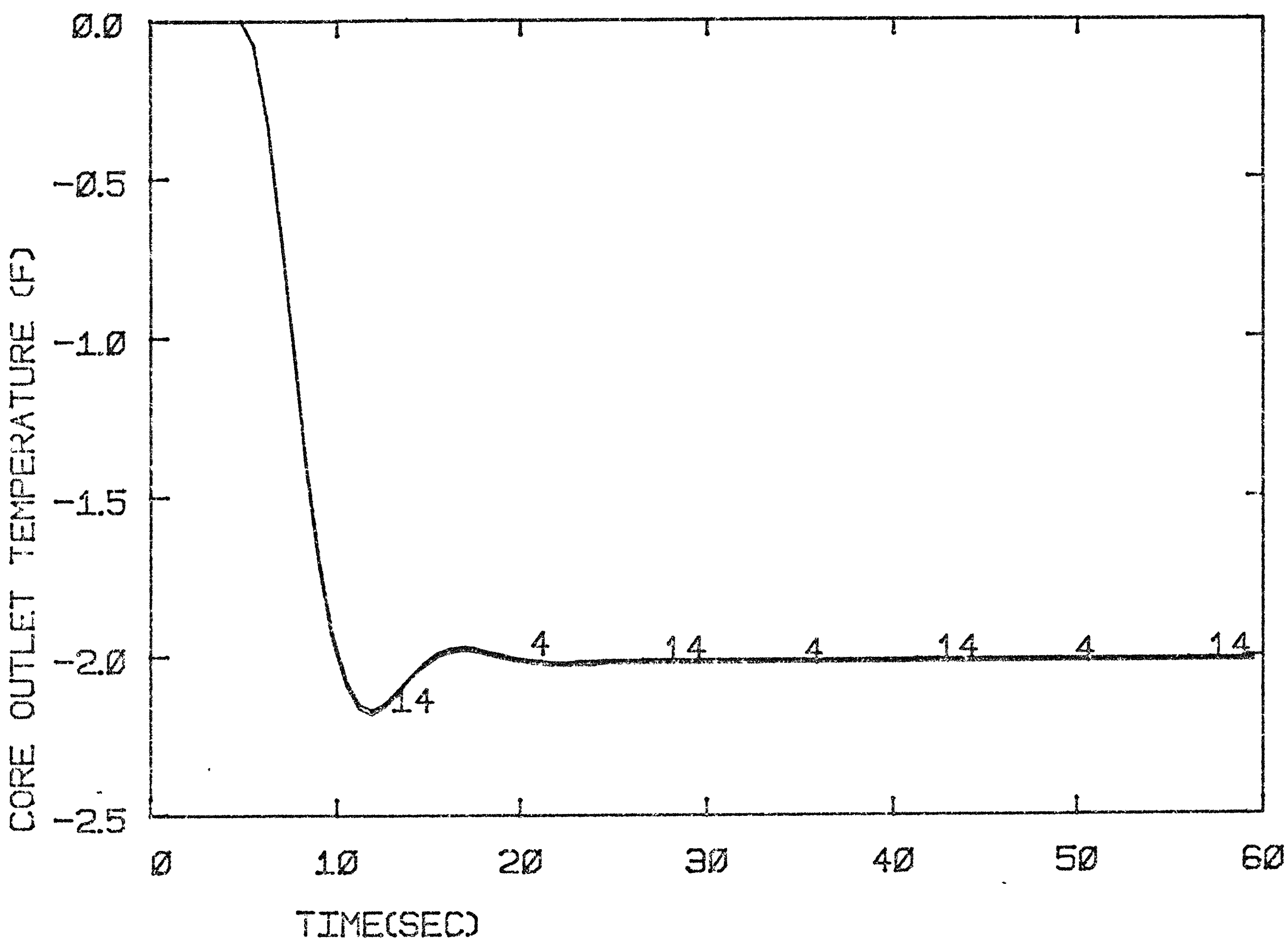

Fig. 6.3.1 (h) Respones of the PWR Power Plant.

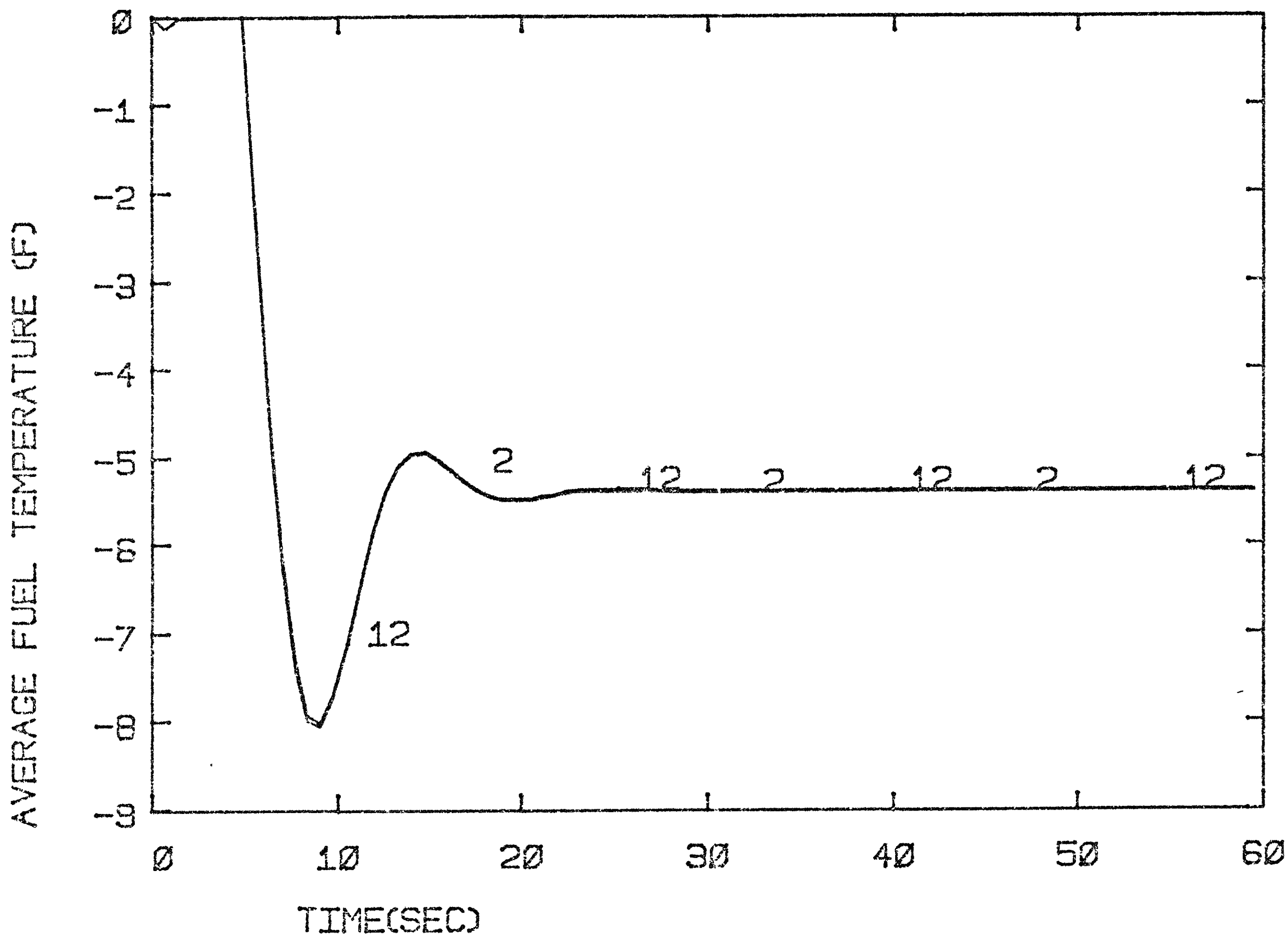

Fig. 6.3.1 (i) Step Responses of the PWR Power Plant.

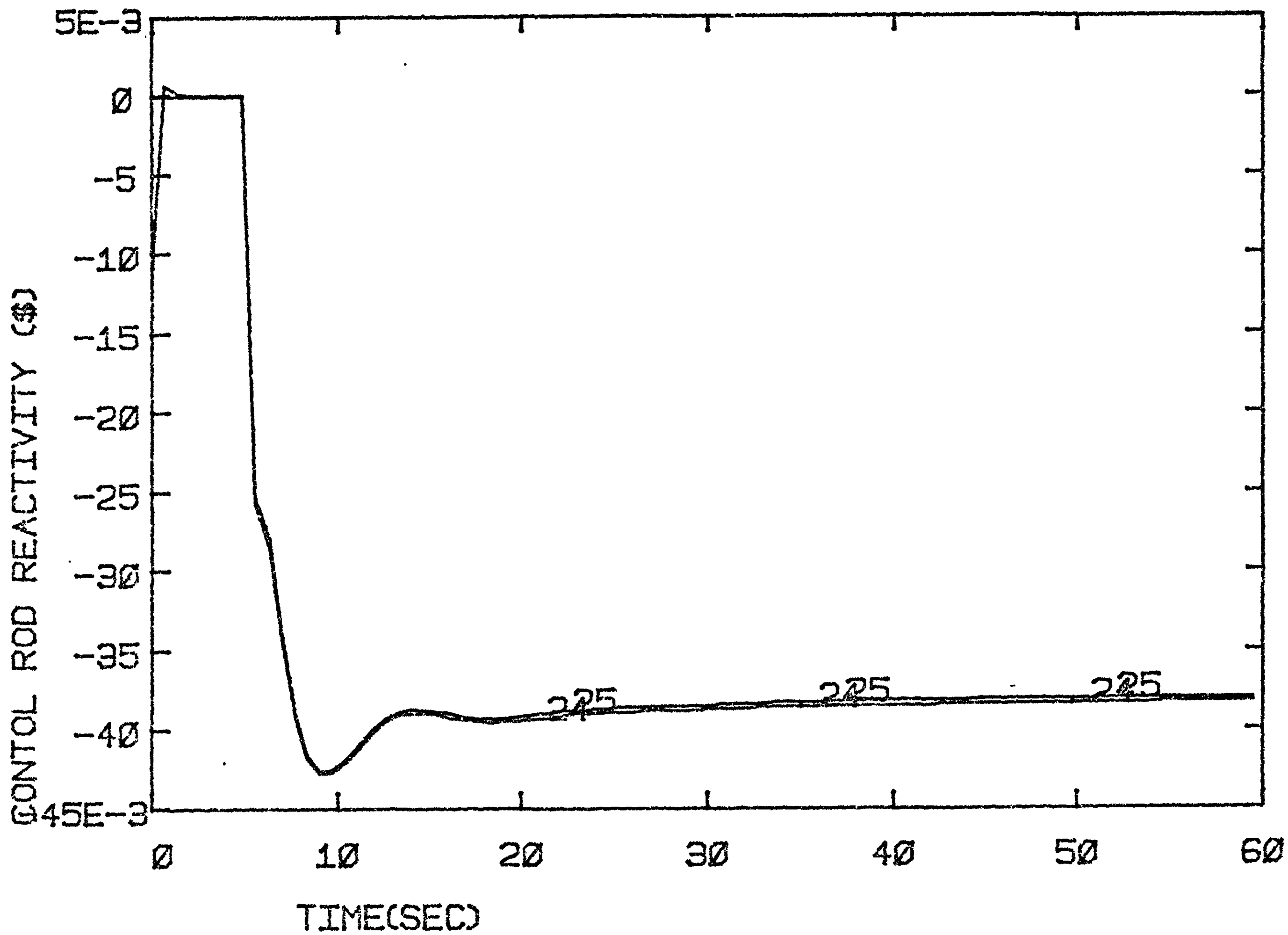

Fig. 6.3.1 (j) Step Respones of the PWR Power Plant.

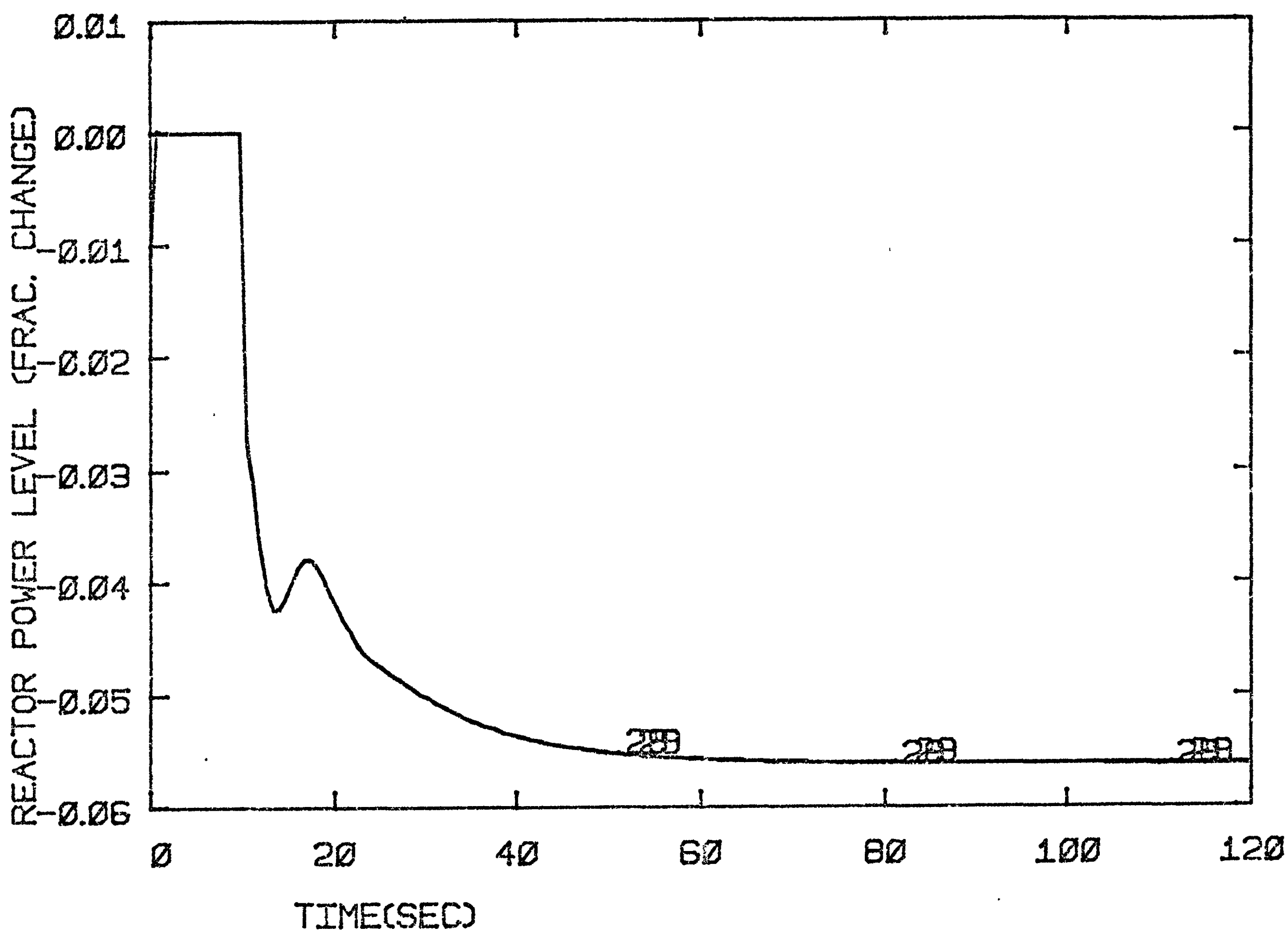

Fig. 6.3.1 (k) Step Responses of the PWR Power Plant.

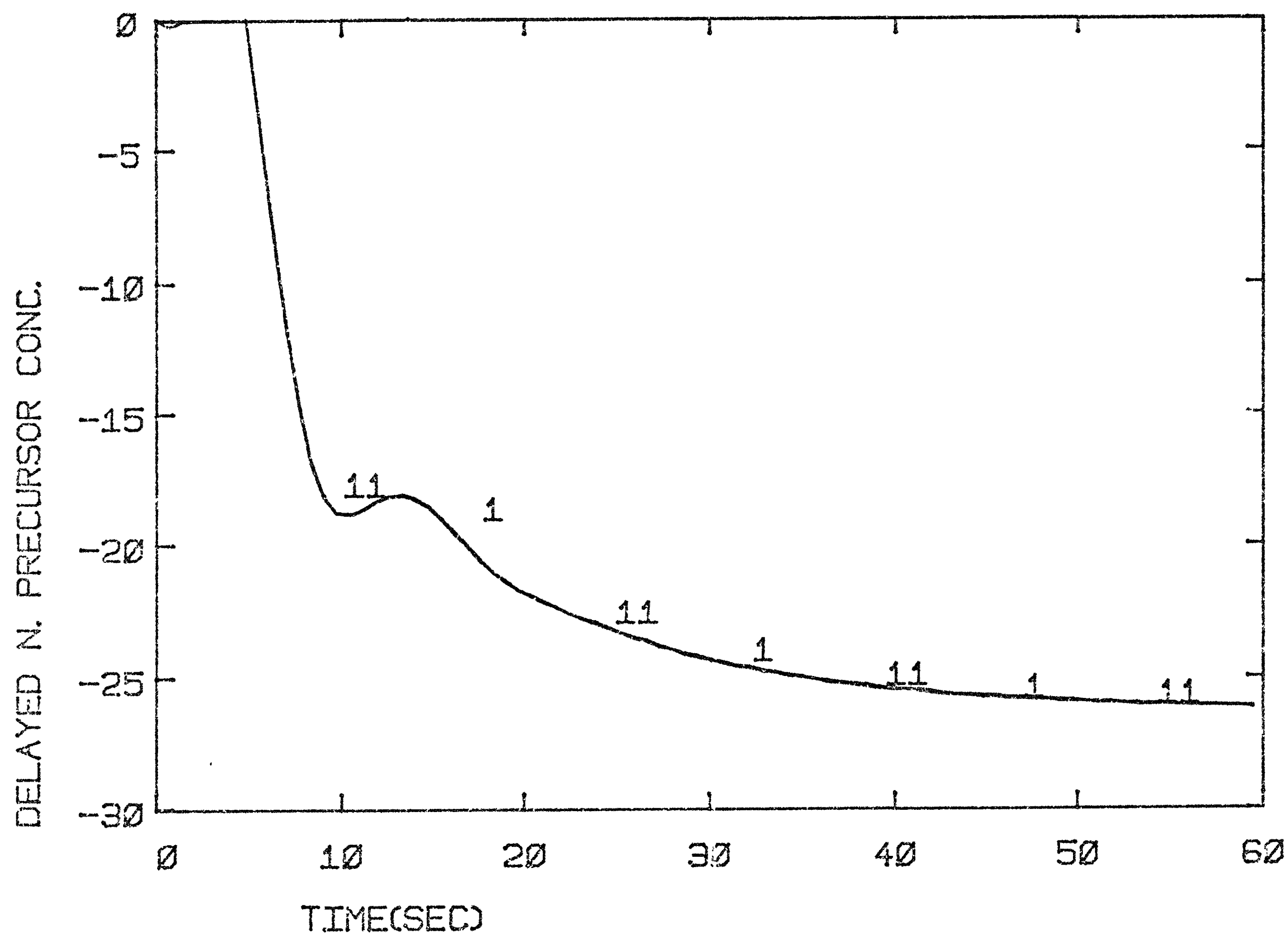

Fig. 6.3.1 (L) Step responses of the PWR Power Plant.

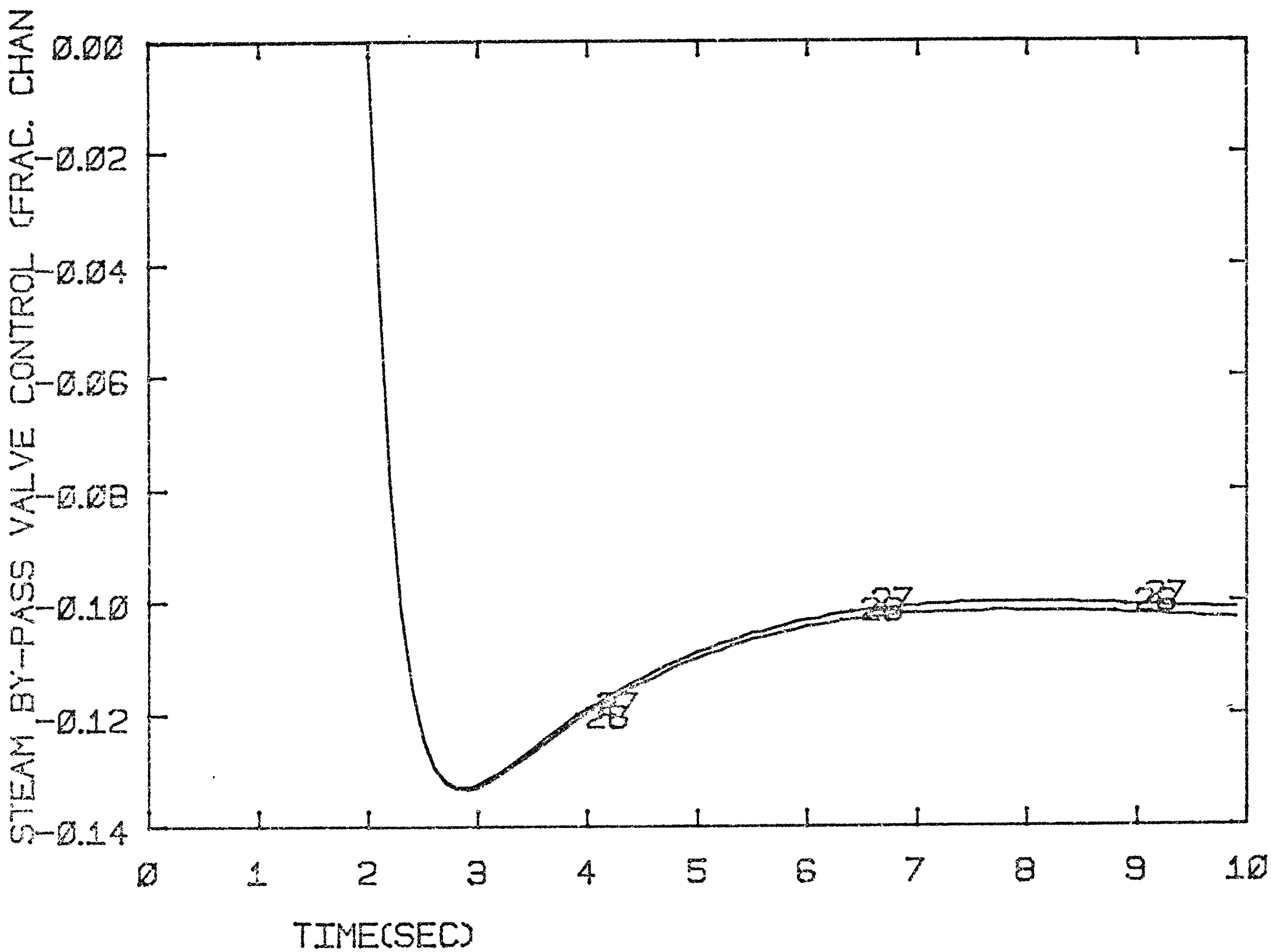

Fig. 6.3.1 (m) Step Respones of the PWR Power Plant.

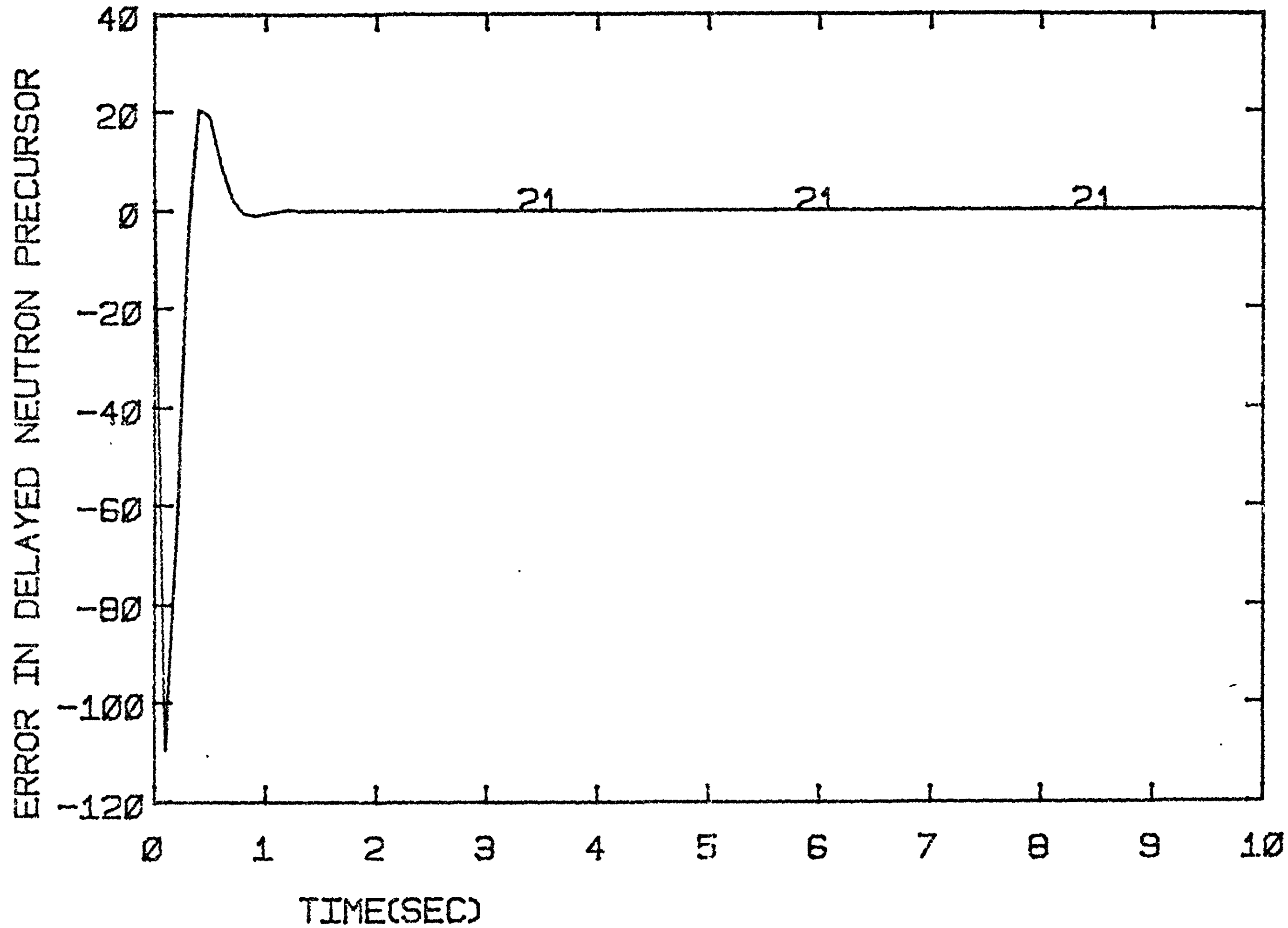

Fig. 6.3.2 (a) Time Respones of the Errors in the PWR Inaccessible State Variables.

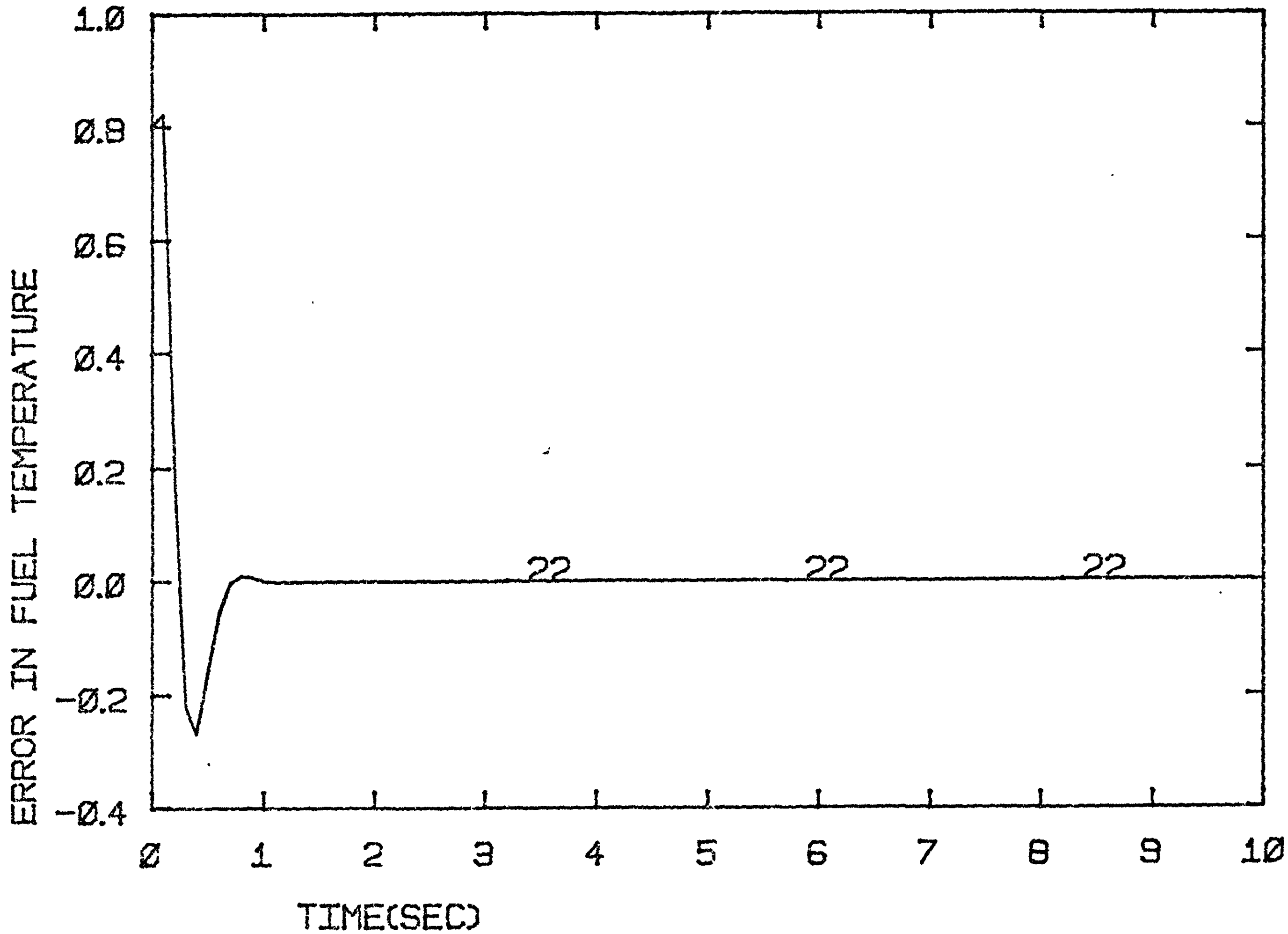

Fig. 6.3.2 (b) Time Responses of the Errors in the PWR Inaccessible State Variables.

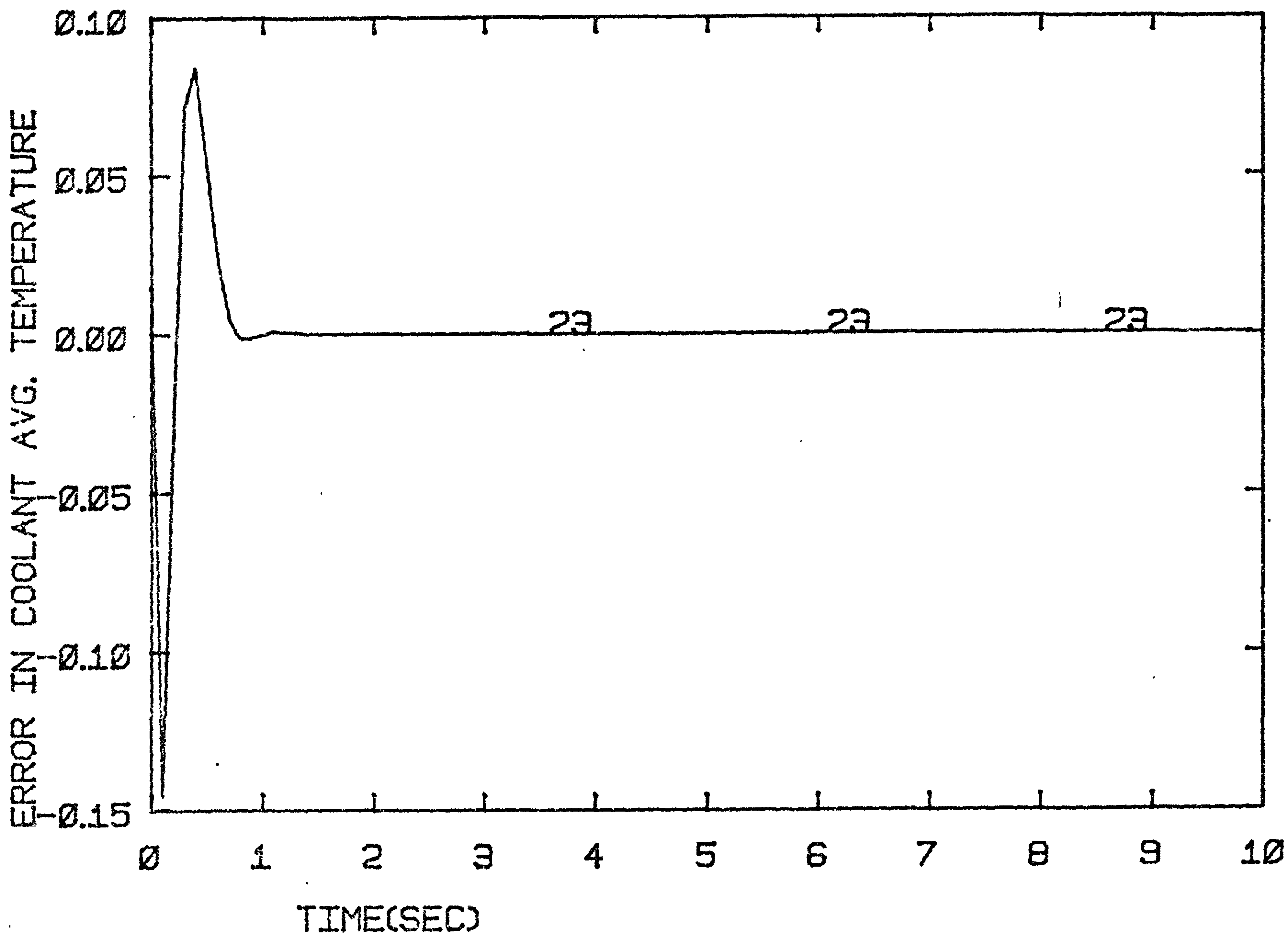

Fig. 6.3.2 (c) Time Responses of the Errors in the PWR Inaccessible State Variables.

Chapter 7

CONCLUSIONS AND RECOMMENDATIONS

This study provides an extension to the Set-Theoretic control synthesis technique as reformulated in (1). Also it demonstrates the applicability of this technique to more practical situations and opens the door for its adaptation to other control problems.

The Set-Theoretic control synthesis technique has been applied to a PWR power plant control problem for two cases. In the first case the full-state vector is assumed available for measurement and in the second case some state variables are inaccessible. A good design of the observer which involves choosing appropriate observation gain matrix can reconstruct the full-state vector without much error. In the application to the power plant, the observer was tested under severe conditions by allocating high initial values to the errors in order to study the applicability of Set-Theoretic control technique under this severe situation. The design of K and L provided by this technique generated results which show that Set-Theoretic Control is an affective and promising scheme. The difference between the time responses of the second case from those given in the first case are small in most of the step responses of the power plant. The other advantage of the Set-Theoretic control technique is that it addresses control problems associated with PWR power plants since keeping critical plant variables within prespecified bounds at all times is a vital requirement. With the full state feedback control structure coordination between the primary and secondary loops is achieved and this helps to yield satisfactory response characteristics for the power plant.

The recommendations for future work in the field of state reconstruction would be to design observers in cases where measurements are noise-corrupted in addition to the process disturbance. Concerning the solution algorithms adopted in this study, they are slow and no attempt has been made to investigate other algorithms since the goal was first to test and implement the state reconstruction to Set-Theoretic control in an existing and working algorithm. Lagrange approach seems to be promising (56). Implementing the state reconstruction to a Set-Theoretic Control using Lagrange approach and also investigating other algorithms then can be used in the Direct Search approach are subjects of interest for future work.

REFERENCES:

1. Usoro, P.B."Set-Theoretic Control Synthesis and Applications", Ph.D. Thesis, M.E. Dpt., MIT, October 1979.

2. Schweppe, F.C., "Recursive State Estimation: Unknown-but-Bounded Errors and System Inputs", IEEE Trans. AC, Vol. AC-13, No. 1, February 1968, pp. 22-28.

3. Schweppe, F.C., Uncertain Dynamic Systems, Prentice-Hall, Inc., Englewood Cliffs, New Jersey, 1973.

4. Hnyilicza, E., "A Set-Theoretic Approach to State Estimation", M.S. Thesis, MIT, Cambridge, Mass., 1967.

5. Witsenhausen, H., "Set of Possible States of Linear Systems Given Perturbed Observations", IEEE Trans. AC, Vol. AC-13, October 1968, pp. 556-558.

6. Schweppe, F.C. and Knudsen, H.K., "Theory of Amorphous Cloud Trajectory Prediction", IEEE Trans. Inform. Theory, Vol. IT-14, May 1968, pp. 415-427.

7. Schaepfer, F.M., "Set-Theoretic Estimation of Distributed Parameter Systems", MIT Electronic Systems Laboratory, Report ESL-R-413, January 1970.

8. Bertsekas, D.P., and Rhodes, I.B., "Recursive State Estimation for a Set-Membership of Uncertainty", IEEE Trans. AC, Vol. AC-16, No. 2, April 1971, pp. 117-128.

9. Delfour, M.C. and Mitter, S.K., "Reachability of Perturbed Systems and Nin-Sup Problems", SIAM J. on Control, Vol. 7, No. 4, pp. 521-533, November 1969.

10. Bertsekas, D.P., and Rhodes, I.B., "On the Minimax Reachability of Target Sets and Target Tubes", Automatrica, Vol. 7, pp. 233-247, Pergamon Press, 1971.

11. Glover, J.D., "Control of Systems with Unknown-but-Bounded Disturbances-Application to Electric Power Systems", Ph.D. Thesis, EE Dept., MIT, Cambridge, Mass., January 1971.

12. Glover, J.D. and Schweppe, F.C., "Control of Linear Dynamic Systems with Set-Constrained Disturbances", IEEE Trans. AC, Vol. AC-16, No. 5, pp. 441-423, Oct. 1971.

13. Sira-Ramirez, H.J., "Set-Theoretic Control of Large-Scale Uncertain Systems", Ph.D. Thesis, EE Dept., MIT, Cambridge, Mass., 1977.

14. Moore, R.L., "Adaptive Estimation and Control for Nuclear Power Plant Load Changes", Ph.D. Thesis, EE Dept., MIT, Cambridge, Mass., May 1971.

15. Fragner, B. and Rao, H.S., "Control of Nuclear Power Plants", IEEE Trans. AC., Vol. AC-23, No. 3, June 1978.

16. Bjørlo, T.J., Grumbach, R. & Josefsson, R., "Digital Control of the Halden Boiling Water Reactor by A Concept Based on Modern Control Theory", Nuclear Science and Engineering: 39, 231-240, (1970).

17. Blomsnes, Bjørn, "Two Applications of Linear Quadratic Theory to LWR Plant Control", Proc.: Joint Automat. Contr. Conf., San Francisco, CA 1977.

18. Frogner B., "System Identification, Estimation and Optimal Feedback Control Theory Applied to the Control of a Nuclear Boiling Water Reactor", Ph.D. Thesis, University of Calfironia, Berkeley, (1974).

19. Gragner, B and Grossman, L.M., "Estimation and Optimal Feedback Control Theory Applied to a Nuclear Boiling Water Reactor", Nuclear Science and Engineering: 58, 265-277 (1975).

20. Godbole, S.S., and Dixon, R.R., "Pressurized Water Reactor Operation and Controls Concept", Proc. Joint Automat. Contr. Conf., San Francisco, CA, 1977.

21. Kerlin, T.W., "Dynamic Analysis and Control of Pressurized Water Reactors", Control and Dynamic Systems, Advances in Theory and Applications, Volume 14, 1978, Edited by C.T. Leondes.

22. Courses: 22.32, Nuclear Power Reactors and 22.39, Nuclear Reactor Operations and Safety, Class Notes, Department of Nuclear Engineering at MIT, Academic Year 1978-79.

23. U.S. Nuclear Regulatory Commission, "Reactor Safety Study, Wash 1400, October 1975.

24. Garber, I., "Application of Control Systems for Pressurized Water Reactors", Proc. of the 11th International ISA Symposium, May 13-15, 1968, Chicago, Ill., Instrumentation in the Power Industry, Volume 11, pp. 98-115.

25. Weaver, L.E., in Nuclear Power Safety, edited by James H. Rust and Lynn E. Weaver, Pergamon Press 1976, pp. 169-208.

26. Lewins, J., Nuclear Reactor Kinetics and Control, Pergamon Press, 1978.

27. Kerlin, T.W., Katz, E.M., Thakkar, J.G., Strange, J.E., "Theoretical and Experimental Dynamic Analysis of the H.B. Robinson Nuclear Plant", Nuclear Technology, Vol. 30, Sept. 1976, pp. 299-316.

28. Thakkar, J.G., "Correlation of Theory and Experiment for the Dynamics of a Pressurized Water Reactors", MS Thesis, Nuclear Engineering Department, The University of Tennessee (March 1975).

29. Freels, J.D., "An Investigation of High Order and Low Order Dynamic Modeling of a Conplete Pressurized Water Nuclear Power Plant", Vol. 2, EPRI PROJECT RP764.4, Nuclear Engineering Department., The University of Tennessee.

30. Girija Shankar, P.V., "Simulation Model of a Nuclear Reactor Turbine", Nuclear Engineering and Design 44 (1977), pp. 269-277.

31. Cooper, K.F., Cain, J.T., "A Pressurized Water Reactor System Model for Control System Design and Analysis", Modeling and Simulation, Vol. 6, 7th Annual Conference, Pittsburgh, 1975.

32. Mehta, K.K., "A Dynamic Simulation of a Nuclear Power Station for Control Analysis", Nuclear Eng. and Design 33 (1975) 403-421.

33. Onega, R.J., Karcher, K.E., "Nonlinear Dynamics of a Pressurized Water Reactor Core", Nuclear Science and Eng. 61(2), Oct. 1976, pp. 276-282.

34. IBM Data Processing Application, "Power Systems Simulator Description of Models," IBM Technical Publications Department.

35. Henry, A.F., Nuclear-Reactor Analysis, The MIT Press, Cambridge, MA 1975.

36. Henry, A.F., "The Applications of Reactor Kinetics to the Analysis of Experiments", Nucl. Sc. and Eng. 3, 52, 1958.

37. Ball, S.J., "Approximate Models for Distributed-Parameter Heat-Transfer Systems", ISA Trans. 3, pp. (38-47), Jan. 1964.

38. Course: Advanced Engineering of Nuclear Reactors, 22.313, "The Response of a PWR Pressurizer to Load Changes", Revised on 2/19/80, Department of Nuclear Engineering, MIT.

39. Baron, R.C., "Digital Model Simulation of a Nuclear Pressurizer", Nucl. Sc. and Eng.: 52, 283-291 (1973).

40. Glasser, T.H., "Basic Equations for Predicting Performance of a Nuclear Power Plant Pressurizer", Sponsored by the American Society of Mechanical Engineers for 1957 Engineering and Science Conference, Paper 95.

41. Nahavandi, A.N., and Batenburg, A,. "Steam Generator Water-Level Control", Journal of Basic Eng., June 1966, pp. 343-354.

42. "Dynamic Models for Steam and Hydroturbines in Power System Studies", IEEE Committee Report, IEEE Trans. Power Apparatus and Systems, Vol. PAS. 92, No. 6, pp. 1904-1915, 1973.

43. Davison, E.J., "A Method for Simplifying Dynamic Systems", IEEE Trans. AC, Vol. AC. 11, No. 1, pp. 93-101, 1966.

44. Lal, M., Mitra, R., and Jain, A.M, "On Schwarz Canonical Form for Large System Simplification," IEEE Trans., AC, April 1975.

45. Course 2.152, Modern Control Theory and Applications, Class Notes, Department of Mechanical Engineering at MIT, Academic Year, 1979-1980.

46. Schultz, D.G. and Melsa, J.L., "State Functions and Linear Control Systems, McGraw-Hill, 1967.

47. Kwakernaak, H. and Sivan R., Linear Optimal Control Systems, John Wiley & Son, 1972.

48. Luenberger, D.G., "Observers for Multivariable Systems", IEEE Transactions on Automatic Control, Vol. AC-11, No. 2, April 1966, pp. 190-197.

49. Luenberger, D.G., "An Introduction to Observers", IEEE Transactions on Automatic Control, Vol. AC-16, No. 6, Dec. 1971, pp. 596-602.

50. Luenberger, D.G., Introduction to Dynamic Systems: Theory, Models and Applications, John Wiley & Son, 1979.

51. Kalman, R.E. and Bucy, R.S., "New Results in Linear Filtering and Prediction Theory", J. Basic Eng., Trans. ASME, Ser. D, 83, pp. 95-108.

52. Luenberger, D.G, "Observing the State of a Linear System", IEEE Trans. on Mil. Electron., Vol. MIL-8, April 1964, pp. 74-80.

53. Cumming, S.D.G., "Designing of Observers of Reduced Dynamics", Electron. Letters, 5, 10, pp. 213-214.

54. Goppinath, B., "On the Control of Linear Multiple Input Systems", Bell System Technical Journal No. 50, March 1971, pp. 1063-1081.

55. Wonhaim, W.M., Linear Multivariable Control: A Geometric Approach, Springer-Verlag, N.Y., 1974.

56. Negahdaripour, S., "A Set-Theoretic Control Algorithm", M.S. Thesis, ME Dept., MIT, May 1980.

57. Youcef Toumi, K., "Reduced-Order observer Subroutine in OPTSYS III", Joint Computer Facility, MIT, Cambridge, MA 02139.

58. Armstrong, E.S., "An Extension of Bass' Algorithm for Stabilizing Linear Continuous Constant Systems", IEEE Trans. AC, Vol. AC-20, Feb. 1975, pp. 153-154.

59. Athay, T.M., "Numerical Analysis of the Lyapunov Equation with Application to Interconnected Power Systems", EE Thesis, EE Dept., MIT, Cambridge, Mass. 1976.

60. Bartels, R.H. and Stewart, G.W., "Solution of the Matrix Equation AX+XB=C", Commun. of A.C.M., Vol. 15, No. 9, Sept. 1972.

61. Kuester, J.L., and Mize, H.H., Optimization Techniques with Fortran, McGraw-Hill Book Co., N.Y., 1973.

62. Peterson, D.W. and Schweppe, F.C., "Code for a General Purpose System Identifier and Evaluator (GPSIE)", IEEE Trans. AC. Vol. AC-19, No. 6, Dec. 1974.

63. Joint Computer Facility, "DYSYS", MIT Cambridge, Mass.

64. LeFrancois, M.P., Safety Group of Yankee Atomic Electric Co., private communication.

65. Final Safety Analysis Report of Maine Yankee, Section 3.

Appendix A

EQUATIONS FOR SIMULATION OF A PWR POWER PLANT

In this Appendix, we present the equations that are the basis for the simulated PWR power plant. The equations for the primary side (reactor core, pressurizer and steam generator of U-tube type) are derived following the modeling procedure presented in (21) and as applied in (27,28,29). The equations for the secondary side (turbine and feedwater heaters) are taken from (29,30). Because the number of these equations is large, we have further reduced the overall power plant model to a set of ten equations in linearized form.

A.1 Neutron Kinetics and Reactivity Feedback

The most commonly known neutron kinetics model is the space-independent point kinetics. This model is derived from the time-dependent neutron transport equation following Henry (35,36) by the use of perturbation weighting functions. A key assumption in the derivation is that the spatial shape of the neutron flux density does not change appreciably as time goes on. The point kinetics equations are given by:

$$\frac{dp(t)}{dt} = \frac{\rho(t)-\beta^*}{\Lambda} P(t) + \sum_{i=1}^{6} \lambda_i C_i, \qquad (A.1)$$

$$\frac{dC_i(t)}{dt} = \frac{\beta_i^*}{\Lambda} P(t) - \lambda_i C_i, \quad i=1,2...6 \qquad (A.2)$$

where

$P(t)$ = reactor power level

$\rho(t)$ = reactivity

β^* = fraction of fission neutrons produced as delayed neutrons. $\beta^* = \sum_i \beta_i$.

β_i^* = delayed neutron fraction for $i^{\underline{th}}$ group.

λ_i = decay constant of the $i^{\underline{th}}$ delayed neutron precursor.

Λ = prompt neutron generation time.

$C_i(t)$ = delayed neutron precursor density in power units.

Reactivity $\rho(t)$ is commonly expressed in units of β^* or equivalently in dollars ($\delta\rho = \beta^*$ is equivalent to \$1).

The point kinetics equation are linearized about an operating condition P_o, C_{io} and zero reactivity. If deviations from the operating values are δP, δC_i and $\delta\rho$ respectively, the linearized point kinetics equations are given as:

$$\frac{d}{dt} \frac{\delta P}{P_o} = -\frac{\beta^*}{\Lambda} \frac{\delta P}{P_o} + \sum_{i=1}^{G} \lambda_i \delta C_i + \frac{\beta^*}{\Lambda} \delta\rho \qquad (A.3)$$

$$\frac{d}{dt} \delta C_i = \frac{\beta_i^*}{\Lambda} \frac{\delta P}{P_o} - \lambda_i \delta C_i, \qquad i=1,2,...6 \qquad (A.4)$$

where,

$\delta\rho$ and δC_i are expressed in terms of the normalized quantities $\delta\rho/\beta^*$ and $\delta C_i/P_o$ respectively.

The reactivity $\delta\rho$ consists of a part $\delta\rho_{ext}$ induced by using the control rods and another $\delta\rho_{fb}$ induced by temperature and/or pressure feedbacks inherent to the reactor:

$$\delta\rho = \delta\rho_{ext} + \delta\rho_{f.b.} \tag{A.5}$$

The inherent feedbacks in Eqn. (A.5) serve as coupling between the point kinetic equations (A.3), (A.4) and the core heat transfer equations as well as the pressurizer. There are other feedbacks inherent to the reactor but they are not considered because their time constants are much longer (hours and days) that those of interest to this study (seconds and minutes).

A.2 Core Heat Transfer

The heat transfer rate from fuel surface to coolant is given by:

$$q_s = A_s h_{fc} \; (_s - T_c) \tag{A.6}$$

where, A_s = heat transfer area
h_{fc} = heat transfer coefficient for fuel-to-coolant
T_s = fuel temperature in surface node
T_c = coolant temperature.

The fuel is divided into 6 nodes as shown in Fig. 2.4.1 with a heat balance of the form:

$$\rho_f C_{pf} V_{fi} \frac{dT_{fi}}{dt} = (\text{heat generated})_i + (\text{heat flow in})_i - (\text{heat flow out})_i, \quad i=1,2,\ldots n \tag{A.7}$$

where,

subscript i denotes node i

ρ_f = fuel density

C_{pf} = fuel specific heat capacity.

V_{fi} = volume of fuel node i.

T_{fi} = temperature of fuel node i.

The average fuel temperature is obtained as follows (18):

$$T_f = \frac{T_{f1}V_{f1} + T_{f2}V_{f2} + \ldots + T_{fi}V_{fi} + \ldots + T_{f6}C_{f6}}{V_{f1} + V_{f2} + \ldots + V_{fi} + \ldots V_{f6}}, \quad i=1,2..,6 \qquad (A.8)$$

By adding the 6 equations of (A.7) we can obtain the heat balance equation for the average fuel temperature

$$\frac{dT_f}{dt} = \frac{f}{(cm_p)_f} P - \frac{A_f h_{eff}}{(mC_p)_f} (T_f - T_c) \qquad (A.9)$$

where,

f = fraction of power released in the fuel.

h_{eff} = overall fuel-to-coolant heat transfer coefficient including resistances in fuel as well as film resistance.

A_f = area chosen as a basis for application of h_{eff}.

The fuel with the effect of cladding is lumped in only one node, and the only state variable is the average fuel temperature, T_f. The entire effect of the cladding is simply a thermal resistance in the overall heat transfer coefficient. The thermal resistance of the fuel is corrected for the fact that the average fuel temperature T_f is used. The thermal resistance across the gas gap depends on the gas in the gap, the gap thickness, the fuel surface properties and power history (21,33).

In the lumped parameter model of the core, two coolant nodes are used for each fuel node to obtain a good approximation to the average coolant temperature (21,27,37). Figure (2.4.2) shows a schematic of the fuel-coolant heat transfer model.

The average coolant temperature of the first node T_{C1} is taken as the temperature to determine the heat transfer rate q_f

$$q_f = A_f \, h_{eff} \, (T_f - T_{C1}) \tag{A.10}$$

The outlet temperature is taken as the average of the second node T_{C2}. Using the heat balance equation (A.7) for the first coolant node and the second coolant node respectively, we get:

$$\frac{dT_{C1}}{dt} = \frac{(1-f)}{(mC_p)_{C_1}} P + \frac{A_f\ h_{eff}}{2(mc_p)_{C_1}} (T_f - T_{C1}) - (\frac{\dot{m}C_p}{mC_p})_{C_1} (T_{c1} - T_{LP}) \tag{A.11}$$

$$\frac{dT_{C2}}{dt} = \frac{(1-f)}{(mc_P)_{C2}} P + \frac{A_f\ h_{eff}}{2(mC_p)C_2} (T_f - T_{c1}) - (\frac{\dot{m}C_p}{mC_p})_{C_2} (T_{C2} - T_{C1}) \tag{A.12}$$

where,

T_{LP} = reactor lower plenum temperature,

m_{ci} = mass of coolant in node i (assumed equal for node 1 and node 2).

c_{PC} = specific heat of coolant.

If deviations from the operating values are δT_f, δT_{C1} and δT_{C2}, the linearized equations for the core heat transfer are:

$$\frac{d}{dt} \delta T_f = \frac{fP_o}{(mC_p)_f} \frac{\delta P}{P_o} - \frac{A_f\ h_{eff}}{(mC_p)_f} (\delta T_f - \delta T_{C1}) \tag{A.13}$$

$$\frac{d}{dt} \delta T_{c1} = \frac{(1-f)P_o}{(mc_p)_{c1}} \frac{\delta P}{P_o} + \frac{A_f\ h_{eff}}{2(mc_P)C_1} (\delta T_f - \delta T_{C1}) - (\frac{\dot{m}}{m})_{C1} (\delta T_{c1} - \delta T_{LP}) \tag{A.14}$$

$$\frac{d}{dt} \delta T_{C2} = \frac{(1-f)P_o}{(mc_P)_{C2}} \frac{\delta P}{P_o} + \frac{A_f\ h_{eff}}{2(mc_p)_{c2}} (\delta T_f - \delta T_{C1}) - (\frac{\dot{m}}{m})_{c2} (\delta T_{c2} - \delta T_{c1}) \tag{A.15}$$

A.3 Piping and Plenums

Piping sections and plenums are modeled as well-mixed volumes (21). It is assumed that the heat transfer to the metal walls in these sections is small and can be omitted and that the plenums perform their mixing function perfectly. The linearized equations are:

$$\frac{d}{dt}\,\delta T_{UP} = \left(\frac{\dot{m}}{m}\right)_{UP}(\delta T_{c2}-\delta T_{UP}) \tag{A.16}$$

$$\frac{d}{dt}\,\delta T_{HL} = \left(\frac{\dot{m}}{m}\right)_{HL}(\delta T_{UP}-\delta T_{HL}) \tag{A.17}$$

$$\frac{d}{dt}\,\delta T_{IP} = \left(\frac{\dot{m}}{m}\right)_{IP}(\delta T_{HL}-\delta T_{IP}) \tag{A.18}$$

$$\frac{d}{dt}\,\delta T_{OP} = \left(\frac{\dot{m}}{m}\right)_{OP}(\delta T_{P}-\delta T_{OP}) \tag{A.19}$$

$$\frac{d}{dt}\,\delta T_{CL} = \left(\frac{\dot{m}}{m}\right)_{CL}(\delta T_{OP}-\delta T_{CL}) \tag{A.20}$$

$$\frac{d}{dt}\,\delta T_{LP} = \left(\frac{\dot{m}}{m}\right)_{LP}(\delta T_{CL}-\delta T_{LP}) \tag{A.21}$$

where,

the subscript UP stands for reactor upper plenum, HL for hot leg pipe, IP for steam generator inlet plenum, OP for steam generator outlet plenum, CL for cold leg pipe and LP for reactor lower plenum.

δT_p is the deviation in the primary coolant temperature in the steam generator.

$\dot{m}$ is mass flow rate

m is mass of coolant.

A.4 Pressurizer

The pressure of the reactor coolant system (RCS) has some feedback on the rest of the system through the pressure coefficient of reactivity α_p in Eqn. (A.5). This is contained in the feedbacks term $\delta\rho_{f.b.}$. The pressurizer maintains the RCS pressure at a constant value during steady-state operation of the plant. Details of its function are found in (21,25,29,38,39,40). Figure 2.4.3 shows a schematic of the pressurizer. During a transient, pressure changes are limited by the pressurizer control system. This system regulates the pressurizer level, pressurizer pressure and reactor coolant pressure. However, there is no feedback from pressurizer water level on the rest of the system.

A pressurizer pressure equation is given in linearized form by (28)

$$\frac{d}{dt}\,\delta P_p = \alpha_1 \delta P_p + \alpha_2 \delta_q + \alpha_3 \delta W_{su} + \alpha_4 \delta W_{sp} + \alpha_5 \delta T_{su} + \alpha_6 \delta T_{sp} \tag{A.22}$$

with $\delta W_{su} = \sum_{i=1}^{N} V_i \beta_i \frac{d\delta T_i}{dt}$

where,

P_p is the pressure of the primary side.

q is the rate of heat addition to the fluid with electric heater.

W_{su} mass flow of surge water into (or out of) the pressurizer depending on the coolant average temperature.

W_{sp} mass flow of spray water.

T_{su} surge water temperature.

T_{sp} spray water temperature

α's are coefficients to be determined from algebraic substitutions.

V_i volume of $i^{\underline{th}}$ coolant node

β_i slope of coolant density versus temperature cuve.

T_i temperature of $i^{\underline{th}}$ coolant node.

Eqn. (A.22) is based on mass, energy, and volume balances and the assumption that saturation conditions always apply for the steam-water mixture in the pressurizer.

$$\frac{dM_w}{dt} = W_{su} + W_{sp} - W_s$$

$$\frac{dM_s}{dt} = W_s$$

$$\frac{dE_w}{dt} = W_{su}h_{su} + W_{sp}h_{sp} - W_s h_s - P_p\dot{V}_w + q$$

$$\frac{dE_s}{dt} = W_s h_s - P_p\dot{V}_s$$

$$V_w + V_s = V_T$$

where,

M_w = mass of water in the pressurizer.

M_s = mass of steam in the pressurizer.

W_s = flashing rate (or condensing rate) in the pressurizer.

E_w, E_s = internal energy of water and steam in the pressurizer respectively.

h_{su}, h_{sp}, h_s = are enthalpies of surger water, spray water and steam respectively.

v_w, v_s, V_T = water volume, steam volume and total volume respectively.

In the reduction process of the overall power plant model, Eqn. (A.22) for the pressurizer as well as that of the pressurizer pressure control system are neglected.

A.5 The Steam Generator

This model (27,28,29) consists of a primary coolant lump, a heat conducting metal lump, and a secondary coolant lump. For the primary coolant lump, an energy balance is made on theprimary coolant which results in the primary coolant temperature, T_p as a state variable. The governing equation is given in linearized form

$$\frac{d\delta T_p}{dt} = \frac{\dot{m}_p C_{pp}}{m_p C_{pp}} (\delta T_{IP} - \delta T_p) - \frac{(h_{eff}\ A)_{pm}}{m_p C_{pp}} (\delta T_p - \delta T_m) \quad (A.23)$$

where,

$m_p, \dot{m}_p$ are mass of primary coolant in the UTSG and its flow rate respectively.

C_{pp} = specific heat of primary coolant.

$(h_{eff})_{pm}$ = heat transfer coefficient for primary coolant to metal (includes portion of the metal resistance as well as the film resistance).

A_{pm} = primary side to U-tube metal heat transfer area.

T_m = U-tube metal temperature.

For the heat conducting metal lump, an energy balance is also made on the tube metal which results in the tube metal temperature T_m as a state variable. The governing equation is given in linearized form

$$\frac{d}{dt}\,\delta T_m = \frac{(h_{eff}A)_{pm}}{m_m C_{pm}} (\delta T_p - \delta T_m) - \frac{(h_{eff}A)_{ms}}{m_m C_{pm}} (\delta T_m - \delta T_{sat}) \quad (A.24)$$

with $$\delta T_{sat} = \frac{\partial T_{sat}}{\partial P_s}\,\delta P_s$$

where,

m_m = mass of tube metal.

C_{pm} = specific heat of tube metal.

A_{ms} = tube metal to secondary coolant heat transfer area.

$(h_{eff})_{ms}$ = heat transfer coefficient for metal to secondary coolant (includes a portion of the metal resistance as well as the film resistance).

$\frac{\partial T_{sat}}{\partial P_s}$ = slope of saturation temperature versus saturation pressure curve.

P_s = steam pressure.

Equation (A.24) is based on the assumption that saturation conditions exist throughout the secondary coolant lump. This assumption leads to consider the steam pressure P_s as a state variable for the secondary coolant lump. The governing equation for the secondary coolant lump is given in linearized form by:

$$\frac{d}{dt}\,\delta P_s = \frac{1}{K}\,\{(h_{eff}A)_{ms}\delta T_m - [(h_{eff}A)_{ms}\frac{\partial T_{sat}}{\partial P_s} + W_s\frac{\partial h_s}{\partial P_s}$$

$$+ \varepsilon_o(h_s - h_{FW})]\delta P_s + W_s C_{ps}\delta T_{FW} - W_s(h_s - h_{FW})\,\frac{\delta\varepsilon}{\varepsilon_o}\} \quad (A.25)$$

where,

T_{FW} = feedwater temperature

$\frac{\delta\varepsilon}{\varepsilon_o}$ = fractional change in value coefficient, ε (equal to a constant x valve area) and zero denotes steady state condition.

K = constant to be determined by algebraic substitutions.

Equation (A.25) is based on the assumption that any drop in the downstream or turbine pressure will not change the steam flow rate W_s from the steam generator. This assumption is commonly known as the "critical flow" assumption. Following this assumption, it is possible to write

$$W_s = \varepsilon P_s$$

or in linearized form

$$\delta W_s = \varepsilon_o \ \delta P_s + W_{so} \ \frac{\delta\varepsilon}{\varepsilon_o} \tag{A.26}$$

where,

zero denostes values at steady state conditions.

Equation (A.25) is obtained by applying mass balances for the water and steam components, an energy balance on the secondary coolant, and a volume balance on all the secondary coolant in the whole steam generator.

The steam generator is equipped with a three element feedwater controller which maintains a programmed water level on the secondary side during normal plant operation. Three signals determine the main feedwater value position as shown in Fig. 2.4.5: the level error signal, the steam flow rate signal, and the feedwater flow rate signal. Details about the steam generator water-level control are given in reference (41). In this study, the feedwater flow is assumed to be controlled perfectly. Perfect feedwater flow control means that at every instant, the feedwater flow is assumed equal to the steam flow

$$W_{FW} = W_s = \varepsilon P_s$$

$$\delta W_{FW} = \varepsilon_o \delta P_s + W_{so} \frac{\delta \varepsilon}{\varepsilon_o} \tag{A.27}$$

A.6 The Turbine and Feedwater Heaters

This model was originally developed by (34) and used with modifications in (29,30). This model is reduced physically in Section 2.4 for computatioal purpose. For a review of dynamic models of some widely used steam turbines and their speed-governing systems, reference (42) may be consulted. Typical parameters are also given.

A block diagram of the model is shown in Fig. 2.4.6. The governing equations are derived (18) by applying physical laws on the different subsystems as follows:

(i) nozzle chest, Fig. A.1.
(ii) high pressure turbine, Fig. A.2.
(iii) reheater and moisture separator, Fig. A.3.
(iv) low pressure turbine, Fig. A.4.
(v) feedwater heater No. 1, Fig. A.5.
(vi) feedwater hater No. 2, Fig. A.6.

The resulting state variables of the model are described in Table A.1.

(i) nozzle chest, Fig. A.1:

A mass balance over the constant volume V_c and an energy balance will result in the following:

$$\frac{dM}{dt} = W_1 - W_2$$

$$\frac{dE}{dt} = W_1 h_s - W_s h_c .$$

The mass can be written as $M=\rho_c V_c$ and the energy stored in V_c can be expressed as $E=Mu_c$. u_c is eliminated by using Callendar's empirical state equation

$$P_c v_c = \frac{1}{g_c} [K_1 h_c - k_2 - k_3 P_c] \tag{A.28}$$

where k_1, k_2, and k_3 are constants. The product $P_c k_3$ is small and can be neglected. The relationship between h_c and u_c that is $(h_c = u_c + P_c v_c)$ becomes

$$\frac{dh_c}{dt} = [1 - \frac{K_1}{g_c}]^{-1} \frac{du_c}{dt} \tag{A.29}$$

After substitution and linearization, the governing equations are:

Table A.1

State Variables of the Turbine and Feedwater Heaters

$\delta\rho_c$	Change in the density of the steam in the nozzle chest ($1bm/ft^3$).
$\frac{\delta h_c}{h_{co}}$	Fractional change in the enthalpy of the nozzle chest.
$\frac{\delta W''_2}{W_{2''_o}}$	Fractional change in the flow rate of steam entering the moisture separator.
$\delta\rho_R$	Density of steam in the reheater tube side ($1bm/ft^3$).
$\frac{\delta h_R}{h_{R_o}}$	Fractional change in enthalpy of reheater tube side.
$\frac{\delta W_{PR}'}{\omega_{PR'_o}}$	Fractional change in flow rate of steam leaving the reheater shell side
δQ_R	Heat transfer in the reheater shell to tube (Mw-hr/sec).
$\frac{\delta W'_3}{W_{2\dot{0}}'}$	Fractional change in flow rate of steam leaving LP turbine to the condenser.
$\delta h'_{FW}$	Change in the enthalpy of feedwater in heater 1 (B/1bm)
δT_{FW}	Change in feedwater temperature leaving heater 2 (°F).
$\frac{\delta W_{HP2}}{W_{HP2}}$	Fractional change in flow rate of fluid leaving heater 2 to heater 1.

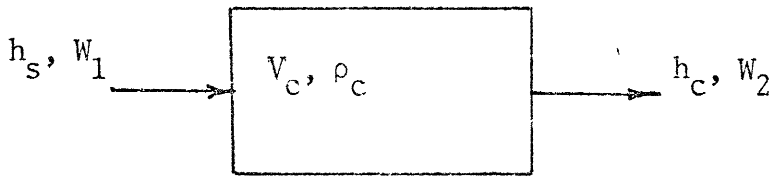

Fig. A.1 Nozzle Chest

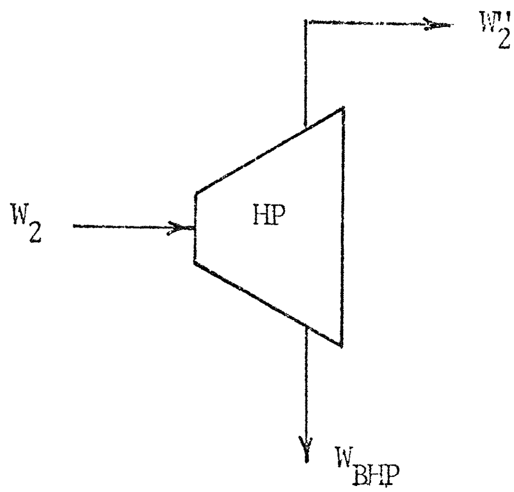

Fig. A.2 HP Turbine

$$\frac{d}{dt}\,\delta\rho_c = \frac{1}{V_c}\,[\delta W_1 - \delta W_2] \tag{A.30}$$

$$\frac{d}{dt}\,\frac{\delta h_c}{h_{co}} = \eta_1\,\delta W_1 + \eta_2\,\delta h_s + \eta_3 \delta W_2 + \eta_4 \frac{\delta h_c}{h_{co}} \tag{A.31}$$

with

$$\delta W_1 = \delta W_s \times \text{NUTSG}$$

$$= [\varepsilon_o \delta P_s + W_{so}\,\frac{\delta\varepsilon}{\varepsilon_o}] \times \text{NUTSG} \tag{A.32}$$

W_2 is given by the empirical relationship [IBM].

$$W_2 = g_c^{0.5} A_{k2}\,[P_c \rho_c - P_R \rho_2]^{0.5} \tag{A.33}$$

where,

η's are coefficients to be determined by algebraic substitutions.

g_c = gravitational constant = 32.2 $lb_m ft/lb_f \cdot sec^2$.

NUTSG = number of U-tube steam generators in the power plant.

A_{k2} = constant

P_R = pressure of steam entering the reheater.

ρ_2 = density of steam leaving HP turbine to the moisture separator.

Equation (A.33) can be expressed in terms of the state variables by using Callender's empirical relationship on P_c and P_R.

$$P_c = \frac{1}{g_c} \rho_c [K_1 h_c - k_2] \tag{A.34}$$

$$P_R = \frac{1}{g_c} \rho_R [K_1 h_R - k_2] \tag{A.35}$$

It is assumed that the quality of the steam entering the nozzle chest and entering the reheater shell side is approximately 1.0. Therefore, the following equations are obtained

$$\delta h_s = \frac{\partial h_s}{\partial P_s} \delta P_s \tag{A.36}$$

$$\delta T_{sat} = \frac{\partial T_{sat}}{\partial P_s} \delta P_s \tag{A.37}$$

$$\delta h_g = \frac{\partial h_g}{\partial P_R} \delta P_R \tag{A.38}$$

$$\delta \rho_2 = \frac{\partial \rho_2}{\partial P_R} \delta P_R \tag{A.39}$$

(ii) <u>high pressure turbine, Fig. A.2</u>

A mass balance will result in

$$\frac{dM}{dt} = W_2 - W_2'' - W_{BHP}$$

Let $W_{BHP} = K_{BHP} W_2$ and $M = \tau_{W2} W_2''$, where K_{BHP} is a constant (a fraction of steam entering the HP turbine that is extracted to feedwater heater 2) and τ_{W2} is a time constant associated with volume of bleed lines. The linearized form of the mass balance

$$\frac{d}{dt}\ \frac{\delta W_2''}{W_{20}''} = \frac{1}{\tau_{W2}}\ [\frac{1-K_{BHP}}{W_{20}''}\delta W_2 - \frac{\delta W_2''}{W_{20}''}\ ] \qquad (A.40)$$

(iii) <u>reheater and moisture separator, Fig. A.3:</u>

A mass balance and an energy balance on the shell side of the reheater will result in the following equations

$$\frac{dM}{dt} = W_2' - W_3$$

$$\frac{dE}{dt} = Q_R + W_2' h_g - W_3 h_R.$$

The reheater volume remains constant, so the mass is given by $M = \rho_R V_R$ and the internal energy is $E=Mu_R$. u_R can be eliminated by using an equation similar to Eqn. (A.29). Upon substitution and linearization, the governing equations are:

$$\frac{d}{dt}\ \delta\rho_R = \frac{1}{V_R}\ [\delta W_2' - \delta W_3] \qquad (A.41)$$

$$\frac{d}{dt}\ \frac{\delta h_R}{h_{RO}} = \eta_5\ \delta W_2' + \eta_6 \delta h_g + \eta_7 \delta W_3 + \eta_8 \frac{\delta h_R}{h_{RO}} + \eta_q \delta Q_R \qquad (A.42)$$

with

$$\delta W_2' = \left(\frac{h_g - h_f}{h_{fg}}\right)\delta W_2'' - \frac{W_2''}{h_{fg}}\delta h_g \tag{A.43}$$

$$W_3 = g_c^{0.5}\ K_3\ [P_R \rho_R]^{0.5} \tag{A.44}$$

where η's are coefficients to be determined δh_g is as given by Eqn. (A.38) and P_R is as given by Eqn. (A.35).

A mass balance on the tube side is given by:

$$\frac{dM}{dt} = W_{PR} - W_{PR}'$$

The reheater is assumed a "well-mixed tank". Let M be given by $M = \tau_{R1}\ W_{PR}'$ where τ_{R1} is a time constant. The governing equation in linearized form is:

$$\frac{d}{dt}\ \frac{\delta W_{PR}'}{W_{PRO}'} = \frac{1}{\tau_{R1}}\ \left[\frac{\delta W_{PR}}{W_{PRO}'} - \frac{\delta W_{PR}'}{W_{PRO}'}\right] \tag{A.45}$$

With W_{PR} following the critical flow, $W_{PR} = \varepsilon_2 P_s$, and δW_{PR}, in linearized form, given by:

$$\delta\ W_{PR} = \varepsilon_{20}\delta P_s + W_{PRO}\ \frac{\delta\varepsilon_2}{\varepsilon_{20}} \tag{A.46}$$

where,

ε_2 is the coefficient of the by-pass valve and ε_{20} is its operating value.

The derivation of the reheater heat transfer Q_R

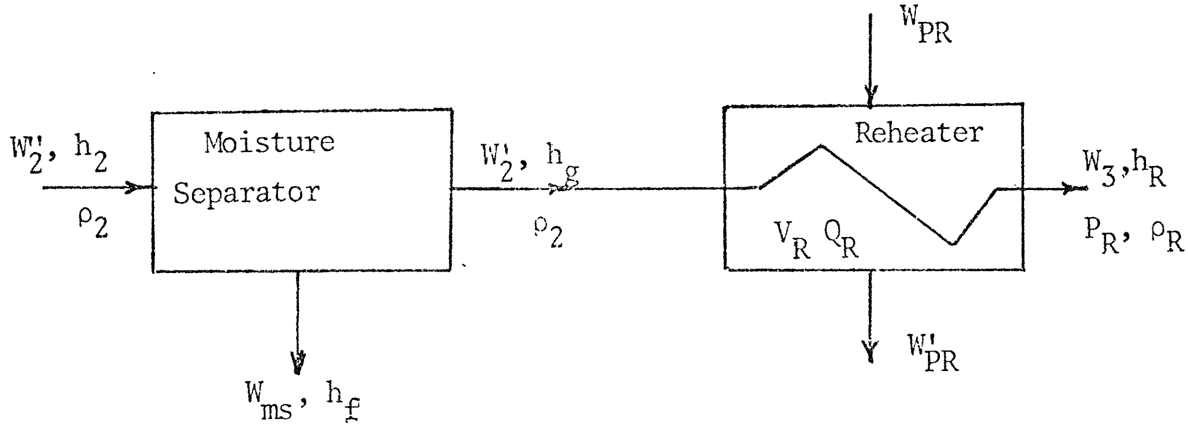

Fig. A.3 Moisture Separator and Reheater.

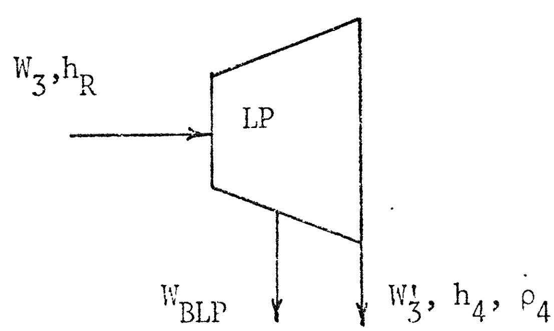

Fig. A.4 LP Turbine.

is based on two assumptions:

(i) the dynamic heat transfer is assumed to be equal to the steady state heat transfer modified by a time constant.

(ii) the heat transfer coefficient for heat transfer across the reheater tubes is assumed to vary linearly with the tube side flow rate.

$$\tau_{R2} \frac{dQ_R}{dt} + Q_R = H_R \left[\frac{W_{PR} + W'_{PR}}{2}\right] (T_S - T_R)$$

where

τ_{R2} is a time constant

T_S is main steam temperature, Eqn. (A.37)

T_R is reheat steam temperature

H_R is overall heat transfer coefficient.

T_R can be expressed in terms of the state variables by assuming that the superheated steam on the tube side of the reheater behaves as an ideal gas, that is $P_R = R\rho_R T_R$. The enthalpy is given by $h_R = u_R + P_R/\rho_R$. The linearized equation of T_R is

$$\delta T_R = [R + C_V]^{-1} \delta h_R \qquad (A.47)$$

where,

R = constant of ideal gas law

C_V = specific heat at constant volume.

The governing equation for Q_R in linearized form is

$$\frac{d}{dt}\,\delta Q_R = \frac{1}{\tau_{R2}}\,[\tfrac{1}{2}H_R(T_S - T_R)(\delta W_{PR} + \delta W'_{PR})$$

$$+\ \tfrac{1}{2}H_R(W_{PR} + W'_{PR})\ (\delta T_s - \delta T_R)\ -\ \delta Q_R] \qquad (A.48)$$

(iv) low pressure turbine, Fig. A.4:

A mass balance will result in:

$$\frac{dM}{dt} = W_3 - W_{BLP} - W'_3$$

Let $W_{BLP} = K_{BLP}W_3$ and $M = \tau_{W3}W'_3$, where K_{BLP} is the fraction of steam entering the LP turbine that is extracted to feedwater heater 1 and τ_{W3} is a time constant associated with volume of bleed lines. The governing equation in linearized form is:

$$\frac{d}{dt}\,\frac{\delta W'_3}{W'_{30}} = \frac{1}{\tau_{W3}}\,[\frac{1 - K_{BLP}}{W'_{30}}]\ \delta W_3 - \frac{\delta W'_3}{W'_{30}} \qquad (A.49)$$

(v) <u>feedwater heater No. 1, Fig. A.5:</u>

An energy balance on the tube side of the heater is:

$$\frac{dE}{dt} = Q_{H1} + h_o W_{FW} - h'_{FW} W_{FW}$$

Let $M = \tau_{H1} W_{FW}$ for a "well mixed tank" assumption where τ_{H1} is a time constant and let the energy be $E = M u'_{FW}$. The fluid is in liquid state and so it is assumed incompressible, the internal energy is $u'_{FW} \cong h'_{FW}$ since the change in $(Pv)'_{FW}$ is very small. The heat transfer from the shell side to the tube side, Q_{H1} is expressed as an effective flow on the shell side multiplied by a constant H_{FW} (34)

$$Q_{H1} = H_{FW} (W_{BLP} + W_{HP2})$$

$$W_{BLP} = K_{BLP} W_3 .$$

Assuming that inlet enthalpy change is zero ($\delta h_o = 0$), the governing equation in linearized form is:

$$\frac{d}{dt} \delta h'_{FW} = \frac{H_{FW}}{\tau_{H1} W_{FW}} [K_{BLP} \delta W_3 + \delta W_{HP2}] - \frac{\delta h'_{FW}}{\tau_{H1}}$$

$$- \frac{h'_{FW}}{\tau_{H1} W^2_{FW}} (K_{BLP} W_3 + W_{HP2}) \delta W_{FW} - \frac{h'_{FW}}{W_{FW}} \frac{d\delta W_{FW}}{dt} \qquad (A.50)$$

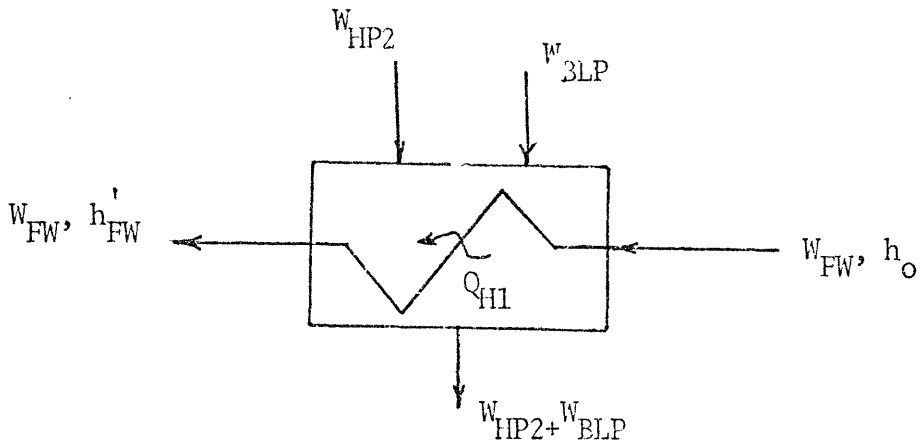

Fig. A.5 Feedwater Heater #1

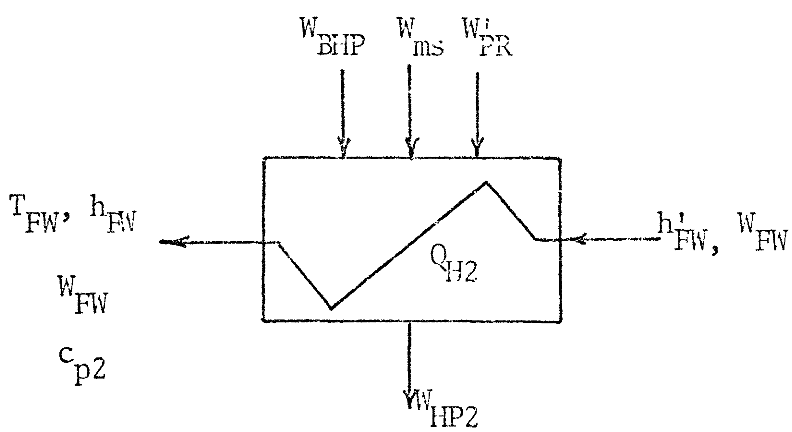

Fig. A.6 Feedwater Heater #2.

Where the constant H_{FW} is the latent heat removed from the steam entering the shell side. δW_3 is given by the linearized form of Eqn. (A.44) and δW_{FW} is given by Eqn. (A.27) and consequently $\frac{d}{dt}\delta W_{FW}$ can be known.

(vi) feedwater heater No. 2, Fig. A.6:

Similarly, an energy balance is done on feedwater heater No. 2 with the same assumptions except that we set $\delta h_{FW} = C_{p2}\delta T_{FW}$ where C_{p2} is the specific heat. The governing equation in linearized form is:

$$\frac{d}{dt}\delta T_{FW} = \frac{1}{C_{P_2}\tau_{H2}}\left[\frac{H_{FW}}{W_{FW}}(K_{BHP}\delta W_2 + \delta W_{ms} + \delta W'_{PR})\right.$$

$$\left. - \frac{H_{FW}}{W_{FW}^2}(K_{BHP}W_2 + W_{ms} + W'_{PR})\delta W_{FW} + \delta h'_{FW}\right]$$

$$- \frac{\delta T_{FW}}{\tau_{H2}} - \frac{h_{FW}}{C_{P_2}W_{FW}}\frac{d\delta W_{FW}}{dt} \qquad \text{(A.51)}$$

where,

$$\delta W_{ms} = \delta W''_2 - \delta W'_2$$

H_{FW} is the latent heat removed from the steam.

A mass balance on feedwater heater No. 2 will give

$$\frac{dM}{dt} = W_{BHP} + W_{ms} + W'_{PR} - W_{HP2}$$

Let $M = \tau_{HP2} W_{HP2}$ for a "well-mixed tank" assumption where τ_{HP2} is a time constant and let $W_{BHP} = K_{BHP} W_2$. Upon linearization and division by W_{HP20}, the governing equation in linearized form is:

$$\frac{d}{dt} \frac{W_{HP2}}{W_{HP20}} = \frac{1}{\tau_{HP2} W_{HP20}} [K_{BHP} \delta W_2 + \delta W_{ms} + \delta W'_{PR}] - \frac{1}{\tau_{HP2}} \frac{\delta W_{HP2}}{W_{HP20}} \tag{A.52}$$

Appendix B

DERIVATION OF THE REDUCED-ORDER OBSERVER

Consider a linear time-invariant dynamic system as

$$\underline{\dot{x}} = A\underline{x} + B\underline{u} + \underline{G}w \tag{B.1}$$

$$\underline{z} = M\underline{x} \tag{B.2}$$

where,

$\underline{x}$ = n-dimensional state vector

$\underline{u}$ = r-dimensional control vector

$\underline{z}$ = m-dimensional measurement outputs vector

w = scalar input disturbance

A,B and M are matrices with appropriate dimensions

$\underline{G}$ = n-dimensional vector.

Let consider a new state vector $\underline{x}_1$ given by

$$\underline{x}_1 = \left[\frac{\underline{z}}{\underline{\eta}}\right] \tag{B.3}$$

So that the first m elements of $\underline{x}_1$ are equal to $\underline{z}$. We need a non-singular transformation relating $\underline{x}$ to the new state vector $\underline{x}_1$.

Assume that the system is observable, m<n, and the rows of M are linearly independent. In this case an (n-m)xn matrix N is selected so that

$$\underline{\eta} = N\underline{x} \tag{B.4}$$

$$\begin{bmatrix} \underline{z} \\ \underline{\eta} \end{bmatrix} = \begin{bmatrix} M \\ N \end{bmatrix} \underline{x} \tag{B.5}$$

$$\underline{x} = \begin{bmatrix} M \\ N \end{bmatrix}^{-1} \underline{x}_1$$

$$\underline{x} = [S_1 S_2] \begin{bmatrix} \underline{z} \\ \underline{\eta} \end{bmatrix}$$

$$\underline{x} = S_1 \underline{z} + S_2 \underline{\eta} \tag{B.6}$$

Equations (B.1), (B.5) and (B.6) give

$$\begin{bmatrix} M \\ N \end{bmatrix}^{-1} \dot{\underline{x}}_1 = A \begin{bmatrix} M \\ N \end{bmatrix}^{-1} \underline{x}_1 + B\underline{u} + \underline{G}w$$

$$\frac{d}{dt} \begin{bmatrix} \underline{z} \\ \underline{\eta} \end{bmatrix} = \begin{bmatrix} M \\ N \end{bmatrix} A \, [S_1 S_2] \begin{bmatrix} \underline{z} \\ \underline{\eta} \end{bmatrix} + \begin{bmatrix} M \\ N \end{bmatrix} B\underline{u} + \begin{bmatrix} M \\ N \end{bmatrix} \underline{G}w$$

$$\frac{d}{dt} \begin{bmatrix} \underline{z} \\ \underline{\eta} \end{bmatrix} = \begin{bmatrix} J & R \\ V & P \end{bmatrix} \begin{bmatrix} \underline{z} \\ \underline{\eta} \end{bmatrix} + \begin{bmatrix} B_1 \\ B_2 \end{bmatrix} \underline{u} + \begin{bmatrix} \underline{G}_1 \\ \underline{G}_2 \end{bmatrix} w \tag{B.7}$$

This may be written as:

$$\dot{\underline{\eta}} = P\underline{\eta} + V\underline{z} + B_2\underline{u} + \underline{G}_2 w \tag{B.8}$$

$$\dot{\underline{z}} = J\underline{z} + R\underline{\eta} + B_1\underline{u} + \underline{G}_1 w \tag{B.9}$$

Let

$$\underline{Z} = \dot{\underline{z}} - J\underline{z} - B_1\underline{u} \tag{B.10}$$

$\underline{z}$ is of order mx1.

Note that the instantaneous values of the variables $\underline{z}$ and $\underline{u}$ are available for measurement and consequently $d\underline{z}/dt$ can be determined.

From Eqns. (B.8) and (B.10), the plant is expressed as:

$$\dot{\underline{\eta}} = P\underline{\eta} + V\underline{z} + B_2\underline{u} + \underline{G}_2 w \qquad (B.8)$$

$$\underline{Z} = R\underline{\eta} + \underline{G}_1 w \qquad (B.11)$$

According to the theory of observers, see Section (4.2), the dynamics of the estimate vector are given by:

$$\dot{\hat{\underline{\eta}}} = P\hat{\underline{\eta}} + V\underline{z} + B_2\underline{u} + \underline{G}_2 w + L(\underline{Z} - (R\hat{\underline{\eta}} + \underline{G}_1 w)) \qquad (B.12)$$

where L is the gain matrix to be determined by the designer. Therefore, by using Eqn. (B. 10)

$$\dot{\hat{\underline{\eta}}} = (P-LR)\hat{\underline{\eta}} + (V-LJ)\underline{Z} + (B_2-LB_1)\underline{u} + (\underline{G}_2-L\underline{G}_1)w + L\dot{\underline{z}} \qquad (B.13)$$

$$\text{Let } \hat{\underline{q}} = \hat{\underline{\eta}} - L\underline{z} \qquad (B.14)$$

Or equivalently, Eqn. (B.14) may be expressed by:

$$\hat{\underline{q}} = [-L \;\; I_\eta] \begin{bmatrix} \underline{z} \\ \hline \hat{\underline{\eta}} \end{bmatrix}$$

$$= T\,\hat{\underline{x}}_1 \qquad (B.15)$$

Similarly, if Eqn. (B.9) is multiplied by the aribtrary gain matrix, L, and subtracted from Eqn. (B.8), we get

$$\dot{\underline{q}} = (P-LR)\underline{\eta} + (V-LJ)\underline{z} + (B_2-LB_1)\underline{u} + (\underline{G}_2-L\underline{G}_1)w$$

where $\underline{q} = \underline{\eta} - L\underline{z}$

$$= [-L \;\; I_\eta] \left[\frac{\underline{z}}{\underline{\eta}}\right] = T\underline{x}_1 \qquad \text{(B.16)}$$

By adding and subtracting the term $(P-LR)L\underline{z}$ in the right-hand side of Eqn. (B.13), we get

$$\dot{\hat{\underline{q}}} = (P-LR)\hat{\underline{q}} + (PL-LRL + V-LJ)\underline{z} + TB_3\underline{u} + T\underline{G}_3w \qquad \text{(B.17)}$$

where

$$B_3 = \left[\frac{B_1}{B_2}\right] = \left[\frac{M}{N}\right]B, \quad \underline{G}_3 = \left[\frac{\underline{G}_1}{\underline{G}_2}\right] = \left[\frac{M}{N}\right]\underline{G}$$

Eqns. (B.16) and (B.17) can be written as:

$$\dot{\underline{q}} = F\underline{q} + C\underline{z} + U\underline{u} + \underline{W}w \qquad \text{(B.18)}$$

$$\dot{\hat{\underline{q}}} = F\hat{\underline{q}} + C\underline{z} + U\underline{u} + \underline{W}w \qquad \text{(B.19)}$$

where

$$F = P-LR$$

$$C = PL-LRL + V-LJ$$

$$U = TB_3$$

$$\underline{W} = T\underline{G}_3 \qquad \text{(B.20)}$$

The estimate $\hat{x}$ is expressed as:

$$\underline{\hat{x}} = \begin{bmatrix} M \\ N \end{bmatrix}^{-1} \underline{\hat{x}}_1$$

$$= [S_1 \ S_2] \begin{bmatrix} z \\ \hat{\eta} \end{bmatrix}$$

$$= S_1\underline{z} + S_2\underline{\hat{\eta}} \qquad (B.21)$$

Using Eqn. (B.14), we may express Eqn. (B.19) as:

$$\underline{\hat{x}} = S_1\underline{z} + S_2(\underline{\hat{q}} + L\underline{z})$$

$$= (S_1 + S_2L)\underline{z} + S_2\underline{\hat{q}} \qquad (B.22)$$

Eqns. (B.18) and (B.20) define an (n-m) state dynamic system that provides an estimate $\underline{\hat{x}}$ of $\underline{x}$.

The dynamics of the error are found by subtracting Eqn. (B.18) from Eqn. (B.19)

$$\underline{\dot{e}} = \underline{\dot{\hat{q}}} - \underline{\dot{q}} = F(\underline{\hat{q}}-\underline{q}) = F\ \underline{e}$$

$$= \underline{\dot{\hat{\eta}}} - \underline{\dot{\eta}} = F(\underline{\hat{\eta}}-\underline{\eta}) = F\ \underline{e} \qquad (B.23)$$

In the case of an observer, the control law is expressed as:

$$\underline{u} = k\underline{\hat{x}} \qquad (B.24)$$

where K is a gain matrix for the controller. From Eqn. (B.21):

$$\underline{u} = K(S_1\underline{z} + S_2\underline{\hat{n}}) \tag{B.25}$$

Adding and Subtracting the term $KS_2\underline{n}$ and making the appropriate substitutions for both $\underline{z}$ and $\underline{n}$ and also recognizing that $S_1M + S_2N = I(nxn)$, we get:

$$\underline{u} = k\underline{x} + KS_2\ \underline{e}. \tag{B.26}$$

The plant with its reduced-order observer may be conveniently described in terms of the state vector $\underline{x}$ and the error vector $\underline{e}$ as follows:

$$\begin{aligned} \dot{\underline{x}} &= A\underline{x} + B(K\underline{x} + KS_2\underline{e}) + \underline{G}w \\ \dot{\underline{e}} &= F\underline{e} = (P-LR)\underline{e} \end{aligned} \tag{B.27}$$

or, in matrix notation,

$$\left[\begin{array}{c} \dot{\underline{x}} \\ \hline \dot{\underline{e}} \end{array}\right] = \left[\begin{array}{c:c} A+BK & BKS_2 \\ \hdashline 0 & P-LR \end{array}\right] \begin{array}{c} \underline{x} \\ \hline \underline{e} \end{array} + \left[\begin{array}{c} \underline{G} \\ \hline 0 \end{array}\right] w \tag{B.28}$$

The computation may be repeated for the case when the disturbance is not observed by the observer, i.e., when the only input to the observer is the control input $\underline{u}$. The result in matrix notation is given by:

$$\left[\begin{array}{c} \dot{\underline{x}} \\ \hline \dot{\underline{e}} \end{array}\right] = \left[\begin{array}{c:c} A+BK & BKS_2 \\ \hdashline 0 & P-LR \end{array}\right] \begin{array}{c} \underline{x} \\ \hline \underline{e} \end{array} = \left[\begin{array}{c} \underline{G} \\ \hline -T\underline{G}_3 \end{array}\right] w \tag{B.29}$$

Appendix C

SUPPORT FUNCTION REPRESENTATION OF SETS (1,2)

Consider a closed convex set Ω of a vector $\underline{x}$ as shown in Fig. C.1. The support function $s(\underline{n})$ defines all the support hyperplanes which touch the boundary of the set Ω, and so, it provides a useful representation of the set. The support function $s(\underline{n})$ is defined by:

$$s(\underline{n}) = \underset{\substack{\text{all } \underline{x} \in \Omega \\ n'n = 1}}{\text{maximum}} \{\underline{x}'\underline{n}\} \tag{C.1}$$

It is shown in (2) that as $\underline{n}$ varies, the support hyperplanes "sweep around" the boundary of Ω. The set Ω can be expressed as:

$$\Omega = \{\underline{x}\colon \underline{x}'\underline{n} \leq s(\underline{n}) \text{ for all } \underline{n},\ \underline{n}'\underline{n} = 1\} \tag{C.2}$$

Let the closed convex set be an ellipsoid defined by

$$\Omega_x = \{\underline{x}\colon [\underline{x}-\underline{x}-_o]'\ \Gamma\ [\underline{x}-\underline{x}_o] < 1\} \tag{C.3}$$

where,

Ω_x denotes the set of vector $\underline{x}$

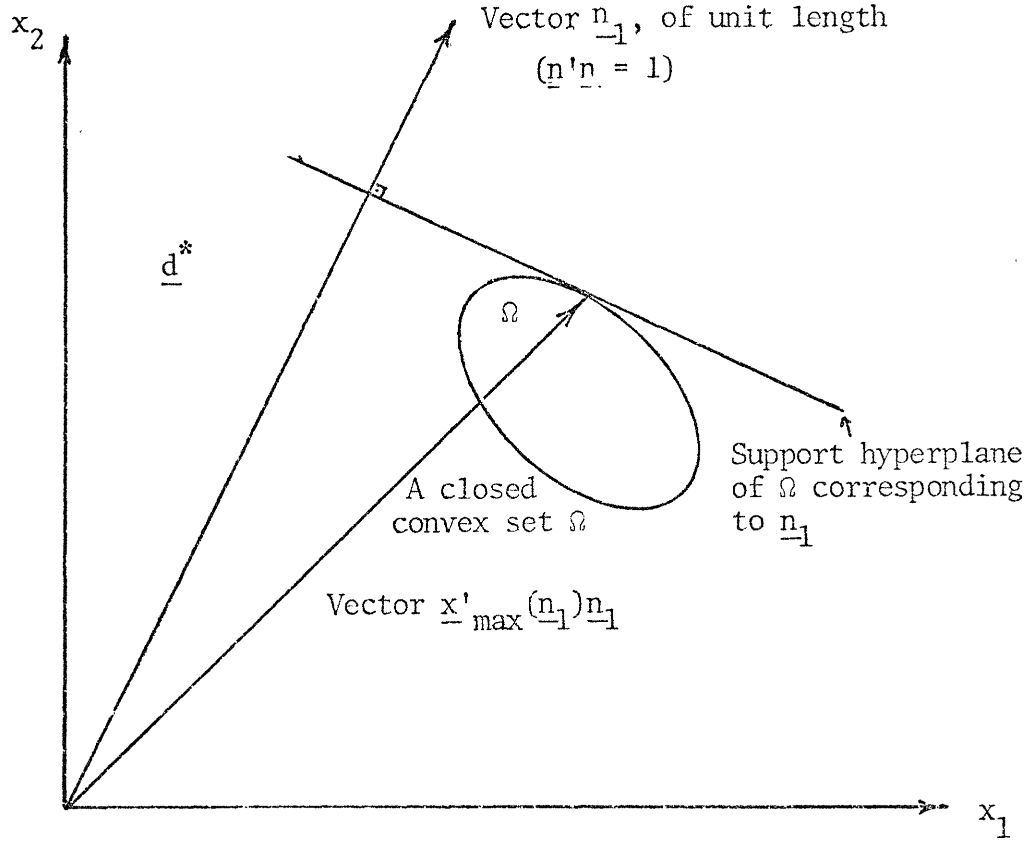

*$\underline{d}$ is a vector in direction of $\underline{n}_1$ with length $d = \underline{x}'_{max}(\underline{n}_1)\underline{n}_1 = s(\underline{n}_1)$

Fig. C.1 Support Function of a Closed Convex Set of Two-Dimensional Vector $\underline{x}$.

$\underline{x}_o$ denotes the center of the ellipsoid

Γ is a positive definite matrix,

If $s(\underline{n})$ denotes the support function of the ellipsoid defined by (C.3), we can find $\underline{x}_{max}(\underline{n})$ of Eqn. (C.1) by introducing a Lagrange multiplier λ and solving the set of equations:

$$\frac{\partial}{\partial \underline{n}} \{\underline{x}'\underline{n} + \frac{\lambda}{2}[(\underline{x}-\underline{x}_o)'\Gamma^{-1}(\underline{x}-\underline{x}_o) - 1]\} = 0 \qquad (C.4)$$

to get

$$\underline{x}_{max}(\underline{n}) = \underline{x}_o - \frac{1}{\lambda}\Gamma\,\underline{n}$$

$$\lambda = \pm\sqrt{\underline{n}'\Gamma\underline{n}} \qquad (C.5)$$

Some of the characteristic properties of the support function for ellipsoid are:

(i) the vector sum of two ellipsoids with Γ_1 and Γ_2 with centers $\underline{x}_{10}$ and $\underline{x}_{20}$ respectively is:

$$S_{1+2})\underline{n})=n'[\underline{x}_{10}+\underline{x}_{20}] + \sqrt{\underline{n}' \ _1\underline{n}} \quad \sqrt{\underline{n}'\Gamma_2 n} \qquad (C.6)$$

Thus the vector sum is not an ellipsoid.

(ii) Consider two ellipsoids Ω_1 and Ω_2 with common centers (say, the origin) defined by Γ_1 and Γ_2. Assume that $\Gamma_1 > \Gamma_2$ so $(\Gamma_1 - \Gamma_2)$ is positive definite. It follows from (C.5) that

$$S_1(\underline{n}) > S_2(\underline{n}), \text{ for all } \underline{n}$$

which means that $\Omega_1 \supset \Omega_2$ (Ω_1 contains Ω_2).

Appendix D

SETS OF REACHABLE STATES (1,2)

Consider a linear dynamic system subjected to an unknown-but-bounded input disturbance w(t)

$$\dot{\underline{x}}(t) = A(t)\underline{x}(t) + G(t)\,\underline{w}(t)$$
$$\underline{x}(0)\,\varepsilon\,\Omega_x(0)$$
$$\underline{w}(t)\,\varepsilon\,\Omega_w(t) \tag{D.1}$$

If the system starts from an initial unknown-but-bounded state $\underline{x}(0)$ in the presence of $\underline{w}(t)$, it undergoes time excursions which depend on the dynamic characteristics of the system and the control action taken at subsequent times. In order for the excursions of the system states to be considered acceptable, the sets of possible states at every instant of time should be contained in the corresponding prespecified target set. This is easily visualized for the discrete time case

$$\underline{x}(n\Delta+\Delta) = \phi(n\Delta)\underline{x}(n\Delta) + \Delta G(n\Delta)\underline{w}(n\Delta)$$
$$\underline{x}(0)\,\varepsilon\,\Omega_x(0)$$
$$w(n\Delta)\,\varepsilon\,\Omega_w(n\Delta) \tag{D.2}$$

where

$$\phi(n\Delta) = I+\Delta A(n\Delta) \tag{D.3}$$

The set $\Omega_x(n\Delta)$ containing all possible $\underline{x}(n\Delta)$ is called the set of reachable states. It follows that

$$\Omega_x(n\Delta+\Delta) = \{\underline{x}: \ \underline{x}=\phi(n\Delta)\underline{x}_1 + \Delta G(n\Delta)\underline{w}, \quad \underline{x}_1 \varepsilon \Omega_x(n\Delta), \ \underline{w}\varepsilon\Omega_w(n\Delta)\} \tag{D.4}$$

$\Omega_x(n\Delta+\Delta)$ can be expressed as a vector sum of two sets as follows:

$$\Omega_x(n\Delta+\Delta) = \tilde{\Omega}_x(n\Delta+\Delta|n\Delta) + \Omega_{Gw}(n\Delta) \tag{D.5}$$

where,

$$\tilde{\Omega}_x(n\Delta+\Delta|n\Delta) = \{\underline{x}: \ \underline{x}=\phi(n\Delta)\underline{x}_1, \underline{x}_1\varepsilon\Omega_x(n\Delta)\} \tag{D.6}$$

$$\Omega_{Gw}(n\Delta) = \{\underline{x}: \ \underline{x} = \Delta\underline{G}(n\Delta)w, \ w\varepsilon\Omega_w(n\Delta)\} \tag{D.7}$$

Using support functions, Eqn. (D.5) is given by:

$$s_{x(n\Delta+\Delta)}(\underline{n}) = s_{\tilde{x}(n\Delta+\Delta|n\Delta)}(\underline{n}) + s_{Gw}(\underline{n}) \tag{D.8}$$

By defining:

$s_{x(n\Delta)}(\underline{n})$ support function $\Omega_x(n\Delta)$

$s_{w(n\Delta)}(\underline{n})$ support function of $\Omega_w(n\Delta)$

Eqn. (D.8) reduces to

$$s_{x(n\Delta+\Delta)}(\underline{n}) = s_{x(n\Delta)}[\phi'(n\Delta)\underline{n}]+s_{w(n\Delta)}[\Delta G'(n\Delta)\underline{n}] \quad (D.9)$$

If $\Omega_x(0)$ and $\Omega_w(n\Delta)$ are ellipsoids defined by

$$\Omega_x(0) = \{\underline{x}:\ (\underline{x}-\underline{x}_o)'\psi^{-1}(\underline{x}-\underline{x}_o) \underline{\leq} 1\} \quad (D.10)$$

$$\Omega_w(n\Delta) = \{\underline{w}:\ \underline{w}'Q^{-1}(n\Delta)\underline{w} \underline{\leq} 1\} \quad (D.11)$$

the corresponding support functions are given by:

$$s_{x(0)}(\underline{n}) = \underline{n}'\underline{x}_o + [\underline{n}'\psi\underline{n}]^{\frac{1}{2}} \quad (D.12)$$

$$s_{w(n\Delta)}(\underline{n}) = [\underline{n}'Q\underline{n}]^{\frac{1}{2}} \quad (D.13)$$

where $\underline{x}_o$ is the center of the states.

Assume that $\Omega_x(n\Delta)$ is bounded by an ellipsoid described by:

$$\Omega_{x,b}(n\Delta) = \{\underline{x}:\ (\underline{x}-\underline{x}_o)'\Gamma^{-1}(n\Delta)(\underline{x}-\underline{x}_o)\underline{\leq} 1\} \quad (D.14)$$

then the corresponding support function is:

$$s_{x(n\Delta),b}(\underline{n}) = n'\underline{x}_o + [\underline{n}'\Gamma\underline{n}]^{\frac{1}{2}} \quad (D.15)$$

Using Eqs. (D.11) and (D.15), equation (D.9) is reduced to

$$s_{x(n\Delta+\Delta)}(\underline{n}) = \underline{n}'\phi(n\Delta)\underline{x}_o + [\underline{n}'\phi(n\Delta)\Gamma(n\Delta)\phi(n\Delta)\underline{n}]^{\frac{1}{2}}$$

$$+[\underline{n}'G(n\Delta)Q(n\Delta)G'(n\Delta)\underline{n}\Delta^2]^{\frac{1}{2}} \qquad \text{(D.16)}$$

Eqn. (D.16) is not the support function of an ellipsoid. A bounding ellipsoid can be obtained by using Holder's inequality

$$(1-\nu)^{-1} b_1^2 + \nu^{-1}b_2^2 \geq (b_1+b_2)^2 \qquad \text{(D.17)}$$

$$0 \leq \nu \leq 1$$

with

$$b_1 = [\underline{n}'\phi(n\Delta)\Gamma(n\Delta)\phi(n\Delta)\underline{n}]^{\frac{1}{2}} \qquad \text{(D.18)}$$

$$b_2 = [\underline{n}'G(n\Delta)\ Q(n\Delta)\ G'(n\Delta)\underline{n}\Delta^2]^{\frac{1}{2}} \qquad \text{(D.19)}$$

Using Holder's inequality, the support function of a bounding ellipsoid is given by:

$$s_{x(n\Delta+\Delta),b}(\underline{n}) = \underline{n}'\phi(n\Delta)\underline{x}_o$$

$$+[\frac{1}{1-\nu}\ \underline{n}'\phi(n\Delta)\Gamma(n\Delta)\phi'(n\Delta)\underline{n}+\frac{1}{\nu}\Delta^2\underline{n}'G(n\Delta)Q(n\Delta)G'(n\Delta)\underline{n}]^{\frac{1}{2}}$$

$$\text{(D.20)}$$

Substituting for $\nu=\Delta\beta(n\Delta)$ in Eqn. (D.20)

$$s_{x(n\Delta+\Delta),b}(\underline{n}) = \underline{n}'\phi(n\Delta)\underline{x}_o$$

$$+[\underline{n}'(\frac{1}{1-\Delta\beta(n\Delta)}\phi(n\Delta)\Gamma(n\Delta)\phi'(n\Delta) + \frac{\Delta}{\beta(n\Delta)}G(n\Delta)Q(n\Delta)G'(n\Delta))\underline{n}]^{\frac{1}{2}} \tag{D.21}$$

It follows that the ellipsoid bounding the set of reachable states is given by:

$$\Omega_{x,b}(n\Delta) = \{\underline{x}: (\underline{x}-\underline{x}_o)'\Gamma^{-1}(n\Delta)(\underline{x}-\underline{x}_o) \le 1\} \tag{D.22}$$

where $\Gamma(n\Delta)$ satisfies

$$\Gamma(n\Delta+\Delta) = \frac{1}{1-\Delta\beta(n\Delta)}\phi(n\Delta)\Gamma(n\Delta)\phi'(n\Delta)+\Delta G(n\Delta)\frac{Q(n\Delta)}{\beta(n\Delta)}G'(n\Delta) \tag{D.23}$$

$$\Gamma(0) = \psi$$

$$\frac{1}{\Delta} \ge \beta(n\Delta) \ge 0$$

The solution for the corresponding continuous-time system described by Eqn. (D.1) is obtained by applying the discrete to continuous time limit: Eqn. (D.3), $\Delta\to o$, $n\to\infty$, and $n\Delta\to t$. The resultant bounding ellipsoid for the set of reachable states is given by:

$$\Omega_{x,b}(t) = \{\underline{x}: (\underline{x}-\underline{x}_o)'\Gamma^{-1}(t)(\underline{x}-\underline{x}_o) \le 1\} \tag{D.24}$$

where $\Gamma(t)$ satisfies

$$\frac{d}{dt}\Gamma(t) = A(t)\Gamma(t) + \Gamma(t)A'(t) + \beta(t)\Gamma(t) + G(t)\,\frac{Q(t)}{\beta(t)}\,G'(t)$$

$$\Gamma(0) = \psi$$

$$\infty \geq \beta(t) \geq 0 \tag{D.25}$$